SKB

TECHNICAL REPORT 96-24

A mathematical model of the shore level displacement in Fennoscandia

Tore Påsse

Sveriges geologiska undersökning, Göteborg, Sweden

December1996

SVENSK KÄRNBRÄNSLEHANTERING AB
SWEDISH NUCLEAR FUEL AND WASTE MANAGEMENT CO
P.O.BOX 5864 S-102 40 STOCKHOLM SWEDEN
PHONE +46 8 665 28 00
FAX +46 8 661 57 19

A MATHEMATICAL MODEL OF THE SHORE LEVEL DISPLACEMENT IN FENNOSCANDIA

Tore Påsse

Sveriges geologiska undersökning, Göteborg, Sweden

December 1996

A mathematical model of the shore level displacement in Fennoscandia

Tore Påsse

Sveriges geologiska undersökning
Göteborg, Sweden

December 1996

Keywords: Shore level displacement, glacio-isostatic uplift, eustasy.

FOREWORD

This study was supported jointly by the Swedish Nuclear Fuel and Waste Management CO (SKB) and Geological Survey of Sweden (SGU).

Göteborg in December 1996.

Tore Påsse

ABSTRACT

The shore level displacement in Fennoscandia is mainly due to two co-operative vertical movements, the glacio-isostatic uplift and the eustatic sea level rise. The course of the glacio-isostatic uplift has recently been made discernible according to an investigation of the lake-tilting phenomenon (Påsse 1996). This new information has made it possible to start an iteration process for detailed estimations of the glacio-isostatic uplift and the eustatic rise using empirical data of the shore level displacement. A*rctan*- functions have proved to be suitable tools for describing the glacio-isostatic uplift.

The model indicates that there are two mechanisms involved in the glacio-isostatic uplift, one slow and the other fast. The main uplift, still in progress, acts slowly. The time of the maximal rate of the slow uplift is isochronous in the entire Fennoscandia, which means that the slow uplift occurred as a sympathetic movement. For the slow uplift there is a relationship between the rate of declining and the crustal thickness. In areas with great crustal thickness the rate of declining of the glacio-isostatic recovery is lower than in areas with thinner crust. The fast mechanism gave rise to a crustal subsidence during the Younger Dryas restored by a fast uplift during Preboreal time. The courses of the fast subsidence and the fast uplift are related to the deglaciation pattern. The fast subsidence was caused by a renewed down-loading of the crust during the glacial advance which culminated during the Younger Dryas.

The existence of the two uplift mechanisms implies that there are two physical processes involved in the glacio-isostatic rebound. The slow mechanism can be linked to viscous flow. The explanation of the fast mechanism may be compression followed by decompression.

The future development regarding the glacio-isostatic uplift, the eustasy and the shore level displacement is predicted in Fennoscandia using the results from the modelling. The predictions are based on the assumption that the crustal and eustatic developments will follow the trends that exist today.

The development of the Baltic have been outlined in this paper.

SAMMANFATTNING

I området som täcktes av den skandinaviska isen under den senaste istiden utgör strandförskjutningen en funktion av två samverkande vertikala rörelser, glacial-isostatisk landhöjning och eustatisk havsytehöjning. Genom sjöstjälpningsmetoden har ett ungefärligt förlopp av landhöjningen kunnat fastställas (Påsse 1996). Denna kunskap har gjort det möjligt att, i kombination med empirisk information från strandförskjutningskurvor och den nuvarande relativa landhöjningen, modellera strandförskjutnings-förloppet. Härigenom har landhöjningens och havsytans förändringar kunnat beskrivas matematiskt. I beräkningarna av landhöjningens förlopp har *arctan*- funktioner använts.

Modelleringen har visat att landhöjningen styrs av två rörelser, en långsam och en snabb rörelse. Den långsamma rörelsen utgör den största delen av den glacial-isostatiska landhöjningen och är en pågående rörelse. Denna sker genom en sympatisk rörelse där tidpunkten, då höjningen var som störst, inföll samtidigt inom hela området. Ett samband har påvisats mellan avklingningshastigheten och jordskorpans tjocklek. I områden med tjock jordskorpa är landhöjningen långsammare än i områden med tunn skorpa. Den snabba landhöjningens förlopp har ett samband med isavsmältnings-mönstret. Den snabba mekanismen orsakade en landsänkning under Yngre Dryas, som sedan ersattes av en snabb landhöjning under Preboreal tid. Landsänkningen orsakades av en förnyad pålastning av is i samband med den isframstöt som kulminerade under Yngre Dryas.

Den tudelade landhöjningsmekanismen visar att två fysikaliska processer är inblandade i den glacial-isostatiska landhöjningen. Den långsamma rörelsen kan kopplas till viskös massförflyttning. En förklaring till den snabba rörelsen kan vara kompression följt av dekompression.

Den framtida utvecklingen, avseende landhöjning, havsyteförändringar och strandförskjutning i Fennoskandia, kan förutsägas genom modellen. Dessa förutsägelser bygger på antagandet att jordskorpans rörelser och havsytans förändringar följer de trender som existerar idag.

Östersjöns utveckling har skisserats i arbetet.

TABLE OF CONTENTS

SUMMARY

The objective of this investigation is to construct a mathematical model of the shore-level displacement in the area covered by the Scandinavian ice during the Weichselian glaciation. The motive for this originally emanates from the desire to determine the shore-level displacement along the Fennoscandian coasts in four dimensions, *i.e.* to determine the shore-level displacement as regards to position (two dimensions), altitude and time.

The shore level displacement (S m) in Fennoscandia was mainly caused by two co-operative vertical movements, the glacio-isostatic uplift (U m) and the eustatic sea level rise (E m). The shore level displacement is estimated by $S = U - E$. Difficulty in modelling the shore level displacement was due to the lack of empirical data concerning the glacio-isostatic uplift and also the lack of reliable data of the eustatic rise. However, according to an investigation of the lake-tilting phenomenon (Påsse 1996) the course of the glacio-isostatic uplift has been made discernible. This new information has made it possible to start an iteration process for detailed estimations of the glacio-isostatic uplift and the eustatic rise using empirical data of the shore level displacement. The modelling also includes information regarding the recent relative uplift (Ekman 1996) and rough information concerning the eustasy (e.g. Fairbanks 1989). The shore level displacement is empirically known from 63 shore level curves in the area affected by the Scandinavian ice during the Late Weichselian.

Arctan- functions have proved to be suitable tools for describing the glacio-isostatic uplift. The basic formula for the land uplift can be expressed as

$$U = 0.6366 \times A \, (arctan \, (T / B) - \, arctan \, ((\, T - t \,) / B))$$

where A is half of the total uplift (m), T (years) is the time for the maximal uplift rate, t (year) is the variable time and B is a declining factor. A formula for expressing the eustatic rise is also presented in this paper. The results of the modelling are presented as comparisons of the congruity between shore level curves available from the literature and calculated theoretical curves, Figures 4-2 to 4-66.

The model indicates that there are two mechanisms involved in the glacio-isostatic uplift, one slow and the other fast. The main uplift is a slow declining movement. This movement is still in progress in the whole area earlier covered by the Scandinavian ice. The peripheral parts of this area, which today seem to be submerged, are thus still affected by a slow uplift. The reason for the submergence is an ongoing eustatic rise. The present annual eustatic rise is estimated to 1.2 mm/y. The time when the maximum uplift rate occurred for the slow uplift mechanism is estimated to 12 500 calendar years *i.e.* 11 300 conventional radiocarbon years BP. This is a constant value which means that the slow uplift occurred as a sympathetic

motion. It also implies that a great part of the uplift, especially in the last deglaciated areas, occurred before the areas finally were ice free. For the slow uplift there is a relationship between the rate of declining and the crustal thickness. In areas with great crustal thickness the glacio-isostatic recovery is slower than in areas with a thinner crust.

The fast mechanism gave rise to a crustal subsidence during the Younger Dryas restored by a fast uplift during the Preboreal. The subsidence is apparent in shore level curves in a peripheral zone outside the Younger Dryas ice margin. The fast uplift is apparent in the same area but also in central Fennoscandia *i.e.* the areas which were rapidly deglaciated during Preboreal time. The course of the fast subsidence and the fast uplift is in response to the deglaciation pattern. The deglaciation of the peripheral parts of the Scandinavian ice, from the maximal Weichselian extension to the Younger Dryas terminal zone, lasted c. 10 000 years while the deglaciation from the Younger Dryas terminal zone to the area in northern Sweden, where the glaciation terminated, lasted c. 1 000 years.

The fast subsidence obviously was caused by a renewed downloading of the crust during that glacial advance that culminated during the Younger Dryas. The shore level curves show that the growth of the ice thickness, at least in the marginal parts of the ice, already started in the beginning of Alleröd or possibly somewhat earlier. The fast subsidence and the fast uplift are visible in shore level curves from sites c. 100 km outside the ice margin. The fast mechanism thus created sympathetic crustal movements more than 100 km outside the ice margin. The positions of maximal uplift, for the slow uplift and fast uplift respectively, are situated in different places. This condition supports the assumption of different causes of the slow and the fast mechanisms. The two mechanisms gave rise to tilting in somewhat different directions in the south- eastern part of Norway and in the western-central part of Sweden.

The existence of the two uplift mechanisms implies that there are two physical processes involved in the glacio-isostatic rebound. Ekman & Mäkinen (1996) have proved that a viscous inflow of mantle is a necessary part of the ongoing uplift process. The present uplift is due to the slow mechanism. That means that this mechanism can be linked to viscous flow and that the fast mechanism needs another explanation. This explanation may be compression followed by decompression.

The future development regarding the glacio-isostatic uplift, the eustasy and the shore level displacement can be predicted in Fennoscandia using the results from the modelling. Some shore level curves from sites in Sweden are shown as examples of these predictions, Figures 6-1 to 6-6. The predictions are based on the assumption that the crustal and eustatic movements follow the trends that exist today.

Shore level curves from the coasts around the Baltic are affected by the raised water levels during two lake stages, the Baltic Ice Lake and the Ancylus Lake. The development of the Baltic has been outlined in chapter 7 and is summarised in Figure 7-4.

1 INTRODUCTION

The objective of this investigation is to construct a mathematical model of the shore-level displacement in the area covered by the Scandinavian ice during the Weichselian glaciation. The motive for that originally emanates from a desire to determine the shore-level displacement along the Fennoscandian coasts in four dimensions, *i.e.* to determine the shore-level displacement as regards to position (two dimensions), altitude and time. During the continuous work the objectives have become more numerous and also include a desire to understand the mechanisms of the glacio-isostatic uplift and also a desire to predicting future shore level development.

It is meaningless to take into account all the more or less incorrect calculations included in the modelling, therefore only the chosen model will be discussed in this presentation. In addition it is impossible to present "the methods" in a logical order as every parameter has been determined gradually and dependent of all the other parameters in a multivariable system. What can prove the validity of the formulas is the congruity between the empirical shore level curves and the theoretically deduced curves.

Most scientists who have tried to calculate the shore level displacement have used exponential functions to express the glacio-isostatic crustal upheaval. However, the exponential function gives rise to several preposterous conditions inconsistent to the course of the glacio-isostatic uplift in a wider perspective. The most obvious absurdity is that the crustal uplift continually increases going backwards in time. The glacio-isostatic recovery is thus better defined by a function that has an inclining course at the beginning and ends with a declining course. A*rctan*- functions have proved to be suitable tools for describing the glacio-isostatic uplift. These functions were used in an investigation of the lake-tilting phenomenon presented by Påsse (1996). This investigation is of fundamental importance to the modelling.

1.1 MODEL PRESUMPTIONS

The shore level displacement (S m) in Fennoscandia is mainly due to two co-operative vertical movements, the glacio-isostatic uplift (U m) and the eustatic sea level rise (E m). The eustatic sea level rise is assumed to be globally constant. The shore level displacement is estimated by

$$S = U - E. \qquad 1\text{-}1$$

The method used in the modelling can be summarised in the following steps:

1. Empirical estimations of the glacio-isostatic uplift have been made by the lake-tilting method (Påsse 1996). This method gives detailed information of the difference in the course of the crustal uplift between two points,

$$U_1 - U_2 = \Delta U \qquad 1\text{-}2$$

Lake-tilting investigations have been performed at four sites on the Swedish west coast (Påsse 1996). An example of the graphs received in the lake-tilting investigations is shown in Figure 1-1. The ΔU functions are not affected by eustatic or geoidal changes.

2. Magnifying ΔU creates a hypothetical uplift function (U_{hyp}).

3. Hypothetical uplift curves are subtracted from the empirical shore level curves and give hypothetical expressions of the eustasy (E_{hyp}).

$$U_{hyp} - S = E_{hyp} \qquad 1\text{-}3$$

An example of these calculations is shown graphically in Figure 1-2.

4. The true uplift formulas are found when

$$U_{hyp1} - S_1 = U_{hyp2} - S_2 = U_{hyp3} - S_3 \ldots\ldots \qquad 1\text{-}4$$

$$\text{or } E_{hyp1} = E_{hyp2} = E_{hyp3}\ldots\ldots \qquad 1\text{-}5$$

5. The results can be restricted by some assumptions:

a. The eustasy is approximately known from off shore information *e.g.* by the data presented by Fairbanks (1989). See Figure 3-9.

b. The functions for the uplift are assumed to be proportional in some respect,

$$U_1 \sim U_2 \sim U_3 \qquad 1\text{-}6$$

which means that there should be some general rules determining the course of the glacio-isostatic uplift.

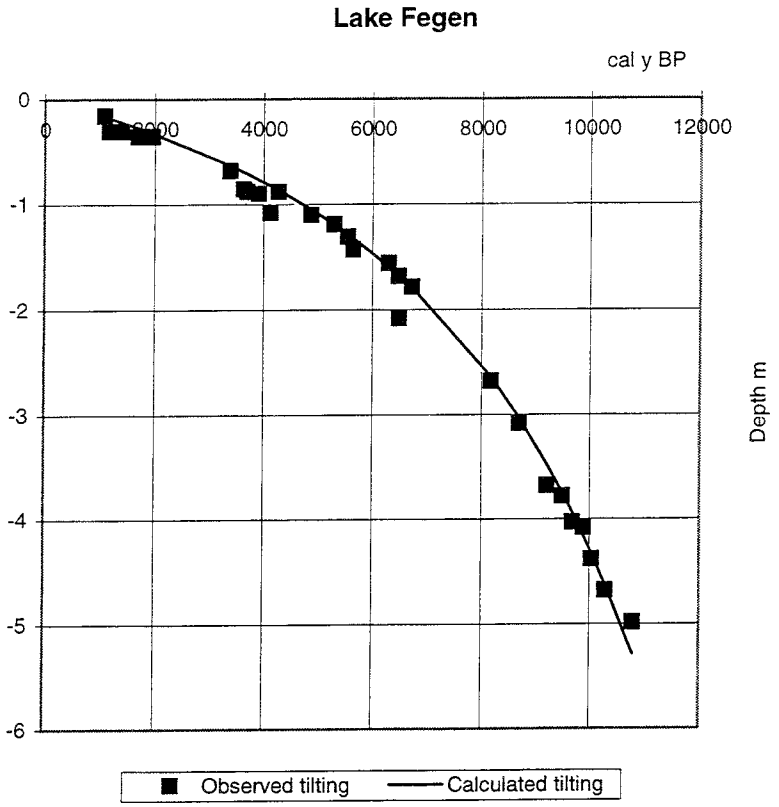

***Figure 1-1**. Radiocarbon dates for ancient lake levels in lake Fegen (Påsse 1990, 1996). The curve shows the difference in land uplift between the outlet and the southern part of the lake expressed by an arctan- function.*

c. The velocity of the present *relative* uplift (v_r mm/y) is recorded from tide gauges and precision levellings (Ekman 1996). The present *relative* uplift (v_o mm/y) is not only dependent on the crustal movement but also on a eustatic component which, however, are the same in the whole area. The present eustatic rise is in the order of 1.2 mm/y according to e.g. Emery & Aubrey (1991), Nakiboglu & Lambeck (1991) and Ekman (1996). The present *absolute* uplift (v_o mm/y) is calculated in the modelling as

U (t) for $t = 1$ 1-7

If the present *relative* uplift (v_r mm/y) is subtracted from the present *absolute* uplift (v_o mm/y) this gives a value of the present eustatic rise. This value should be equal at each site. This condition can be used to evaluate the results in the modelling.

6. Calendar years are used in the modelling.

7. Gravity or geoidal changes have not been taken into consideration in the modelling. Before a serious discussion regarding influences of gravity on the crustal uplift can be brought about it is important to be aware of the uplift mechanisms. Adding more unknown factors at this stage would probably only result in confusion.

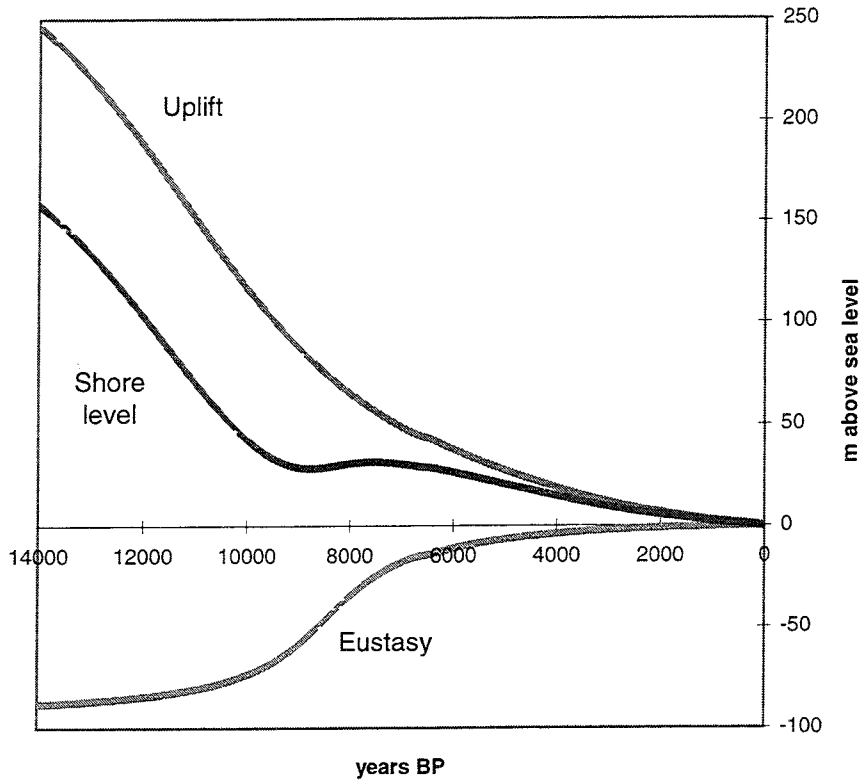

Figure 1-2. *The eustasy (E) and the crustal uplift (U) determine the shore level displacement (S), by S = U - E.*

2 THE RECENT UPLIFT

The recent relative uplift is recorded by precision levellings and tide gauge data. In Finland records are presented by Kääriäinen (1963, 1966) and Suutarinen (1983), in Sweden by RAK (1971, 1974), in Denmark by Simonsen (1969) and Andersen *et al.* (1974), in Norway by Bakkelid (1979). Ekman (1996) has compiled information of the present rate of crustal movements in Fennoscandia mainly from these sources and also in a special map with emphasis on the tide gauge measurements. The maps, presented by Ekman (1996), are used in this report and are shown in Figures 2-1 and 2-2.

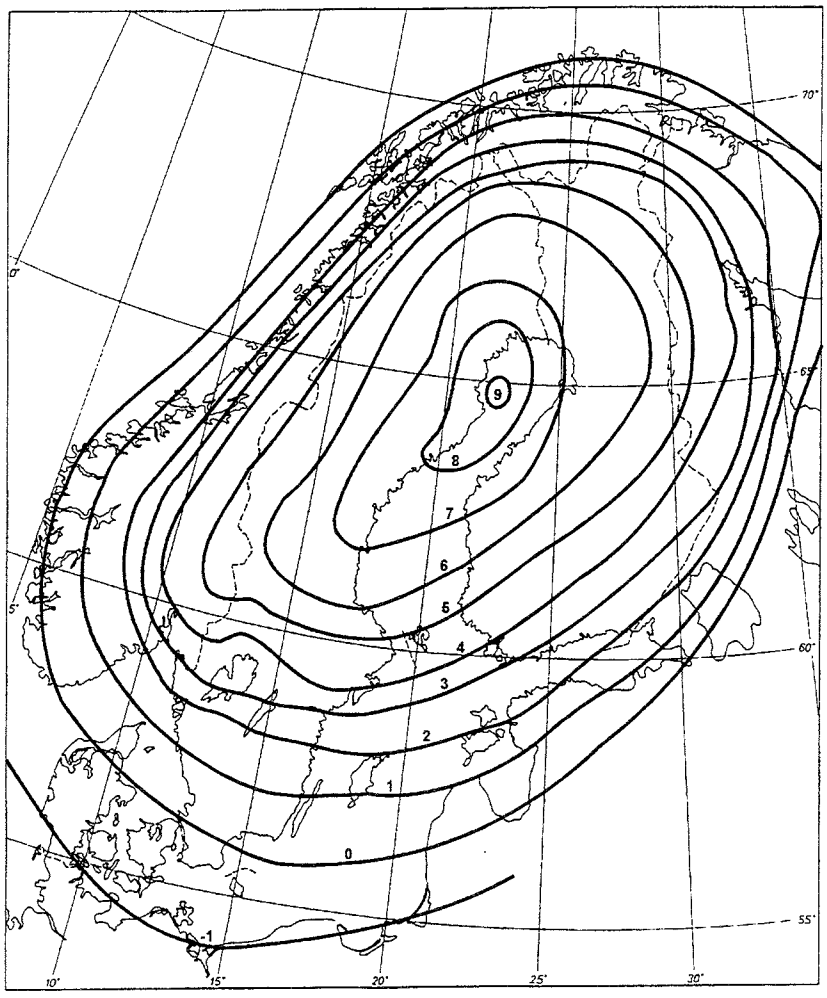

Figure 2-1. *The recent relative uplift, v_r (mm/ y), recorded by precision levellings and tide gauge data. The map is redrawn from Ekman (1996).*

The recent *relative* uplift recorded by tide gauge data includes eustatic changes. A eustatic rise in the order of 1 mm/ year has been reported, among others by Lizitzen (1974), Mörner (1977, 1980a) and Ekman (1986). Compilations by Emery & Aubrey (1991) and Nakiboglu & Lambeck (1991) indicate a present eustatic rise in the order of 1.2 mm/ year.

All isoline maps of the recent relative land uplift in Fennoscandia show an approximately elliptical uplift structure where most of the area emerges. However, a submerging peripheral zone is distinguishable. The southernmost part of Sweden is part of this submerging peripheral zone. As the shore lines are raised in this area, the glacio-isostatic uplift must, at least recently, have been active in this submerging area. This fact indicates that this submergence is caused by a present eustatic rise and not by crustal subsidence.

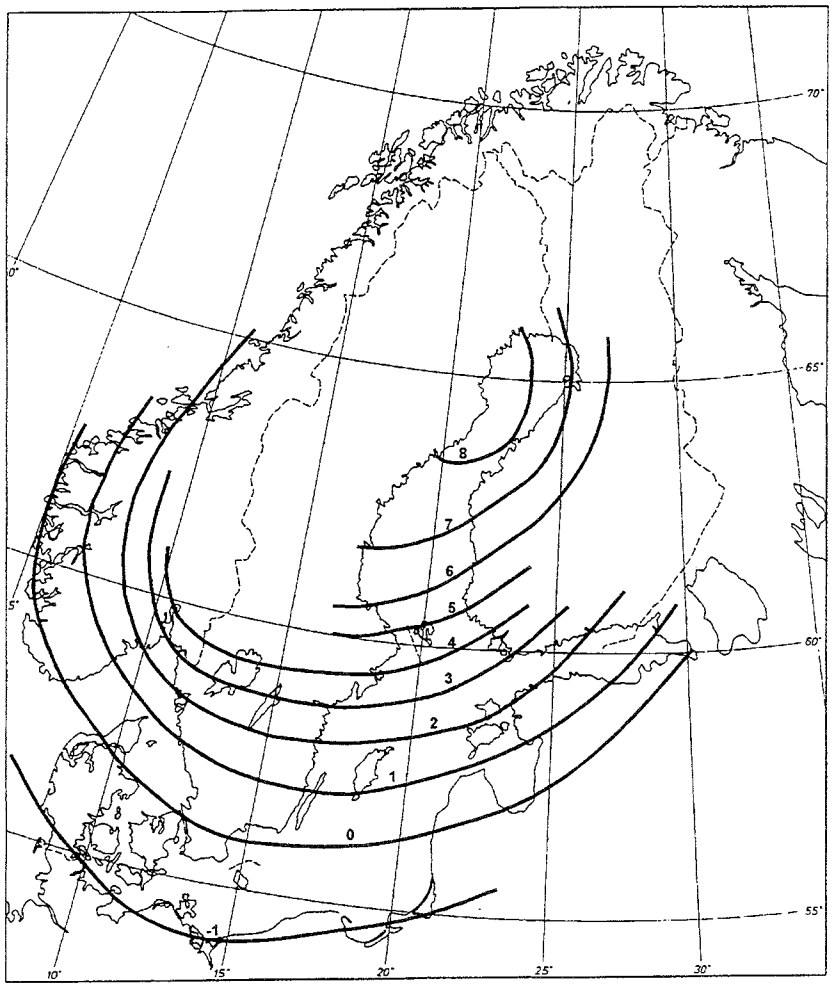

Figure 2-2. *The recent relative uplift, v_r (mm/ y), derived from records of tide gauge data. The map is redrawn from Ekman (1996).*

3 FORMULAS USED IN THE MODELLING

3.1 CALIBRATION OF ^{14}C - VALUES

The assumption of an essentially steady concentration of ^{14}C in the atmosphere is fundamental to the radiocarbon method. However, in detail, this assumption is invalid and the dates given by the radiocarbon method are not the same as calendar dates. The ^{14}C- chronology is furthermore defective because of a systematic error due to the half- life time used. The original half-life established by Libby (1955), with a value of 5568 years, is conventionally used instead of the revised half-life of 5 730 years estimated by Olsson (1968). The dates given by the laboratory can be converted, according to the half-life established by Olsson (1968), by multiplying the given dates by 1.03.

The discrepancy between conventional ^{14}C-dates and calendar dates is usually neglected when ^{14}C-values are used to date e.g. pollen-analytical or deglaciation events. A special ^{14}C-chronology has therefore been established by Quaternary geologists which is convenient for the purposes mentioned but hazardous for other purposes. When comparing the ^{14}C- chronology with other absolute dating methods, such as varve chronology or dates determined by the TL-method, it is necessary to make the comparison in calendar years. This is also necessary when using astronomical information in Quaternary geology and for calculations of the glacio- isostatic uplift.

A calibration of the radiocarbon-chronology has been established for the last 8 000 years by ^{14}C-datings of dendrochronological dated tree-rings (e.g. Damon *et al.* 1966, 1978, Suess 1970, Klein *et al.* 1982). However, when dealing with Late Weichselian chronology this calibration is not applicable. Recently Becker *et al.* (1991) has presented a floating Late Weichselian and Early Holocene chronology of pine (*Pinus sylvestris*) which extend the calibrations backwards to 11 370 calendar years BP. A tentative calibration curve based on radiocarbon datings of annually laminated lake sediments has been carried out by Lotter (1991) comprising the interval 10 600-12 700 calendar years BP. A calibration of the ^{14}C timescale over the past 30 000 years, using mass spectrometric U-Th ages from corals, has been carried out by Bard *et al.* (1990).

Stuiver & Reimer (1993) have developed a computer program for calibrating ^{14}C -dates. Close to 10 000 years BP there is a rapid change during a very short interval in this calibration program which is not in accordance with the results presented by Lotter (1991) and Becker *et al.* (1991). Påsse (1996) suggests a linear calibration in the order of 1.095 for Late Weichselian dates.

A mathematical expression for converting conventional ^{14}C-dates to calendar dates is derived in this paper. This function is carried out by combining the linear expression, for dates > 8 000 years BP, with an adoption of the calibrations given by Stuiver & Reimer (1993) for dates < 8 000 years BP. The formula used in the modelling for converting dates is written as:

$$t = 59.6\text{-}206.9 \times \textit{arctan}\ ((4000\text{-}\ 1.095t_{con})/800) + 63.66 \times \textit{arctan}\ ((7200\ \text{-}$$

$$\text{-}\ 1.095t_{con})/100)) + 95.5 \times \textit{arctan}\ ((750\ \text{-}\ 1.095t_{con})/200) + 1.095t_{con} \qquad 3\text{-}1$$

where t is the calibrated date, while t_{con} is the conventional radiocarbon date. When calendar years are used, this is pointed out by writing cal years BP, while conventional ^{14}C -years are denoted as years BP.

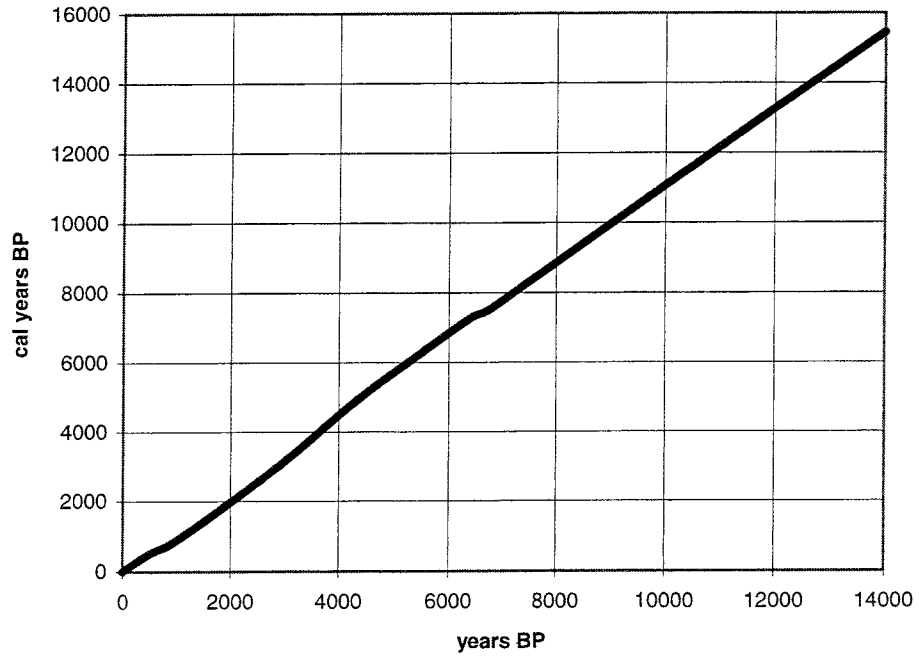

Figure 3-1. *The difference between calibrated dates (cal years BP) and conventional ^{14}C- dates (years BP) received by formula 3-1.*

3.2 THE UPLIFT FORMULA

Physical models of the glacio-isostatic recovery have been presented during the last years *e.g.* by Cathles (1975), Peltier (1976, 1988, 1991), Clark *et al.* (1978), Nakada & Lambeck (1987, 1989), Fjeldskaar & Cathles (1991), Lambeck (1991) and Nakiboglu & Lambeck (1991). The formulas for the course of the glacio-isostatic uplift, used in these models, are derived according to rheological parameters. However there are quite different opinions regarding the rheological parameters among these authors. Påsse (1996) has made investigations of the glacio-isostatic uplift based on the lake-tilting method. The point with the empirical lake-tilting investigations is that the course of the glacio-isostatic uplift can be expressed in mathematical terms without using rheological assumptions.

According to Andrews (1970) the glacio-isostatic movement starts slowly, reaches a maximal rate and after that follows a declining course. Different S-shaped functions have been tested for describing the glacio-isostatic uplift from lake-tilting information (Påsse 1996) and shore level data. *Arctan*-functions turned out to be the most suitable way of describing the glacio-isostatic uplift.

The *arctan*-functions can be divided into two symmetrical parts, one is inclining and the other is declining. To say that the initial inclining phase of the uplift is symmetrical to the declining phase is an overstatement as there is too little information accessible for testing the inclining phase. The lack of data is due to the fact that the main part of the uplift, during the inclining phase, occurred beneath a cover of ice. Only the declining phase of the function can be tested for its validity of describing the glacio-isostatic uplift. The land uplift following the unloading of ice (U in m) can then be described with the function

$$U = A - R - (2A/\pi) \times arctan\ ((T - t)/B) \qquad 3\text{-}2$$

where A is half of the total uplift (m), R is the remaining uplift (m) in present time, T (years) is the time for the maximal uplift rate, *i.e.* the middle of the function, t (year) is the variable time and B is a declining factor.

When $t = 0$, $U = 0$ yields

$$R = A - (2A/\pi) \times arctan\ (T / B) \qquad 3\text{-}3$$

The basic formula for the land uplift can thus be expressed as

$$U = A - (2A/\pi) \times arctan\ ((T - t)/B) - (A - (2A/\pi) \times arctan\ (T / B)) \qquad 3\text{-}4$$

simplified as

$$U = 0.6366 \times A\ (arctan\ (T / B) - arctan\ ((T - t) / B)) \qquad 3\text{-}5$$

In the calculations T and t are counted in calendar years according to the formula 3-1. However, within all graphs the dates are reported in conventional ^{14}C- years as these dates are more familiar to most geologists.

The modelling has shown that the glacio-isostatic uplift is composed of two mechanisms, one slow and the other fast. The fast mechanism has been detected from shore level curves from that area which was covered by ice during the Younger Dryas, but also from a peripheral zone outside the Younger Dryas ice marginal, Figure 5-5. The nature of the two mechanisms will be further discussed in Chapter 5. Both mechanisms can be expressed by the general uplift function, 3-5, but the values of A, T and B differ considerably. These parameters are designated as A_1, T_1 and B_1 for the slow uplift. The parameters A_1 and B_1 are related to the position while T_1 seems to be regionally constant and is estimated to 12 500 calendar years BP *i.e.* 11 300 years BP counted in the conventional radiocarbon chronology. The formula for the slow uplift can thus be written as

$$U = 0.6366 \times A_1 \, (arctan \, (12\,500 / B_1) - arctan \, ((12\,500 - t) / B_1)) \qquad 3\text{-}6$$

The graphs of two different uplift curves are shown in Figure 3-2.

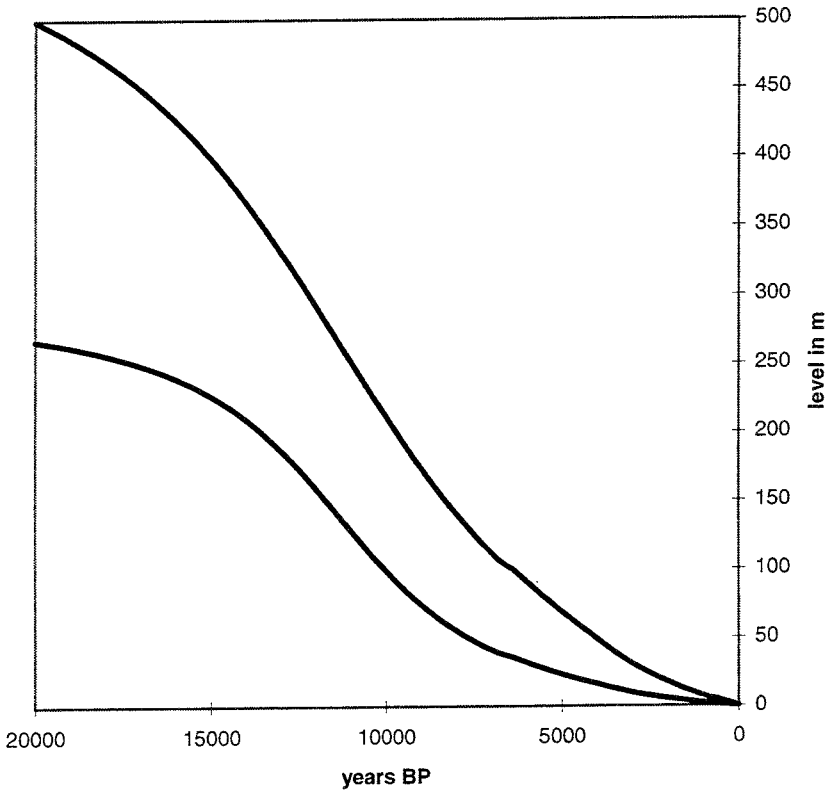

Figure 3-2. *Graphs of the slow glacio-isostatic uplift calculated by different values of A_1 and B_1. The uppermost curve is calculated with A_1 = 380 m and B_1 = 6500 and the lowermost curve with A_1 = 170 m and B_1 = 3800.*

In the southern parts of Scandinavia the glacio-isostatic recovery can be calculated using a formula comprising only the slow mechanism. Shore level curves from Norway and from the northern parts of the Swedish west coast, *i.e.* areas outside but close to the Younger Dryas ice border, show fast crustal movements during the Alleröd, Younger Dryas and Preboreal zones. The fast movement started with a crustal subsidence which later was restored by a fast uplift during the final deglaciation. The subsidence is interpreted to be caused by thickening of the ice which gave rise to the Younger Dryas glacial advance.

The crustal subsidence can be calculated by the general uplift formula letting B be negative. The parameters in the uplift formula are designated as A_2, T_2 and B_2 for the fast subsidence. The parameters related to the fast uplift are designated as A_3, T_3 and B_3. The course of the crustal movements caused by the fast mechanisms are shown graphically in Figures 3-3 and 3-4. The course of the crustal movement caused by the combination of the fast subsidence and the fast uplift is shown in Figure 3-5.

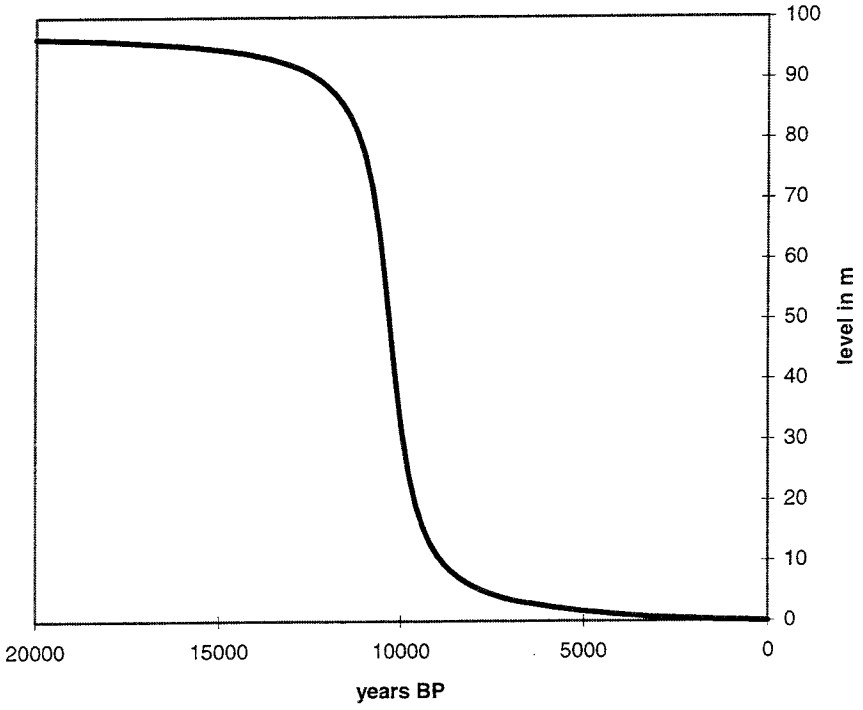

Figure 3-3. *Graph of the fast glacio-isostatic uplift calculated with A_3 = 50 m, T_3 = 11 400 cal y BP and B_3 = 600.*

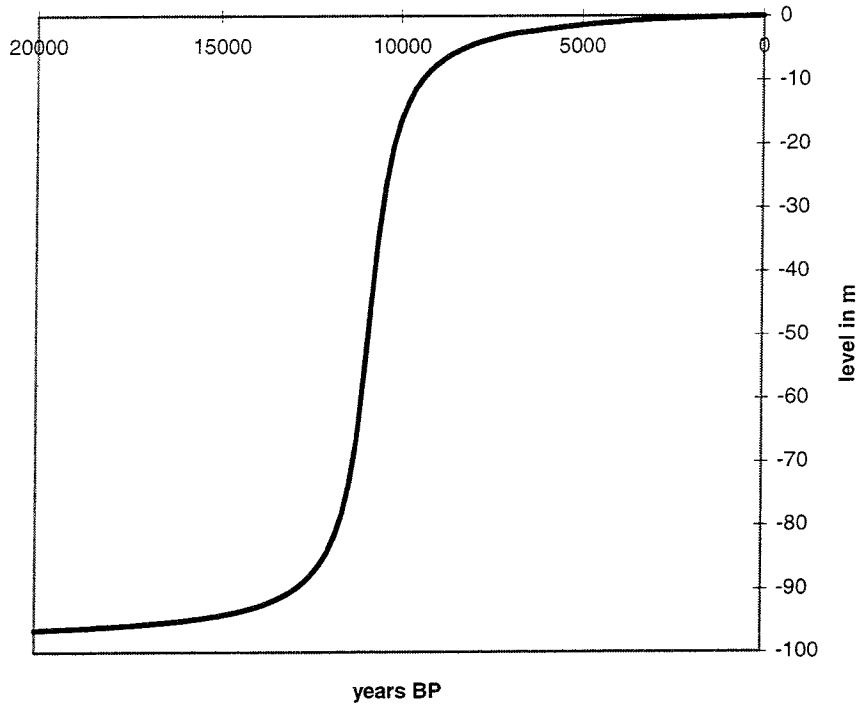

Figure 3-4. *Graph of the fast glacio-isostatic subsidence calculated with A_2 = 50 m, T_2 = 12 000 cal y BP and B_2 = -600.*

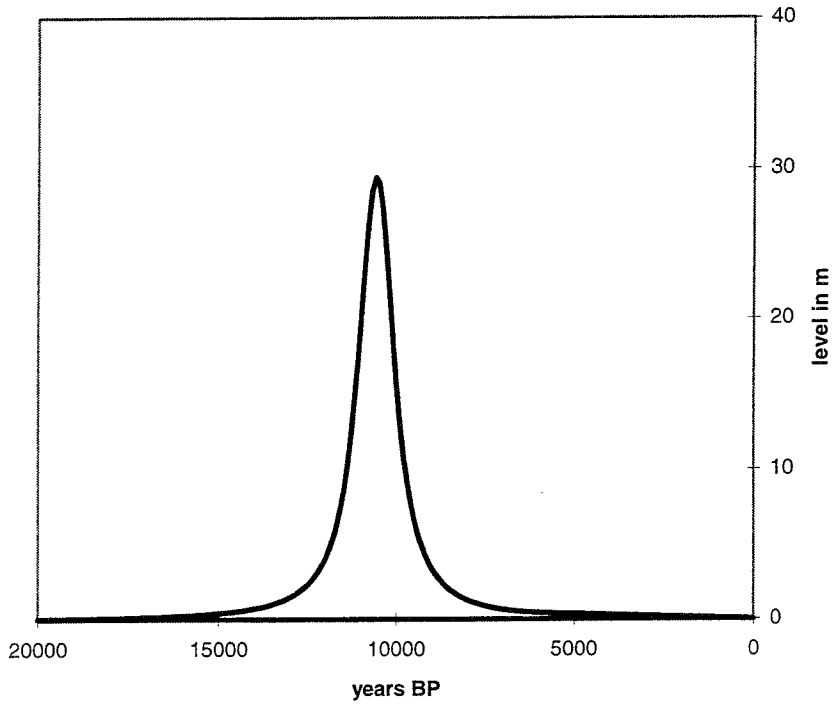

Figure 3-5. *Graph of the combination of the crustal movements shown in Figures 3-3 and 3-4.*

The slow uplift was still under progress when the subsidence occurred. This produced a retardation of the crustal movement during Younger Dryas time and an acceleration during Preboreal time which indicate the bipartite mechanism of the uplift.

The total glacio-isostatic uplift can be calculated by combing the effects of the slow and fast movements according to formula 3-7.

$$U = 0.6366 \times A_1 \, (arctan \, (12\,500 / B_1) - arctan \, ((12\,500 - t) / B_1)) +$$
$$+ 0.6366 \times A_2 \, (arctan \, (T_2 / B_2) - arctan \, ((T_2 - t) / B_2)) +$$
$$+ 0.6366 \times A_3 \, (arctan \, (T_3 / B_3) - arctan \, ((T_3 - t) / B_3)) \qquad 3\text{-}7$$

Figure 3-6 shows the combined effect of the glacio-isostatic movements used in the model.

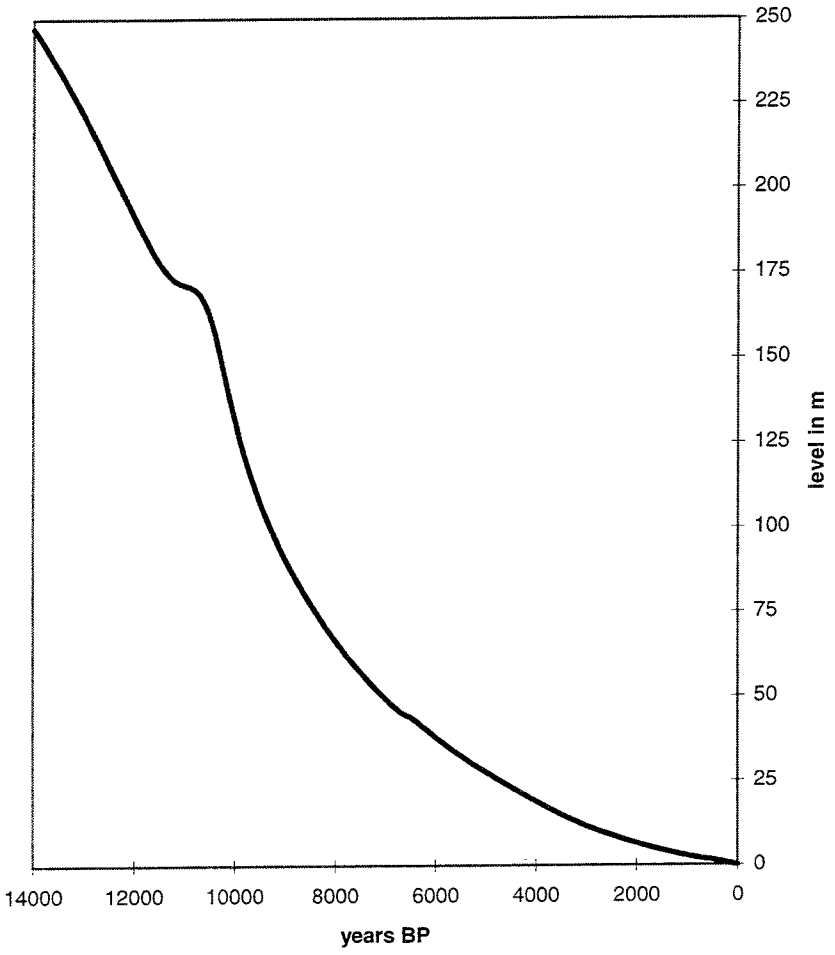

Figure 3-6. Graph showing the combined effect of the different glacio-isostatic movements used in the modelling. The parameters used for this calculation are A_1=200 m, T_1=12 500 cal y BP, B_1=3800, A_2=50 m, T_2=12 000 cal y BP, B_2=-600, A_3=50 m, T_3=11 400 cal y BP and B_3=600.

3.3 THE EUSTASY

The shore level changes in Fennoscandia were noticed and discussed as early as the eighteenth century by Celsius (1743) who interpreted this phenomenon as a lowering of the global sea level (water decrease). Later Lyell (1835) concluded that this and similar phenomena were caused by land uplift rather than a "water decrease". Suess (1885) introduced the theory of a rising sea level and also the term eustasy. The sea level rise was interpreted by Suess (1885) as being caused by a continuous addition of sediments in the sea basins.

The first publication ever of a well-documented shore-level curve is from Göteborg and was made by the Geological Survey of Sweden (Sandegren & Johansson 1931). This curve shows a transgression during the Holocene which was interpreted as land subsidence following the Late Glacial uplift. It was not until Daly (1934) introduced the theory of glacio-eustasy that this transgression was correctly interpreted as a rise of the global sea level. The glacio-eustasy is a climatically controlled movement caused by removal or addition of water under conditions of glaciation and deglaciation.

Ever since Godwin *et al.* (1958), Fairbridge (1961), Jelgersma (1961) and Shepard (1963) presented eustatic curves of the global sea level rise there have been several subsequent curves which on the whole show the same trend but differ in detail. Fairbanks (1989) has published a eustatic curve which is generally accepted. This curve is from Barbados and based on radiocarbon dated corals. The curve goes back to 18 000 years BP and the global sea level was then measured to c. - 120 m.

A eustatic curve is obtained as a result of the modelling. The main course of the eustatic rise may be expressed as:

$$E = 0{,}6366 \times 50 \times (\arctan(9\,350/1375) - \arctan((9\,350 - t)/1375)) \qquad 3\text{-}8$$

This relation is shown in a graph in Figure 3-7. Figure 50 in formula 3-8 designates half of the total eustatic rise (in m). This figure shows that, since the glacial maximum, the eustatic rise is 100 m according to formula 3-8. However, information concerning the eustasy has only been calculated back to 14 000 y BP in the modelling

Function 3-8 for the eustasy only takes the main rise into consideration. In areas where the tidal effect is very low and raised shore levels exist, it is obvious that the sea level not only rose continuously during the Holocene but also changed in an oscillatory way (*cf.* Påsse 1983). The size and periodicity of these oscillations are not satisfactorily known but it is difficult to leave such information unnoticed in this context. The sinusoidal function may be added to the main eustatic formula in order to attain more detailed information regarding transgression and regression phases.

The sinusoidal function is preliminary given a periodicity of *c.* 475 years (Påsse 1983) and an amplitude of 0.5 m. The cyclic function can be written as:

$$C = 0{,}5 \times \sin((t - 100) \times 0{,}013) - 0.48 \qquad 3\text{-}9$$

Figure 3-8 shows the eustatic changes when function 3-9 is added to 3-8.

Most curves, interpreted as eustatic curves, are derived from off shore information. According to Bloom (1967) the sea floor is affected by the change of load caused by the increase of water during the eustatic rise. Bloom (1967) named this phenomenon the hydro-isostatic effect. The eustatic curves compiled from submarine information, e.g. Fairbanks curve (1989), ought to be corrected for the hydro-isostatic effect. A eustatic curve, constructed by subtracting the shore level displacement from a "known" glacio-isostatic uplift, does not need this adjustment provided the shore level curve is compiled from an area situated above the present sea level.

The present shore-line modelling started with the assumption that the eustasy was close to the curve presented by Fairbanks (1989). However, this curve was inconsistent to the results of the calculations. The eustatic curve, which is obtained from the modelling, is supposed to illustrate more clearly the trends in the global eustasy than *e.g.* the curve presented by Fairbanks (1989). A comparision between Fairbank´s curve and the calculated curve is described in Figure 3-9.

3.3.1 Water level changes in the Baltic

The shore level curves from the Baltic basin are influenced not only by the eustasy but also by water level changes during two lake stages, the Balic Ice Lake and the Ancylus Lake. The differences between the sea level and the lake levels within the Baltic basin were possible to calculate during the modelling. The results of these calculations are presented in Chapter 7.

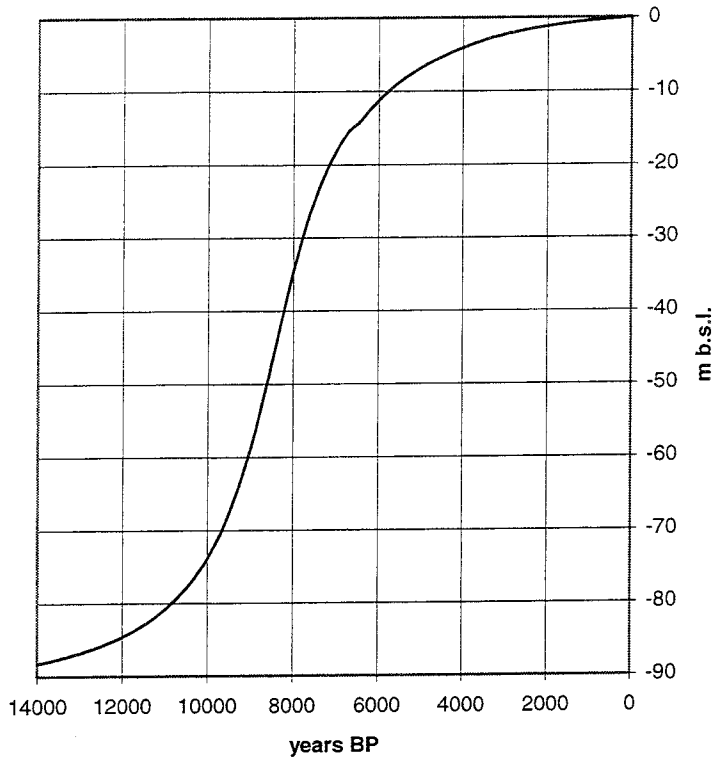

Figure 3-7. *A graph of the eustatic rise calculated with formula 3-8.*

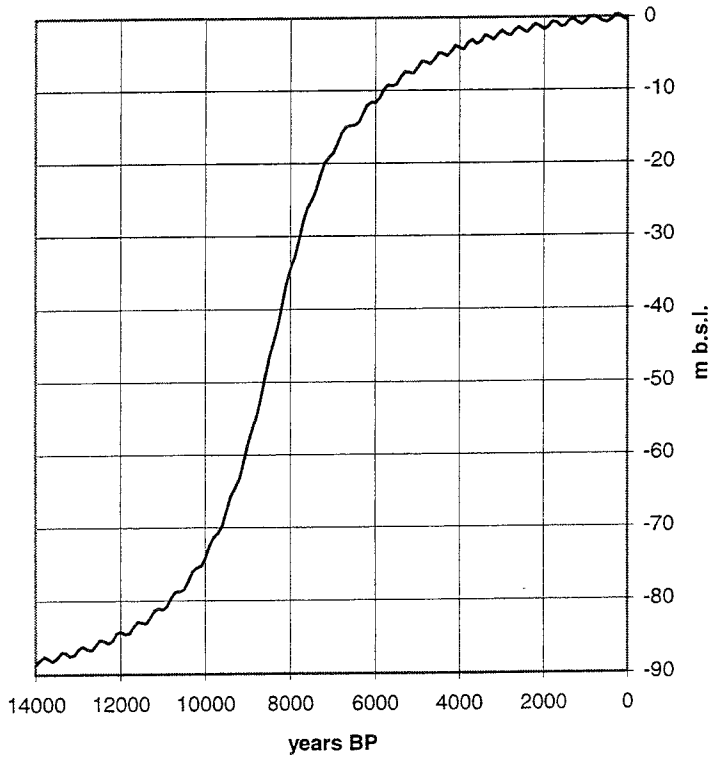

Figure 3-8. *The eustatic rise calculated by a combination of formulae 3-8 and 3-9.*

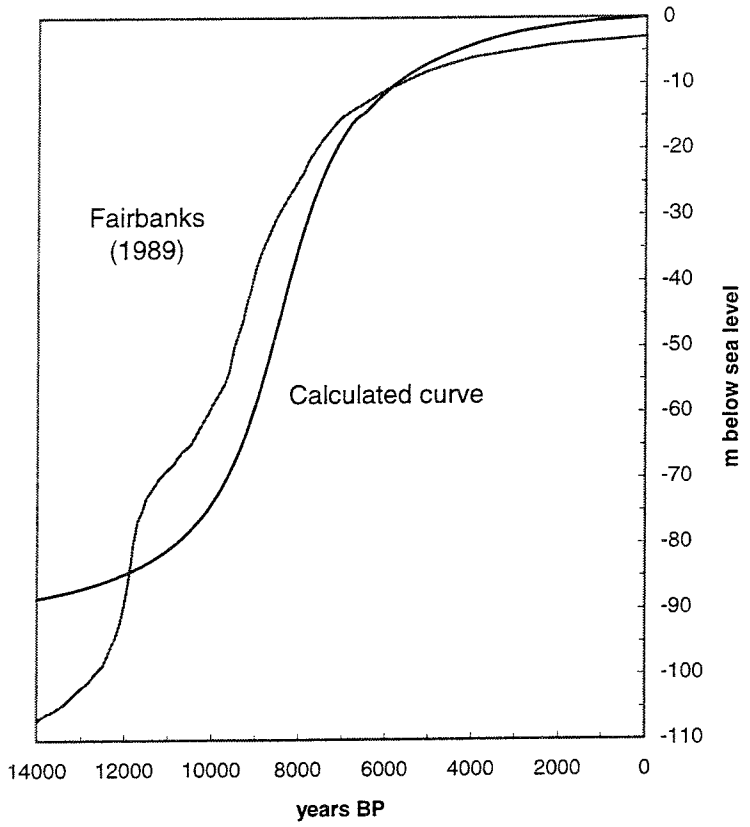

***Figure 3-9**. A comparision between Fairbanks (1989) eustatic curve and the curve resulting from the calculations.*

4 RESULTS OF THE MODELLING

4.1 GENERAL

In this chapter shore level curves within the investigation area available from the literature are compared to the theoretical curves deduced from the formulas presented in Chapter 3. Each shore level curve is shown with a graph where the original curve is drawn in grey and the theoretical curve in black. The lines of original curves have unfortunately in some cases become somewhat rugged during the transformation to the computer. Original data for constructing the curves are shown by black squares in the graphs. 63 shore level curves have been used in the modelling. The position of each curve used in the text is designated with a site number. The geographical positions of the sites are presented in Figure 4-1. The reference of each shore level curve is presented in the text and in Table 4-1. Some shore level curves are extended by new data from nearby sites. Certain curves are commented regarding notable divergence's or uncertainties but it is insurmountable to start a debate of each divergence in this context. Most of the theoretical curves are calculated without using the oscillation formula, 3-9. The uplift parameters, achieved as a result of the modelling, are reported in Table 5-1.

The shore level displacement is a four-dimensional system which includes time (t) and three co-ordinates determining the position, (x, y, z). When shore level information is presented by conventional methods one or two of these co-ordinates are chosen as invariable for making the presentation comprehensible. In shore level curves x and y are invariable. In shore-line diagrams t is invariable and x and y are converted into a position co-ordinate. In isobase maps t is invariable. The method of using *arctan*-formulas is a four-dimensional system, which includes t and z, while x and y are replaced by the uplift parameters related to specific positions.

The declining course of the uplift can only be univocally solved using shore level information that extends over a long time span. There are several shore level curves that range just over one or two thousand years. They may be very detailed but due to the short extension of these curves the calculations of the uplift would be unreliable using these. Shore level curves comprising long time intervals may be constructed by approximate datings but may in spite of this give better qualifications for uplift calculations than shorter more detailed curves.

Table 4-1. Number, names and references of the sites used in the calculations.

Nr	Sites	References
1	Varanger	Donner 1980
2	Andöja	Vorren et al. 1988
3	Tromsö	Hald & Vorren 1983
4	Lofoten	Möller 1984, Vorren & Moe 1986
5	Näröy	Ramfjord 1982
6	Verdalsöra	Sveian & Olsen 1984
7	Frosta	Kjemperud 1986
8	Bjugn	Kjemperud 1986
9	Hitra	Kjemperud 1986
10	Fröja	Kjemperud 1986
11	Leinöy	Svendsen & Mangerud 1990
12	Fonnes	Kaland 1984
13	Sotra	Krzywinski & Stabell 1984, Kaland et al 1984
14	Bömlo	Kaland 1984
15	Yrkje	Anundsen 1985
16	Jären	Thomsen 1982, Bird & Klemsdal 1986
17	Kragerö	Stabell 1980
18	Porsgrunn	Stabell 1980
19	Vestfold	Henningsmoen 1979
20	Oslo	Hafsten 1983
21	Östfold	Danielsen 1970
22	Ski	Sörensen 1979
23	Vendsyssel	Rickardt 1996
24	Vedbäck	Christensen 1993
25	Söborg SÖ	Mörner 1976
26	St Bält & Fakse Bugt	Christensen 1993, Bennike & Jensen 1995
27	Kroppefjäll	Björck & Digerfeldt 1991
28	Hunneberg	Björck & Digerfeldt 1982
29	Central Bohuslän	Miller & Robertsson 1988
30	Ljungskile	Persson 1973
31	Risveden	Svedhage 1985
32	Göteborg	Påsse 1983
33	Sandsjöbacka	Påsse 1987
34	Fjärås	Påsse 1986
35	Varberg	Påsse 1990b, Berglund 1995
36	Falkenberg	Påsse 1988
36	Bjäre Peninsula	Mörner 1980
37	Halmstad	Caldenius & Linman 1949, Caldenius et al. 1966, Berglund 1995.
38	Bjäre	Mörner 1980b
39	Barsebäck	Digerfeldt 1975, Persson 1962, Ringberg 1989
40	Blekinge	Björck 1979, Liljegren 1982
41	Oskarshamn	Svensson 1989
42	Gotland	Svensson 1989
43	Rejmyra	Persson 1979
44	Stockholm area	Åse 1970, Miller & Robertsson 1982, Brunnberg et al. 1985, Risberg 1991
45	Eskilstuna	Robertsson 1991
46	Gästrikland	Asklund 1935
47	Hälsingland	G. Lundqvist 1962

48	Ångermanland	Cato 1992
49	S. Västerbotten	Renberg & Segerström 1981
50	Rovaniemi	Saarnisto 1981
51	Lauhanwuori	Salomaa 1982, Salomaa & Matiskainen 1983
52	Satakunta	Eronen 1983
53	Olkiluoto	Eronen et al 1995
54	Åland	Glückert 1978
55	Turku	Glückert 1976, Salonen et al. 1984
56	Karjalohka	Glückert & Ristaniemi 1982
57	Tammisaari-Perniö	Eronen et al 1995
58	Lohja	Glückert & Ristaniemi 1982
59	Espo	Hyvärinen 1980, 1984, Glückert & Ristaniemi 1982, Eronen & Haila 1982
60	Porvoo	Eronen 1983
61	Hangassuo	Eronen 1976
62	Tallin	Kessel & Raukas 1979
63	Western Baltic	Winn et al 1986, Klug 1980

There are discernible regional characteristics between the shore level curves presented, which are due to different mechanisms involved but also due to different geographical conditions and different scientific traditions.

Norway wins the Nordic championship for producing shore level curves. The Norwegian curves are generally well dated and comprise extensive time spans. The area is affected by down-loading during the Younger Dryas. Especially at those sites which were deglaciated before the Younger Dryas this phenomenon can be better studied than at any other place. The Norwegian coast is affected by tidal changes. This is probably the main reason why small oscillations are not usually included in Norwegian shore level curves.

On the west and south coasts of Sweden the oscillation chronology has been studied more intensely than in other areas. In this area the tidal effect is negligible. Shore level information is derived from both threshold and shore deposits (*cf.* Påsse 1983).

Shore level information from Denmark is scarce which is partly due to the fact that past shore levels in most parts of Denmark have to be studied using offshore methods.

Shore level curves from the coasts around the Baltic are affected not only by the mechanisms already presented but also to the raised water levels during the Baltic Ice Lake and the Ancylus Lake. This means that only some parts of the curves can be compared directly with the marine shore levels. The shore levels during the lake stages have to be reduced for comparison with marine shore levels. However, these reductions are equivalent within the whole Baltic area and can therefore be calculated satisfactory. The shore level development in Finland and in central and northern Sweden is affected by the down-loading during the Younger Dryas. In this area it is difficult to estimate this effect partly due to the existence of the Baltic Ice Lake and the Ancylus Lake but also partly due to the late deglaciation of this area. The

shore level investigations in Finland are mainly focused on the Ancylus transgression

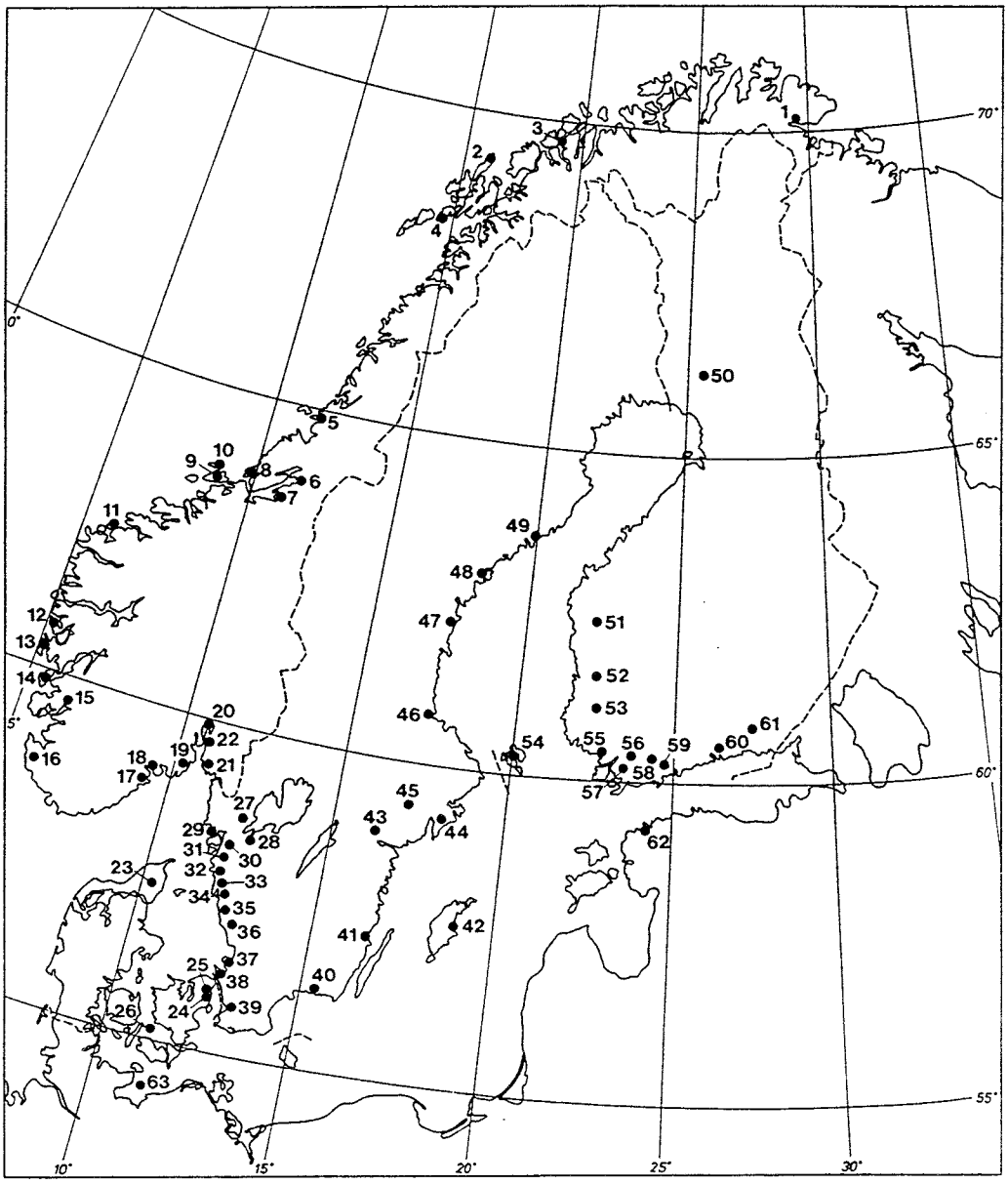

Figure 4-1. The position of the shore level curves used in the modelling. The numbers refer to Table 4-1, where the names of the sites and references are listed.

4.2 SHORE LEVEL CURVES

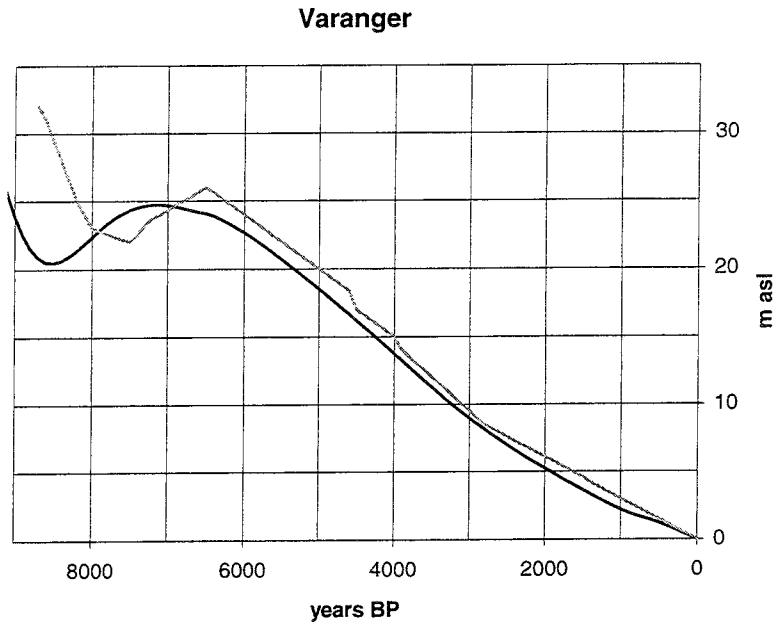

Figure 4-2. Site 1. Shore level displacement at the Varangerfjord according to Donner (1980), grey line. The calculated curve is black.

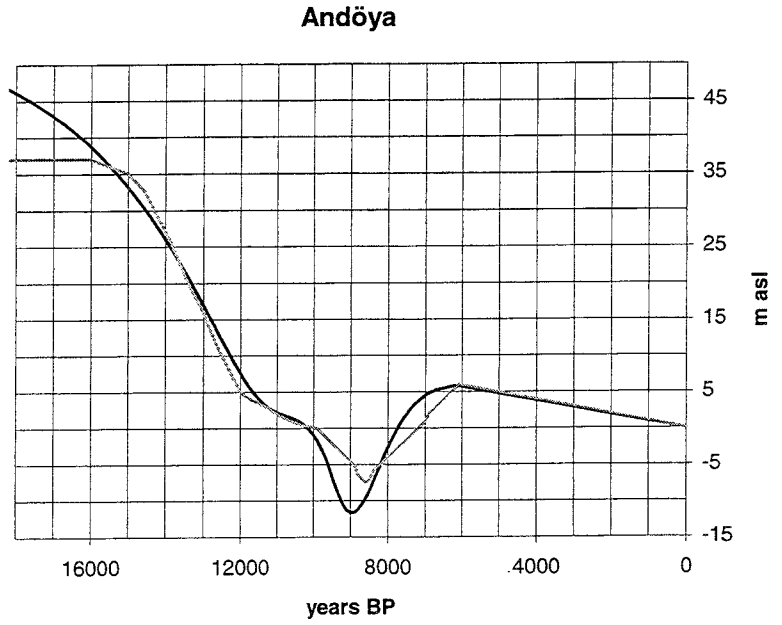

Figure 4-3. Site 2. Shore level displacement at Andöya according to Vorren et al. (1988). This area was unglaciated during the Late Weichselian and the original curve starts c. 18 000 years BP. The Holocene part of this curve is an interpolation of the curve shown at site 4. The calculated curve is somewhat to high between 18 000 - 16 000 years BP.

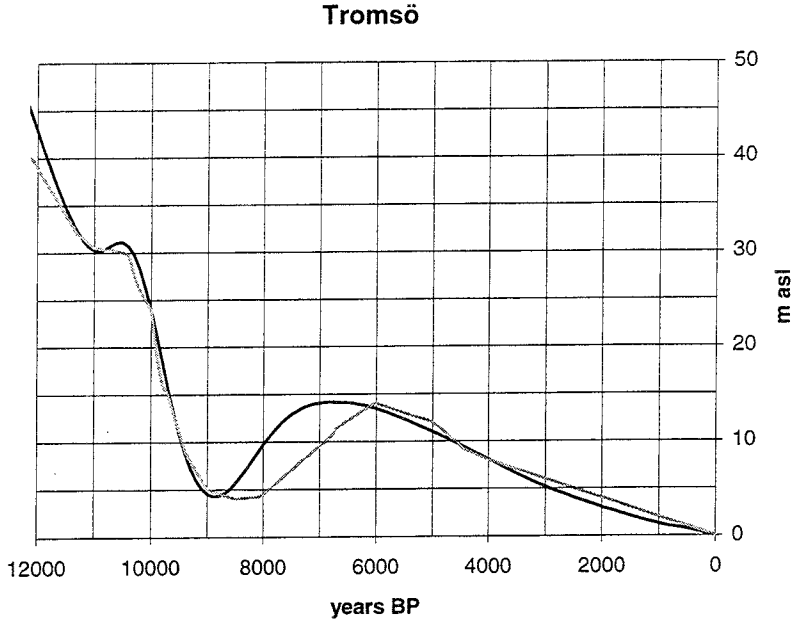

***Figure 4-4**. Site 3. Shore level displacement at Tromsö according to Hald & Vorren (1983). The shore level curve for Tromsö is based on modern data in the Late Weichselian- Preboreal part but relies on unmodern data for the Tapes transgression.*

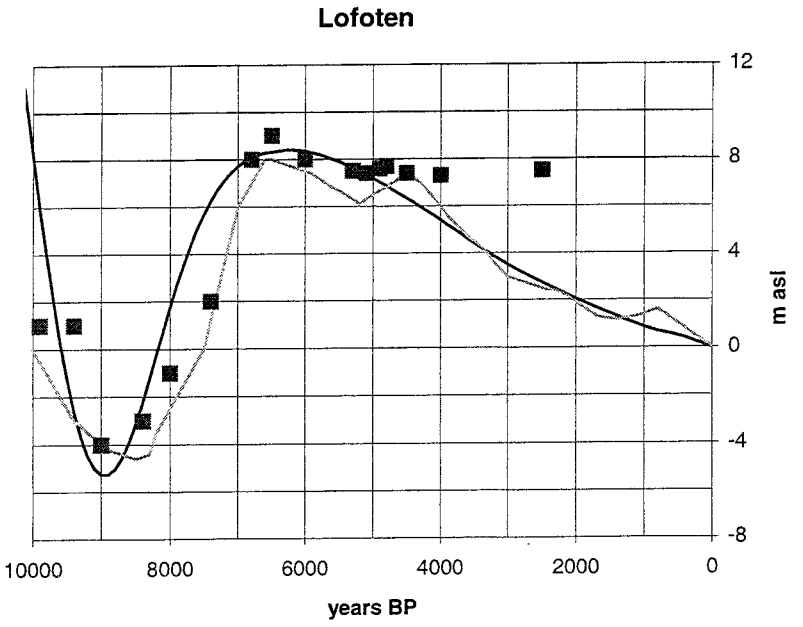

***Figure 4-5**. Site 4. Shore level displacement at Lofoten according to Möller (1984) and Vorren & Moe (1986). Möller (1984) has combined data from Lofoten and Vesterålen. Vorren & Moe (1986) have added some information concerning the period 10 000 - 7 000 years BP to the curve.*

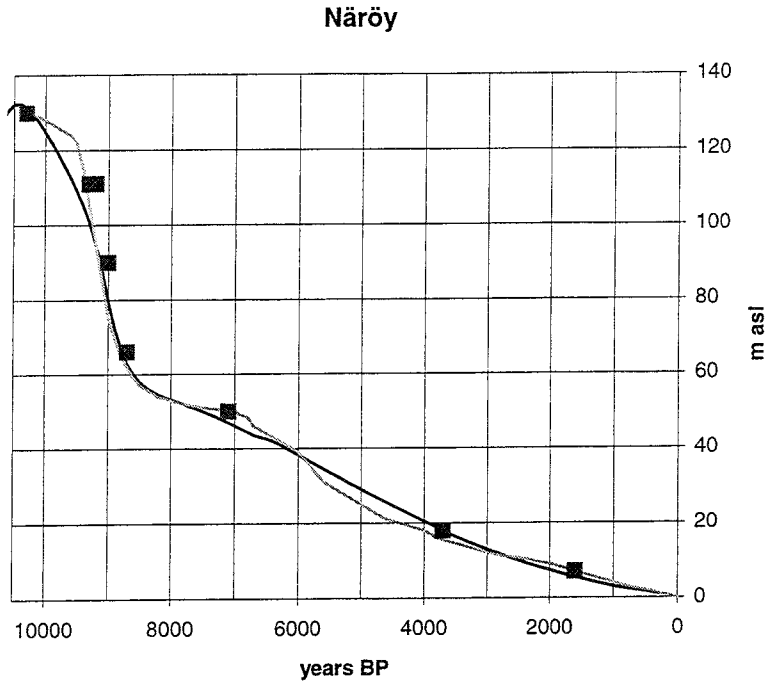

Figure 4-6. Site 5. Shore level displacement at Näröy according to Ramfjord (1982).

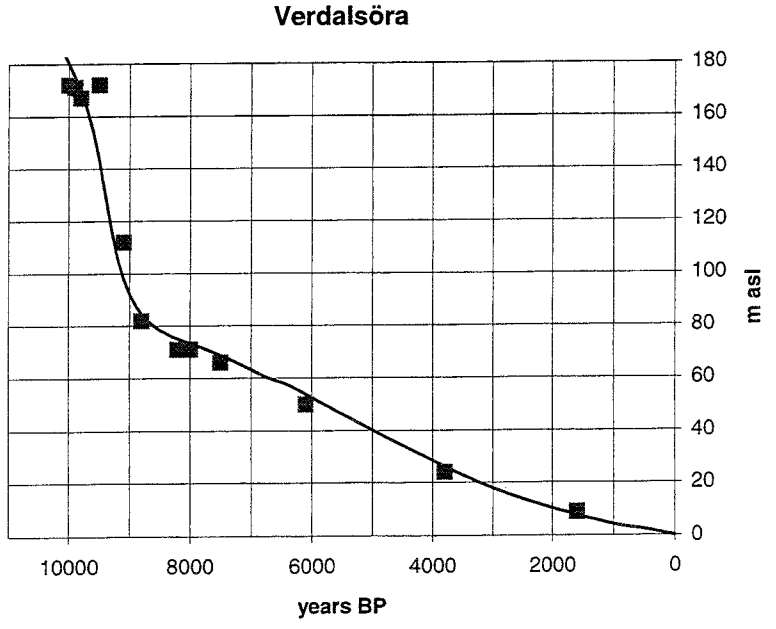

Figure 4-7. Site 6. Shore level displacement at Verdalsöra according to Sveian & Olsen (1984). The shore level displacement is illustrated just by squares as in the original paper.

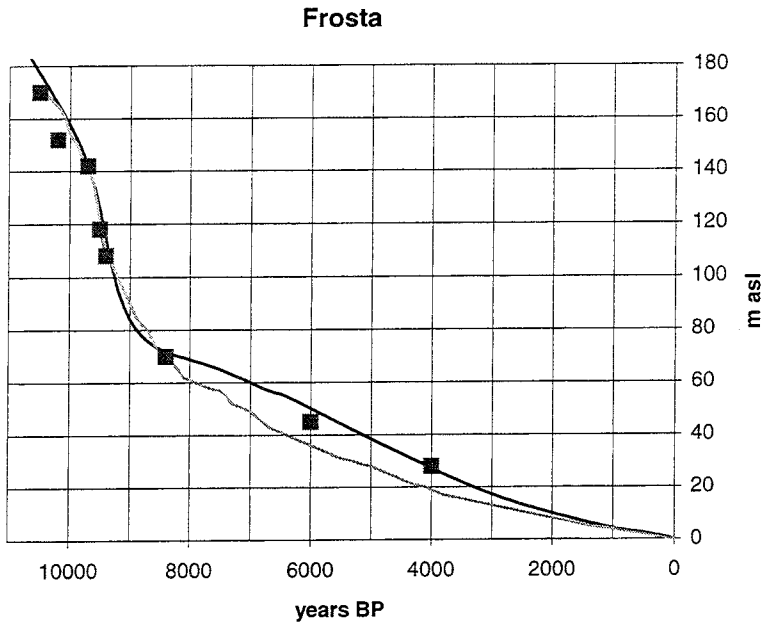

Figure 4-8. *Site 7. Shore level displacement at Frosta according to Kjemperud (1986). Kjemperud (1986) has used calendar corrections for dates younger than 8000 y BP in his original drawing of the curve. This is the reason why the data points and the calculated curve diverge from the original curve.*

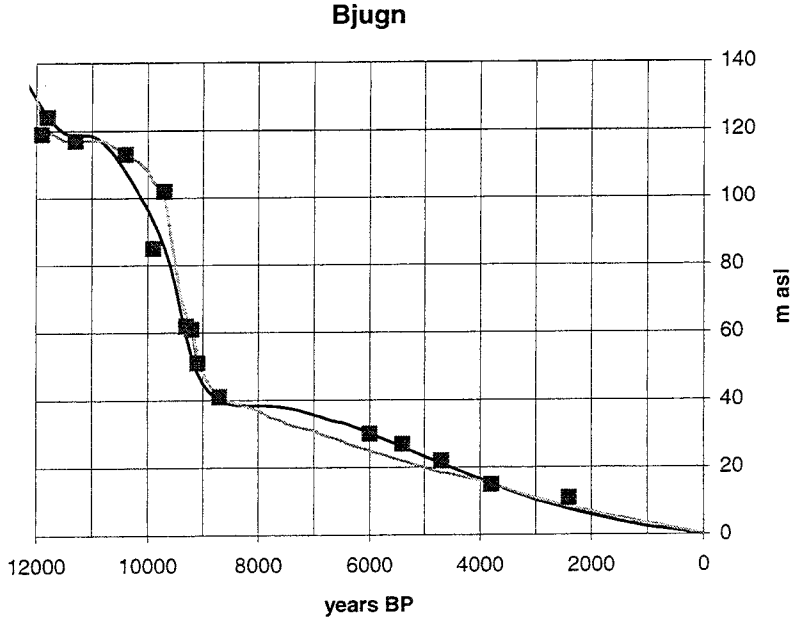

Figure 4-9. *Site 8. Shore level displacement at Bjugn according to Kjemperud (1986). The divergence between the curves during the Holocene is explained in Figure 4-8.*

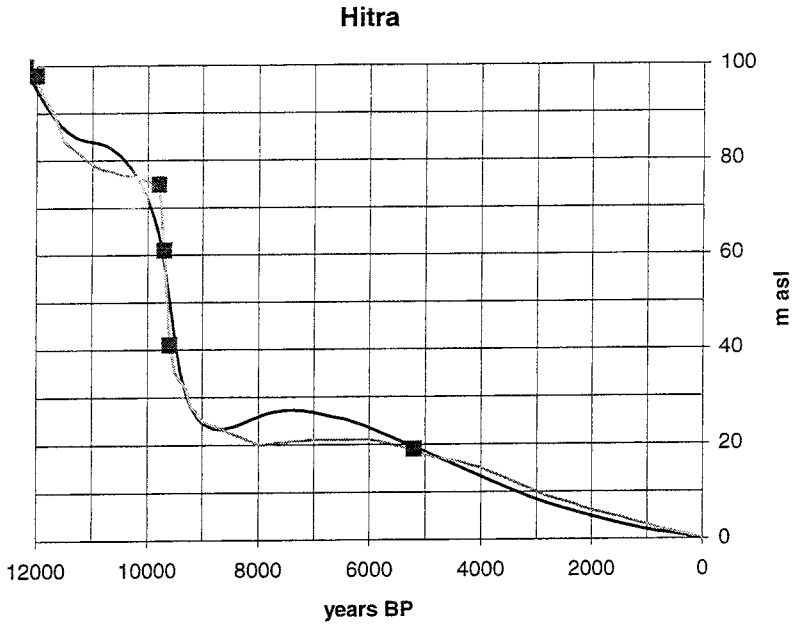

Figure 4-10. *Site 9. Shore level displacement at Hitra according to Kjemperud (1986).*

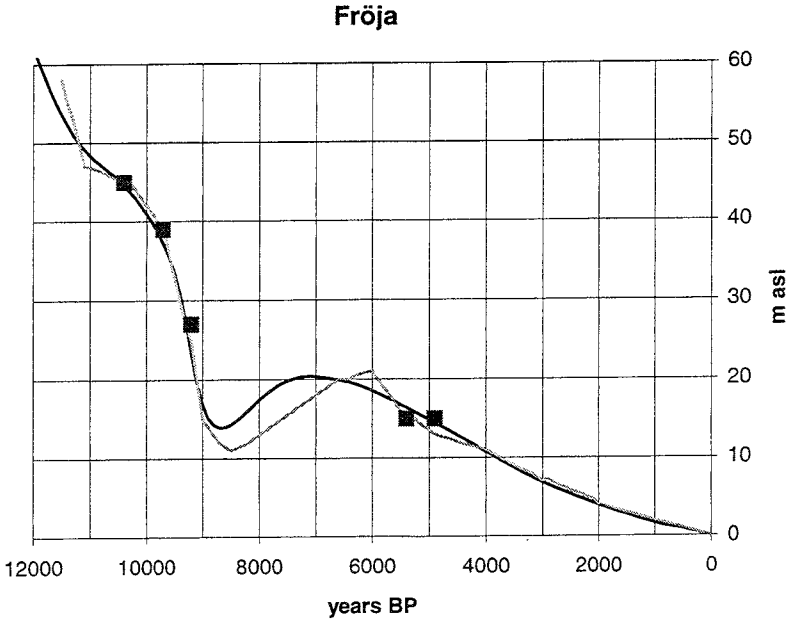

Figure 4-11. *Site 10. Shore level displacement at Fröja according to Kjemperud (1986).*

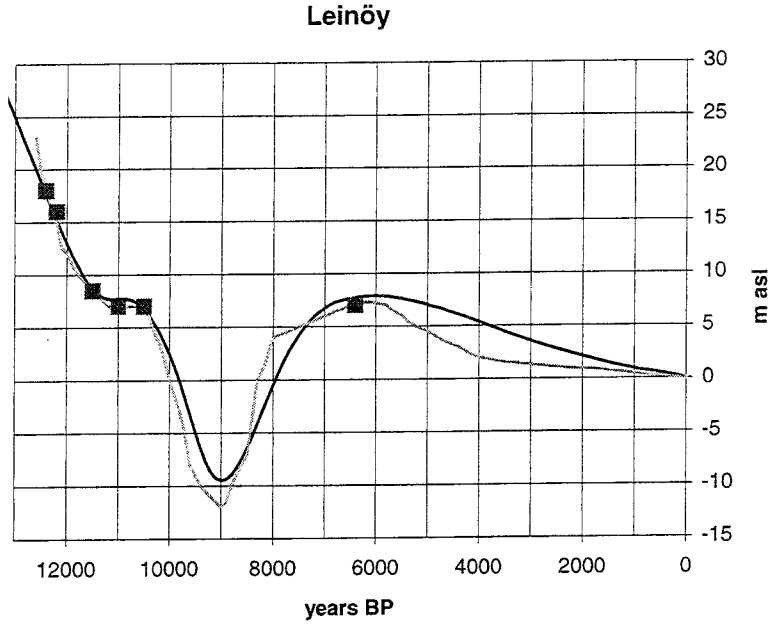

Figure 4-12. *Site 11. Shore level displacement at Leinöy according to Svendsen & Mangerud (1990).*

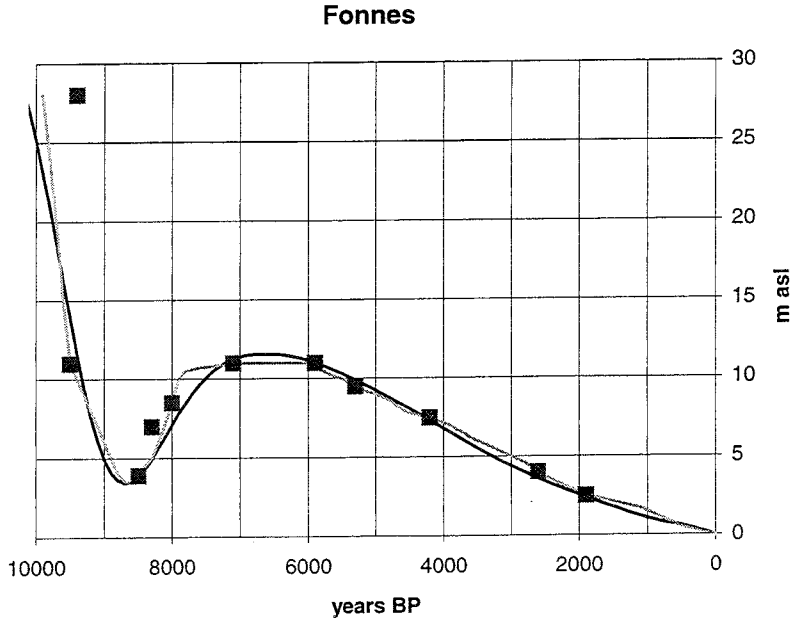

Figure 4-13. *Site 12. Shore level displacement at Fonnes according to Kaland (1984).*

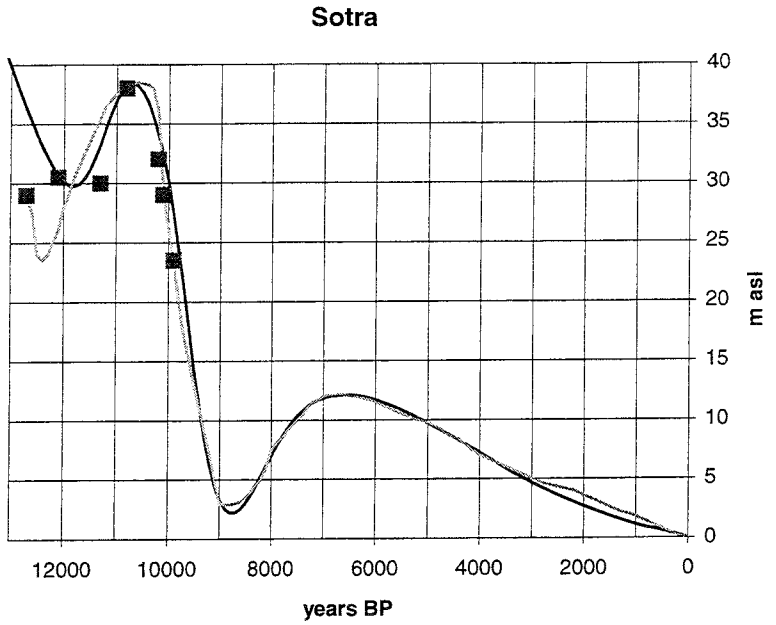

Figure 4-14. *Site 13. Shore level displacement at Sotra according to Krzywinski & Stabell (1984) and Kaland et al. (1984).*

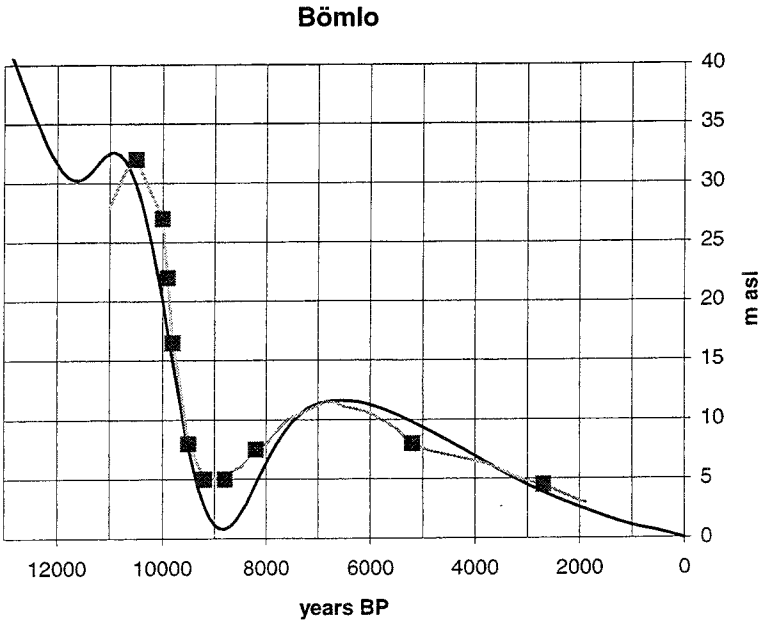

Figure 4-15. *Site 14. Shore level displacement at Bömlo according to Kaland (1984).*

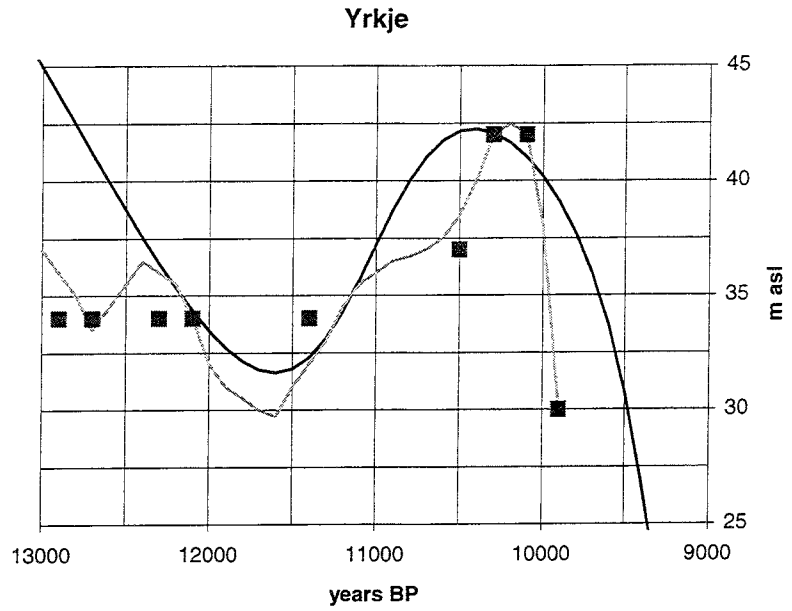

Figure 4-16. *Site 15. Shore level displacement at Yrkje according to Anundsen (1985).*

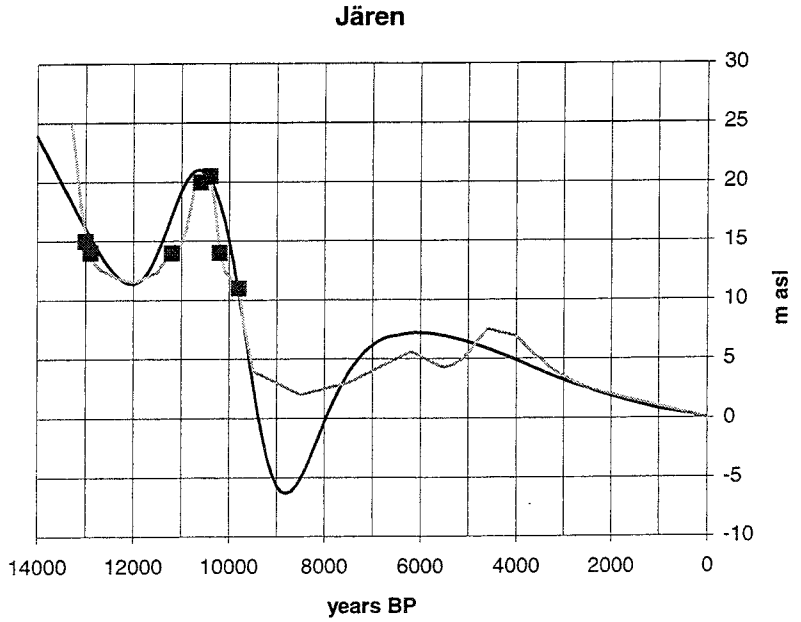

Figure 4-17. *Site 16. Shore level displacement at Jären according to Thomsen (1982) and Bird & Klemsdal (1986).*

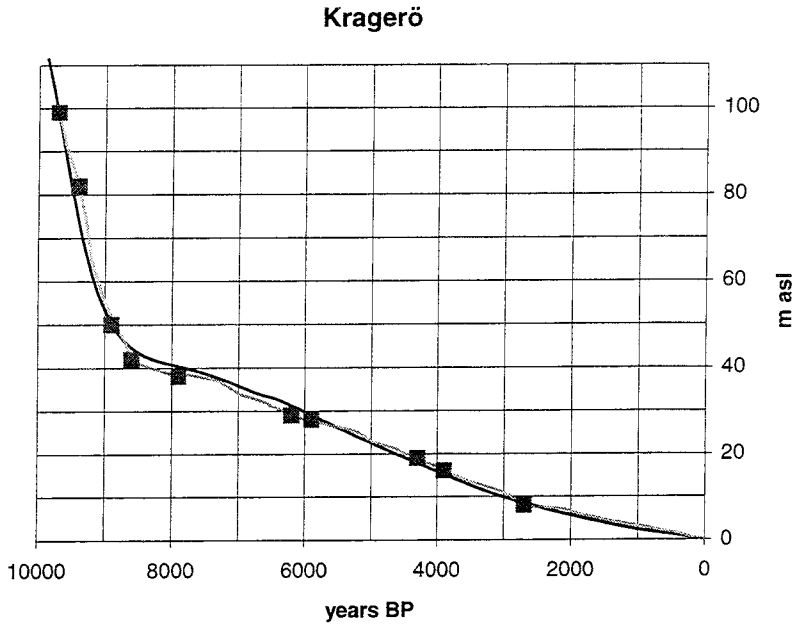

***Figure 4-18**. Site 17. Shore level displacement at Kragerö according to Stabell (1980).*

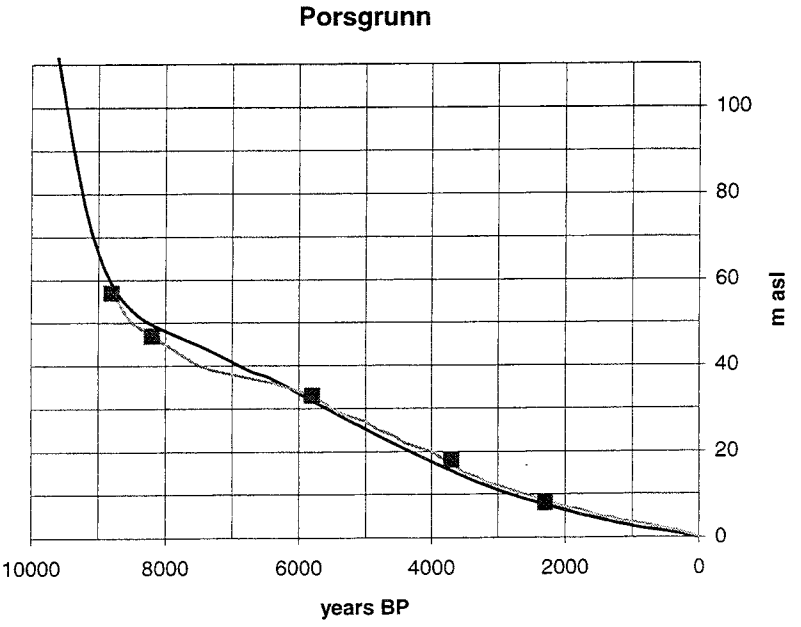

***Figure 4-19**. Site 18. Shore level displacement at Porsgrunn according to Stabell (1980).*

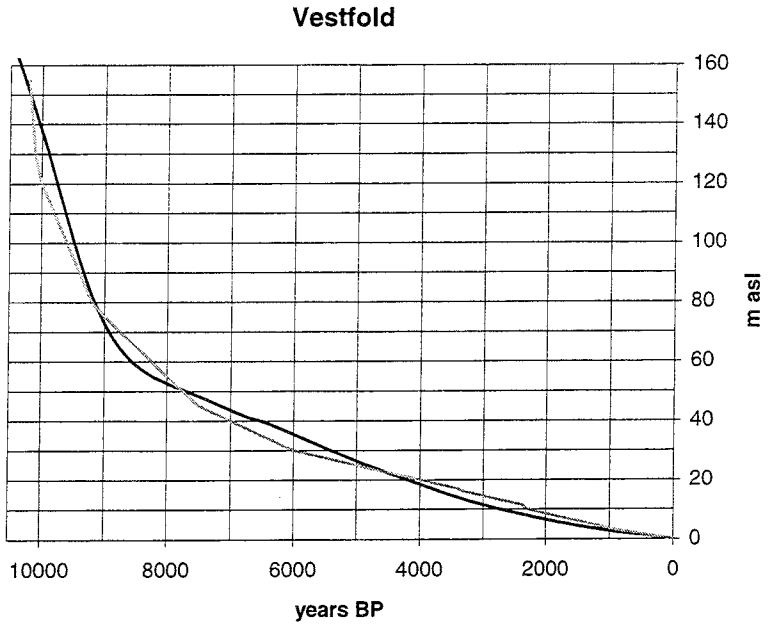

Figure 4-20. *Site 19. Shore level displacement at Vestfold according to Henningsmoen (1979).*

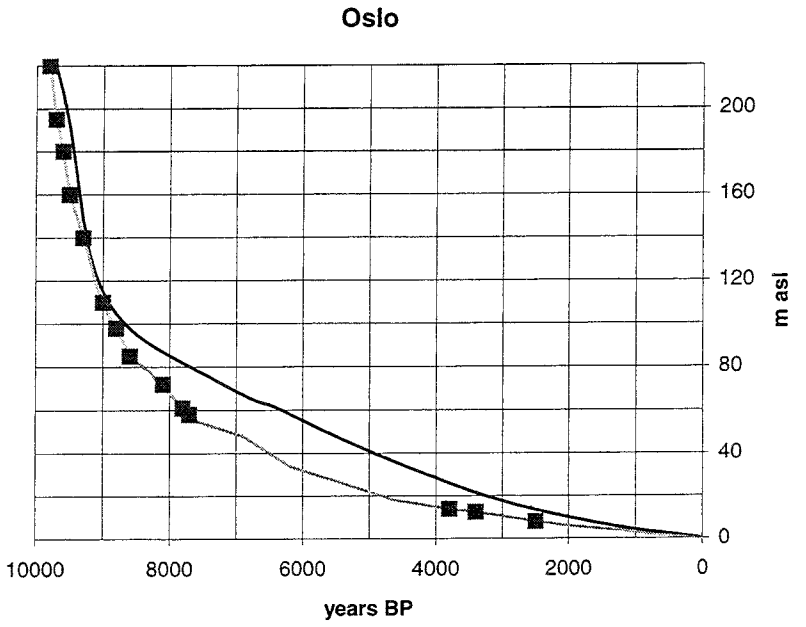

Figure 4-21. *Site 20. Shore level displacement at Oslo according to Hafsten (1983). This curve is dated by pollen-analysis. The correspondence between the curves below 80 m above sea level is not satisfactory. However, when compared to the well dated curve at Ski (Sörensen 1979), site 22, the calculated curve seems to be the most likely one.*

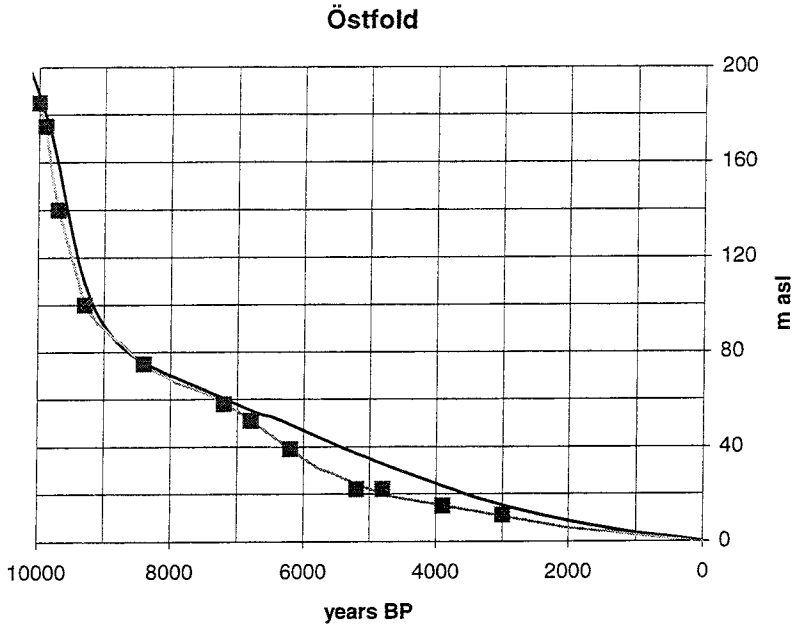

Figure 4-22. *Site 21. Shore level displacement at Östfold according to Danielsen (1970). This curve is dated by pollen-analysis. The investigated basins are from too vast an area. The descrepancy between the curves for the period < 6 000 years BP is most probably explained by the fact that the data for this period is from an area much further to the south.*

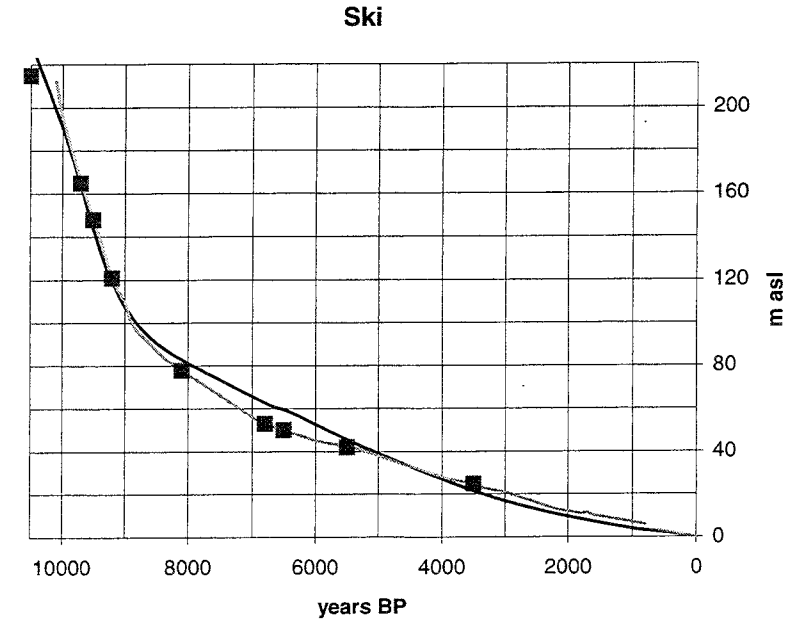

Figure 4-23. *Site 22. Shore level displacement at Ski according to Sörensen (1979).*

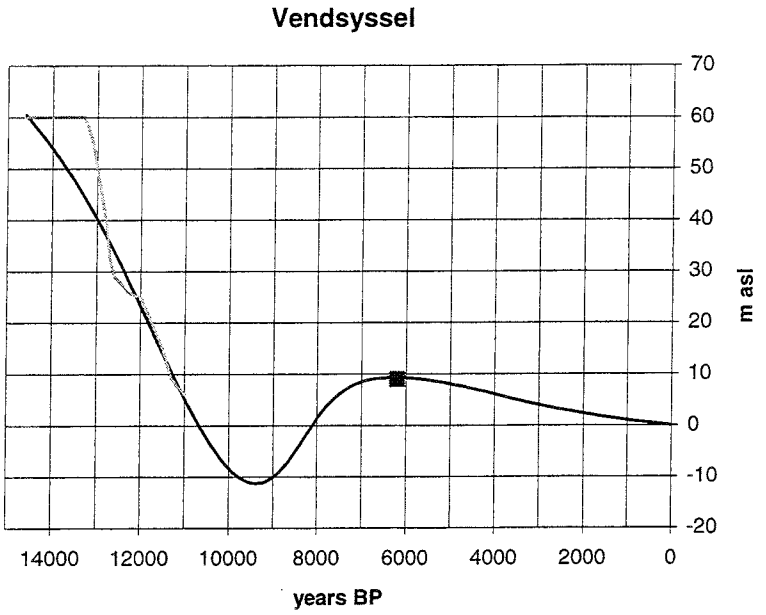

Figure 4-24. *Site 23. Shore level displacement during the Late Weichselian at Vendsyssel according to Richardt (1996). The postglacial transgression maximum, shown with a square, is according to Madsen et al. (1928).*

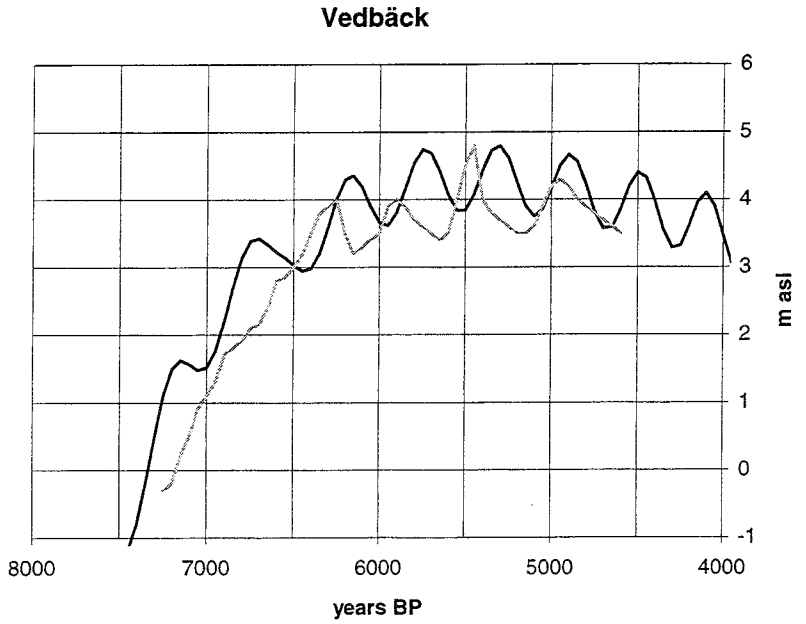

Figure 4-25. *Site 24. Shore-line displacement curve from Vedbäck (Christensen 1993). The oscillation formula is included in the calculations. The shore-line curve is based on numerous radiocarbon dates from archaeological sites.*

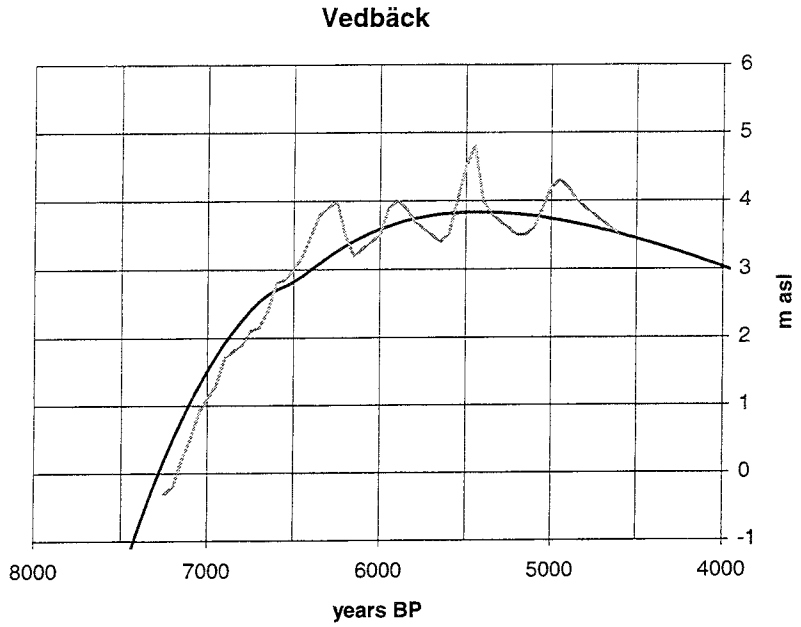

Figure 4-26. *Site 24. The same shore-line displacement curve from Vedbäck (Christensen 1993) as shown in Figure 4-25 but the oscillation formula is excluded in this graph.*

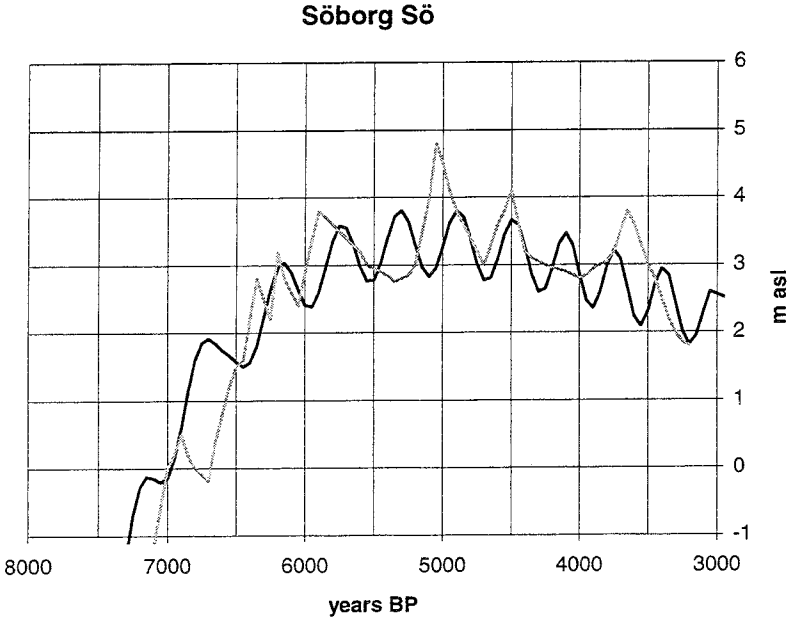

Figure 4-27. *Site 25. Shore level displacement at Söborg Sö according to Mörner (1976). The oscillation formula is included in the calculations.*

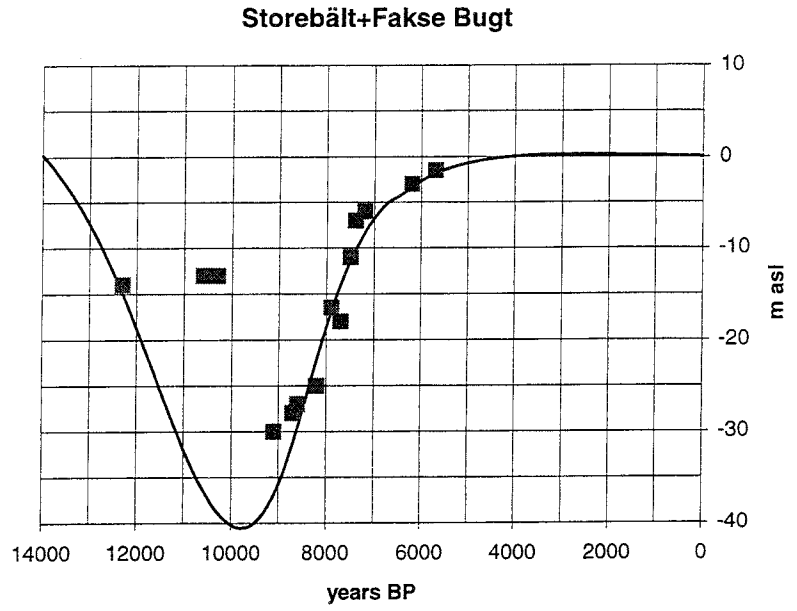

Figure 4-28. *Site 26. Shore level displacement at Storebält (Christensen 1993) combined with Late Weichselian data from Fakse Bugt (Bennike & Jensen 1995). The squares, which are situated above the calculated curve before 8 000 BP, represent data from the Baltic Ice Lake and the Ancylus Lake.*

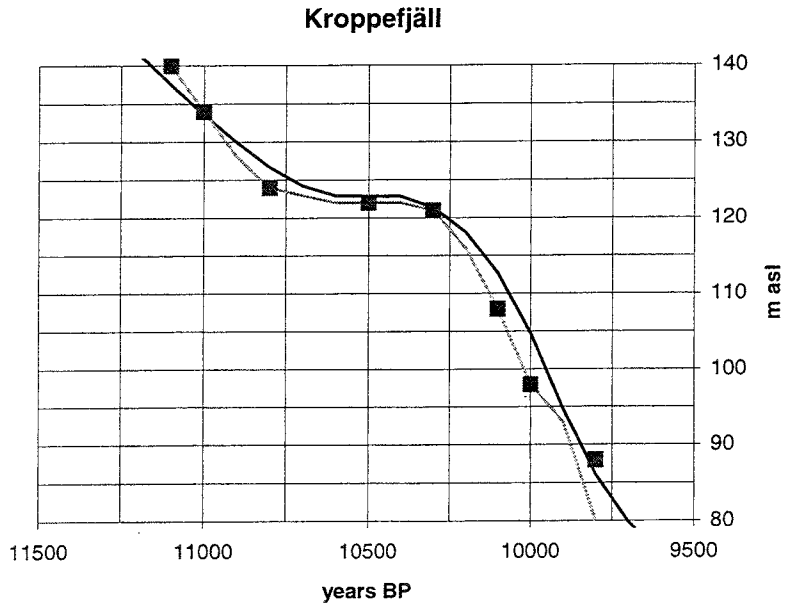

Figure 4-29. *Site 27. Shore level displacement at Kroppefjäll according to Björck & Digerfeldt (1991).*

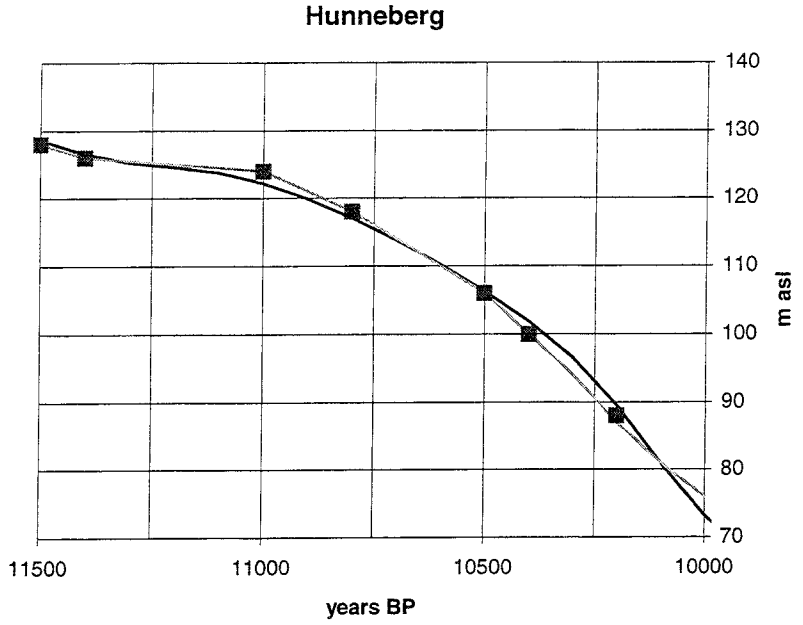

Figure 4-30. *Site 28. Shore level displacement at Hunneberg according to Björck & Digerfeldt (1982).*

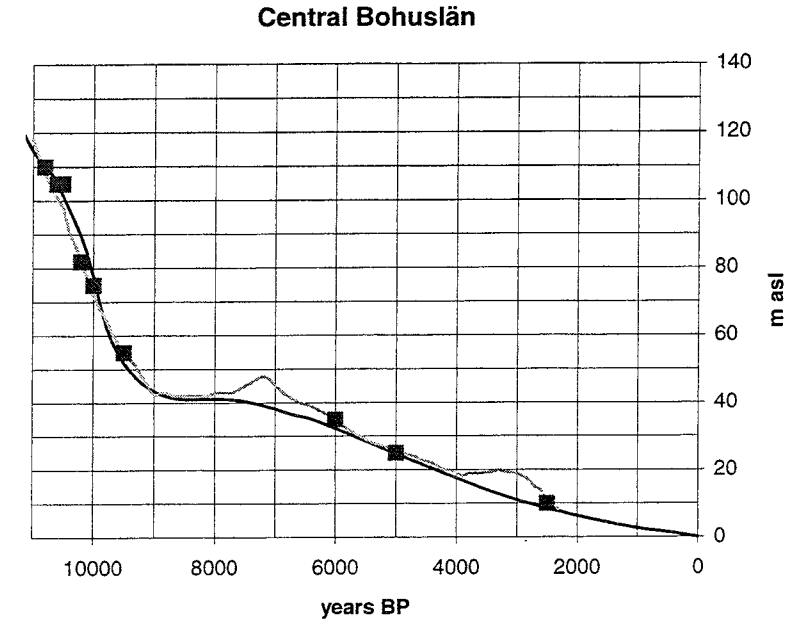

Figure 4-31. *Site 29. Shore level displacement from the central part of Bohuslän county according to Miller & Robertsson (1988).*

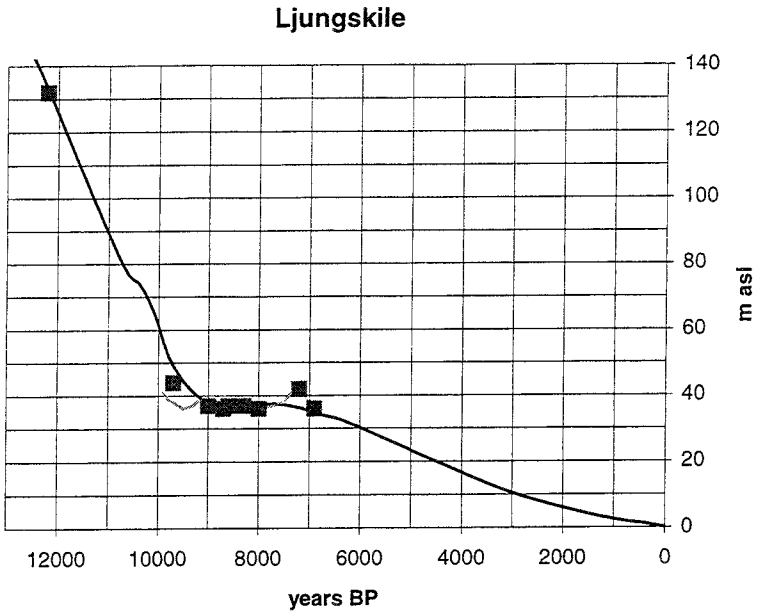

Figure 4-32. *Site 30. Shore level displacement at Ljungskile according to Persson (1973). A value for the highest coastline is inserted in the figure.*

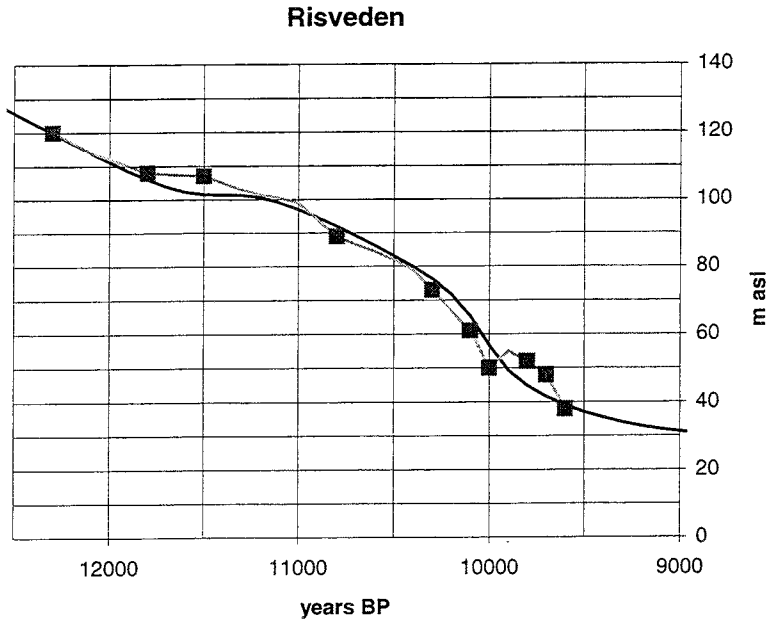

Figure 4-33. *Site 31. Shore level displacement at Risveden according to Svedhage (1985).*

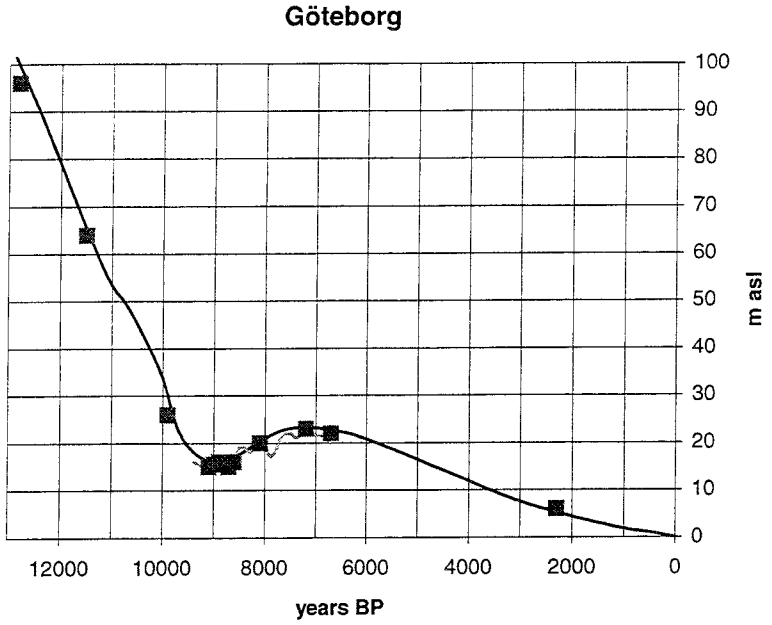

***Figure 4-34**. Site 32. Shore level displacement at Göteborg according to Påsse (1983).*

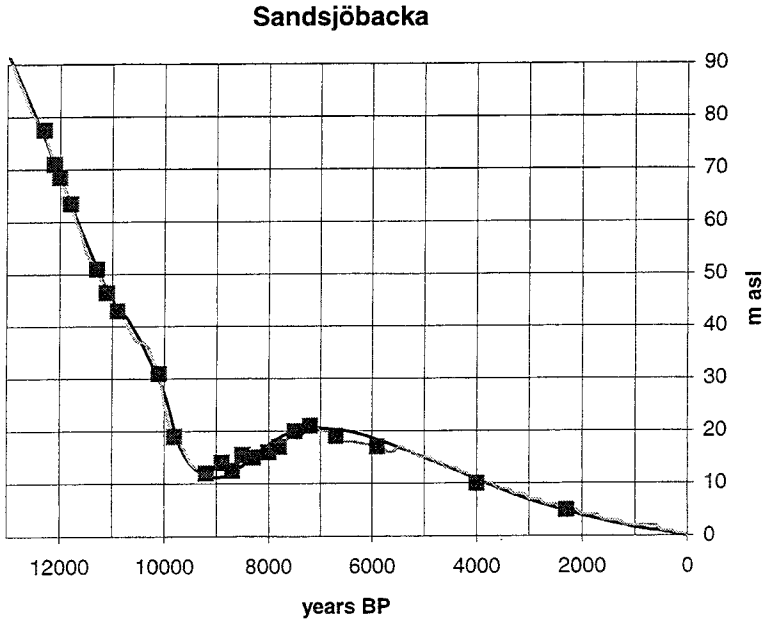

***Figure 4-35**. Site 33. Shore level displacement at Sandsjöbacka according to Påsse (1983, 1987).*

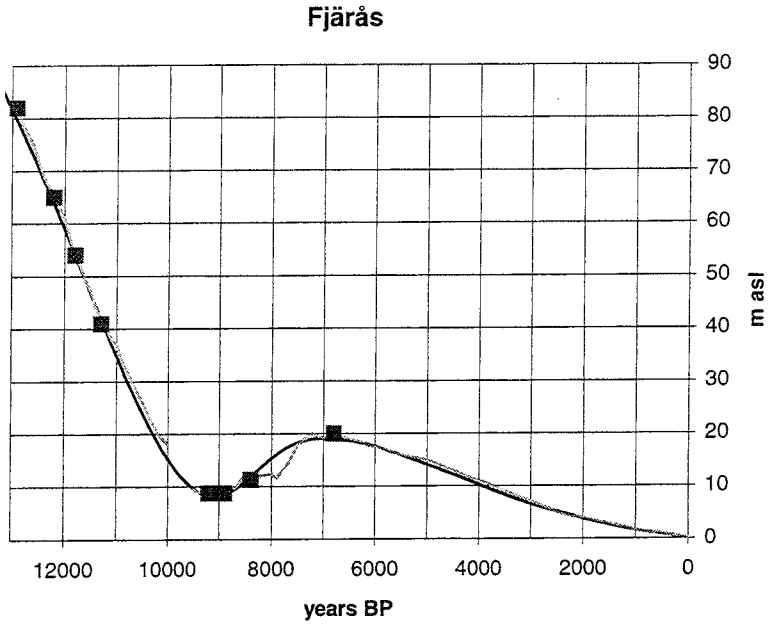

Figure 4-36. *Site 34. Shore level displacement at Fjärås according to Påsse (1986).*

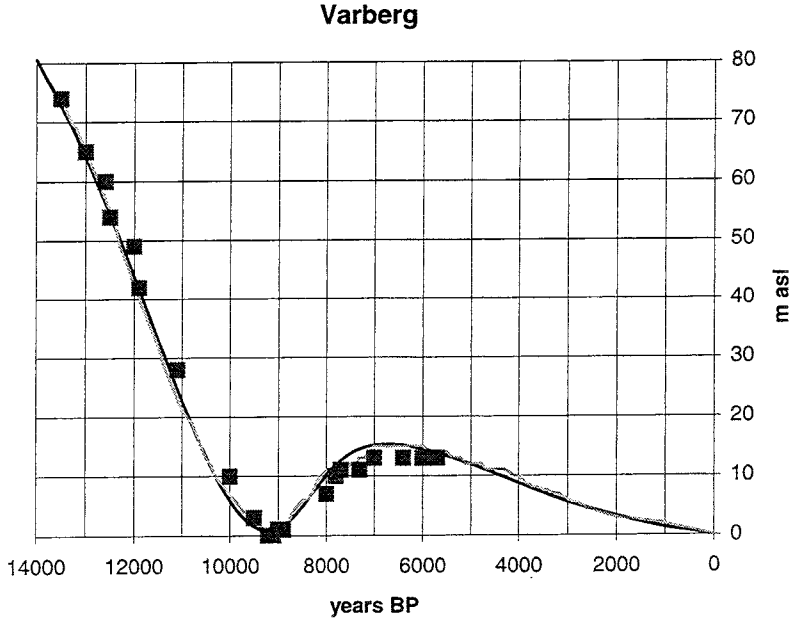

Figure 4-37. *Site 35. Shore level displacement at Varberg according to Påsse (1990b). The data designated with squares in the Late Weichselian part is from Berglund (1995).*

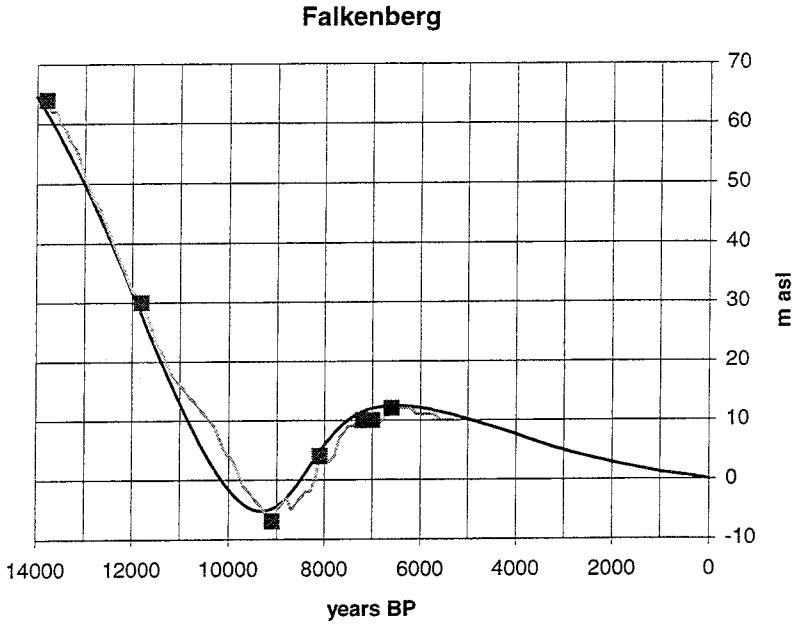

***Figure 4-38**. Site 36. Shore level displacement at Falkenberg according to Påsse (1988).*

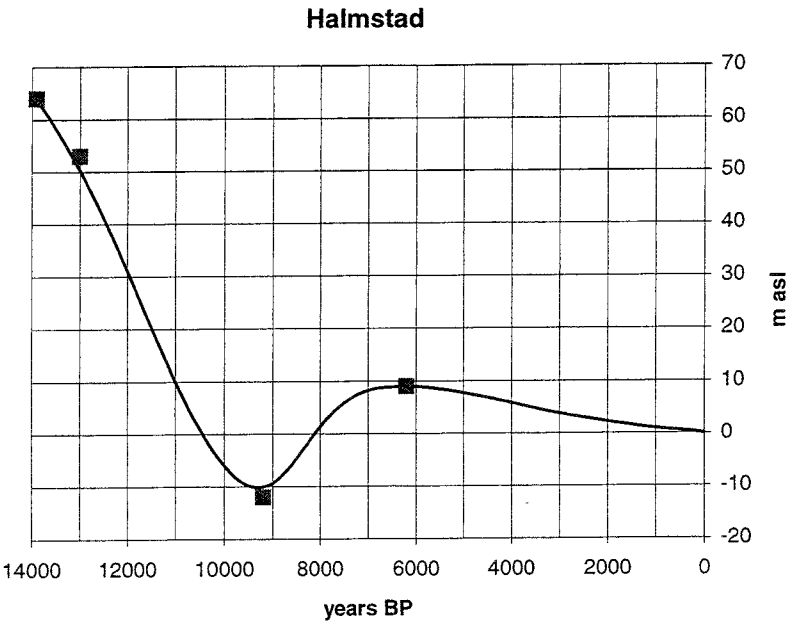

***Figure 4-39**. Site 37. Shore level displacement at Halmstad according to data from Caldenius & Linman (1949), Caldenius et al. (1966) and Berglund (1995).*

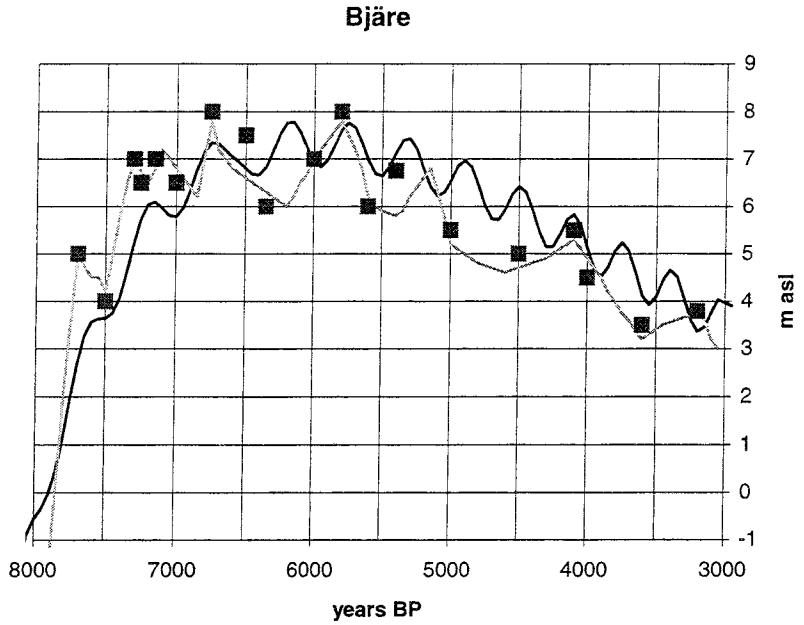

***Figure 4-40**. Site 38. Shore level displacement at Bjäre according to Mörner (1980b). The oscillation formula is used in the calculation.*

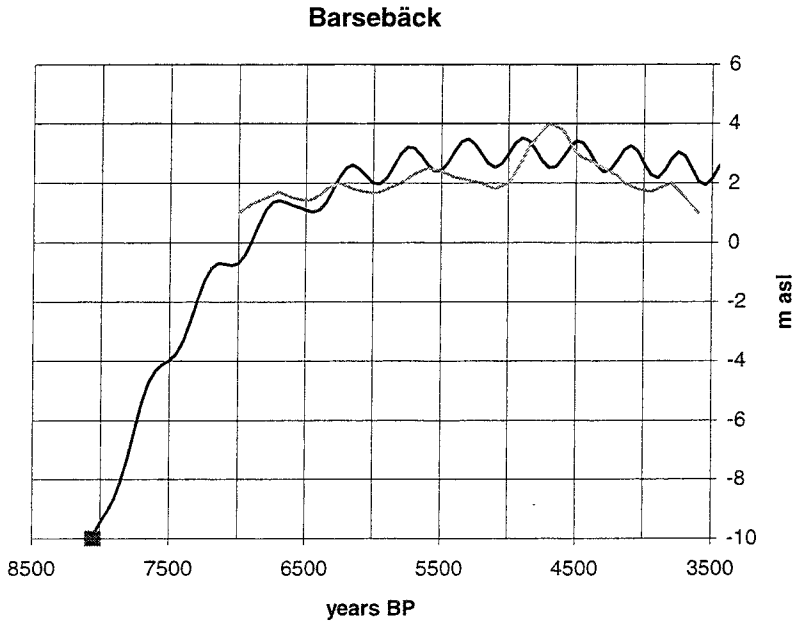

***Figure 4-41**. Site 39. Shore level displacement at Barsebäck according to Digerfeld (1975), complemented with an obsevation from Persson (1962). The oscillation formula is used in the calculation.*

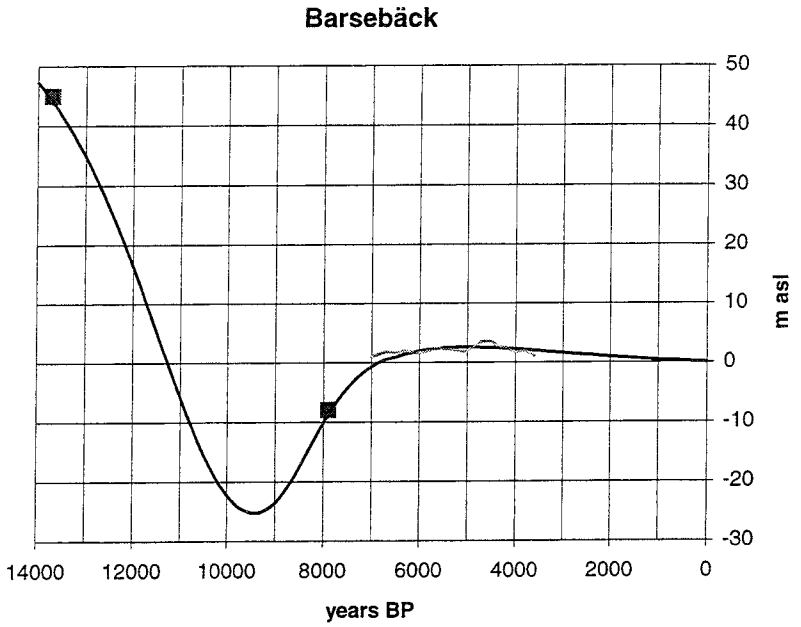

***Figure 4-42**. Site 39. Shore level displacement according to the same data used in figure 4-41 but complemented with the level of the highest coastline according to Ringberg (1989). The oscillation formula is not used in this calculation.*

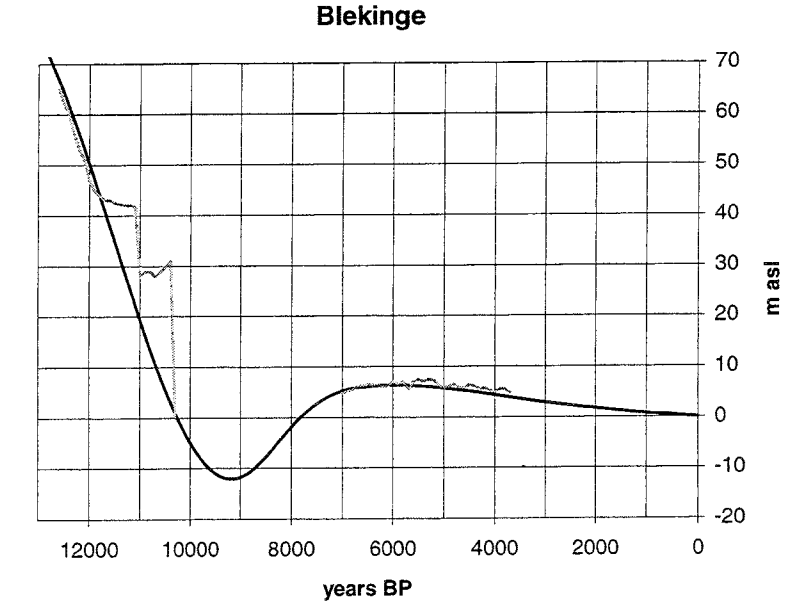

***Figure 4-43**. Site 40. Shore level displacement at Blekinge according to Björck (1979) and Liljegren (1982). The calculations indicate that the Baltic Ice Lake started to exist at c. 12 000 years BP.*

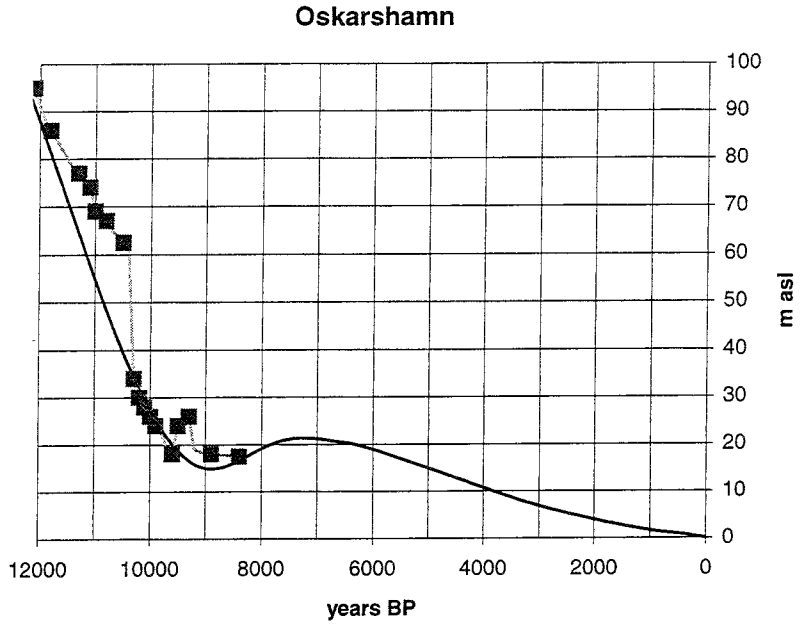

Figure 4-44. *Site 41. Shore level displacement at Oskarshamn according to Svensson (1989). The calculations indicate that the Baltic Ice Lake started to exist at c. 12 000 years BP. The data points that fall above the calculated curve represent the lake stages in the Baltic basin.*

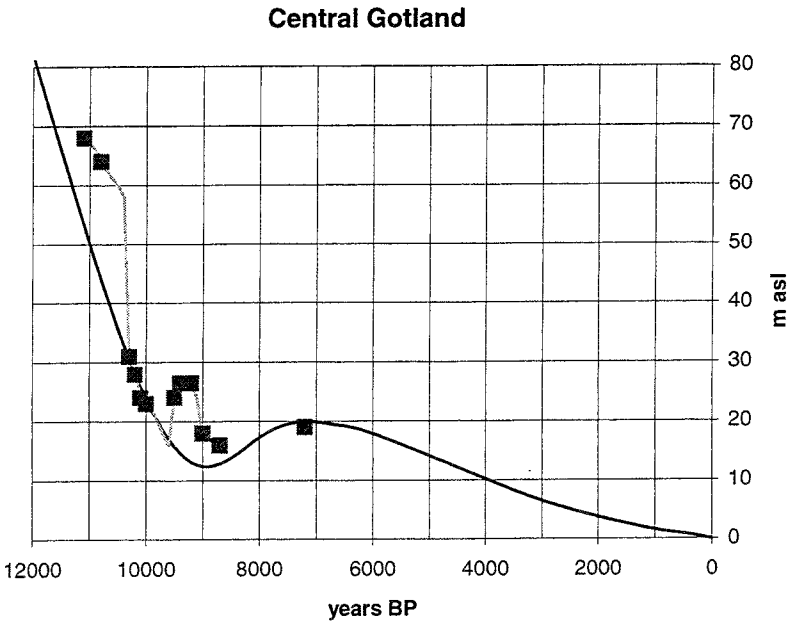

Figure 4-45. *Site 42. Shore level displacement at central Gotland according to Svensson (1989). The data points that fall above the calculated curve represent the lake stages in the Baltic basin.*

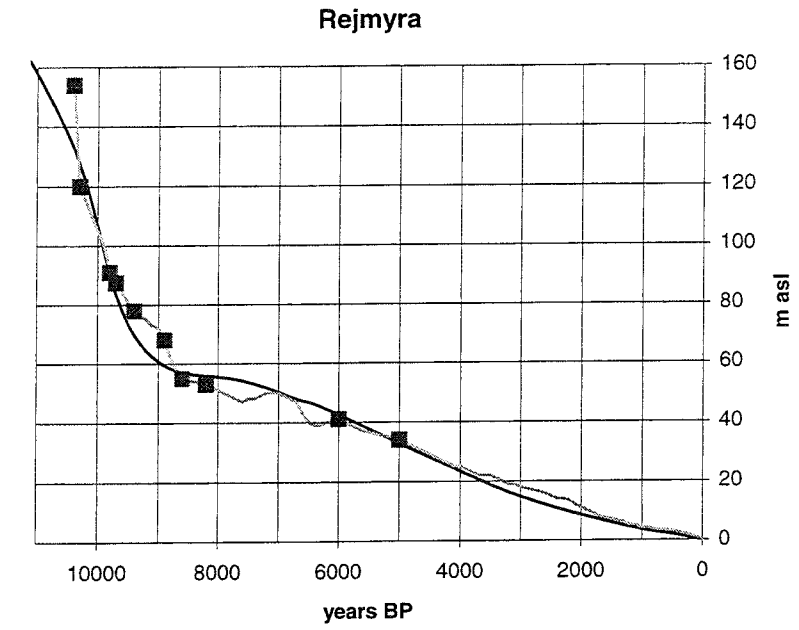

***Figure 4-46**. Site 43. Shore level displacement at Rejmyra according to Persson (1979). The data points that fall above the calculated curve represent the lake stages in the Baltic basin.*

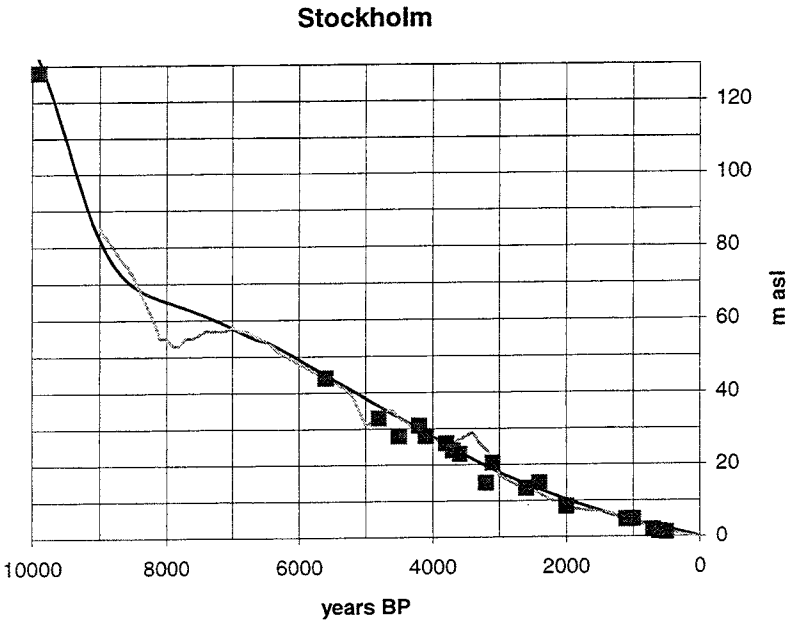

***Figure 4-47**. Site 44. Shore level displacement at Stockholm according to Åse (1970), Miller & Robertsson (1982), Brunnberg et al. (1985) and Risberg (1991).*

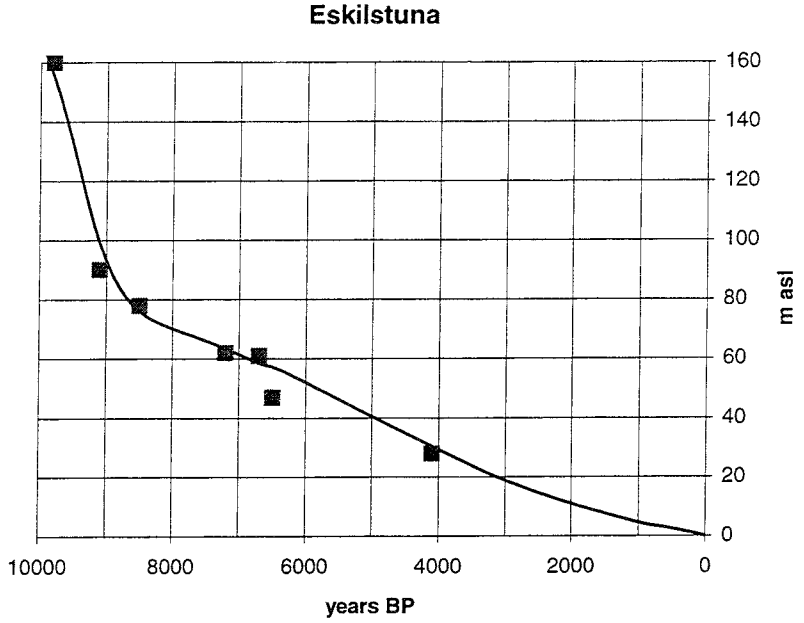

Figure 4-48. *Site 45. Shore level data from Eskilstuna according to Robertsson (1991).*

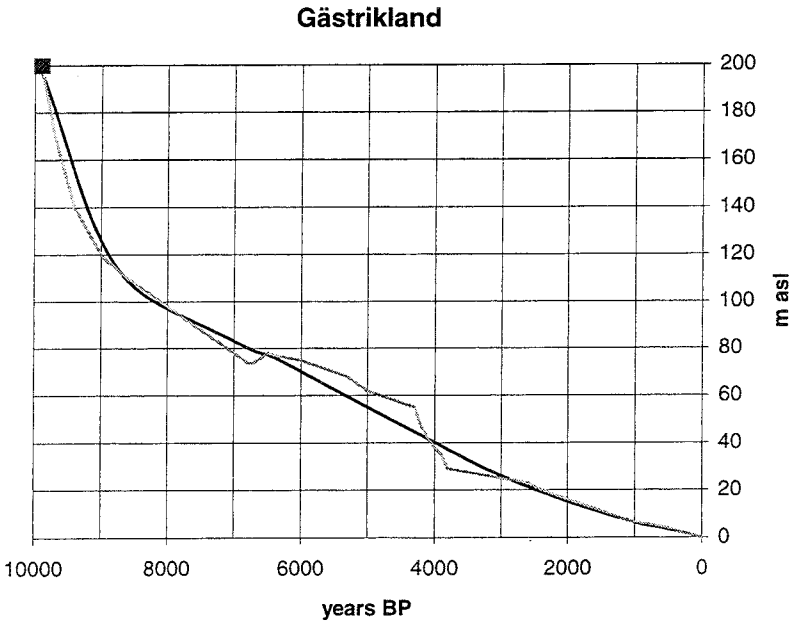

Figure 4-49. *Site 46. Shore level displacement from the central part of the county of Gästrikland according to Asklund (1935). The curve is based on obselete pollen analytical datings. The curve is redrawn in the oldest part.*

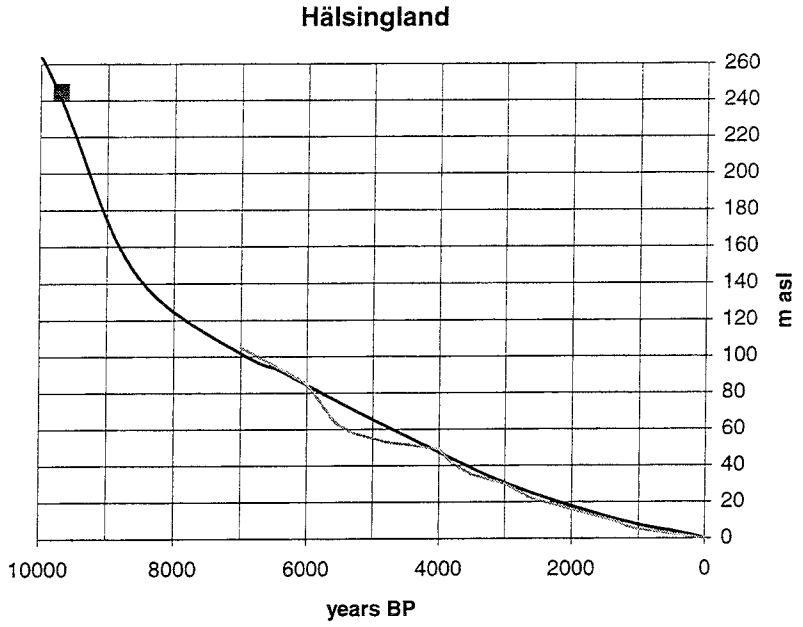

Figure 4-50. *Site 47. Shore level displacement from the northern part of the county of Hälsingland according to G. Lundqvist (1962). The curve is redrawn and simplified.*

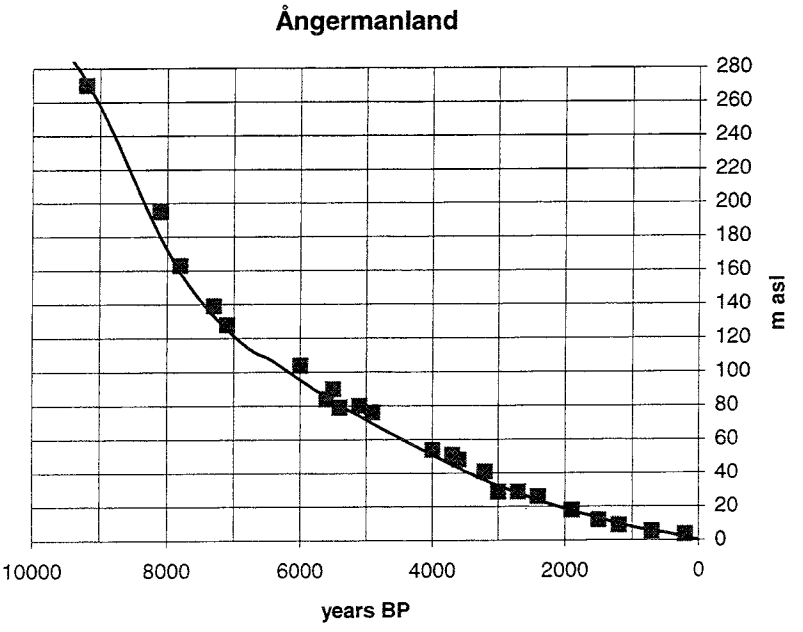

Figure 4-51. *Site 48. Shore level displacement from the county of Ångermanland according to Cato (1992). The shore level data are based on varve datings.*

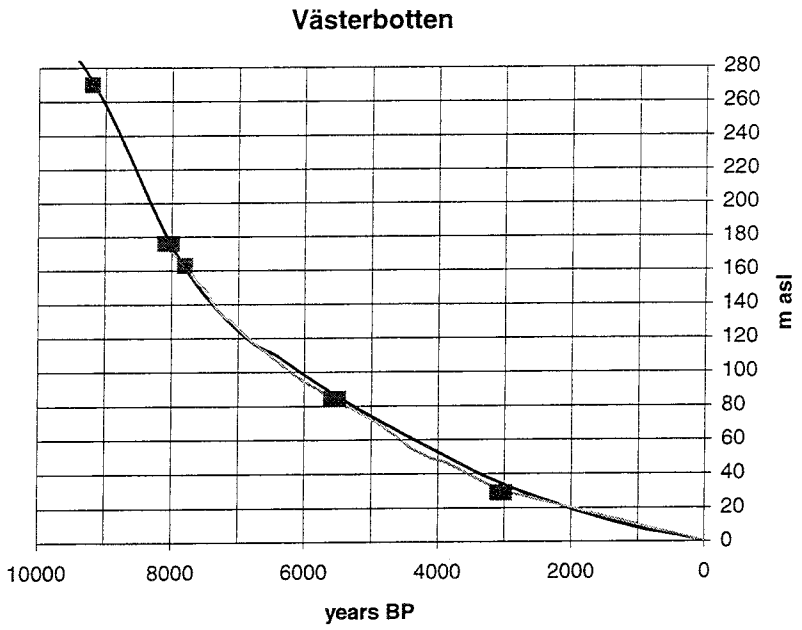

Figure 4-52. *Site 49. Shore level displacement from the southern part of the county of Västerbotten according to Renberg & Segerström (1981). The curve is dated by varve-counts on lake sediments.*

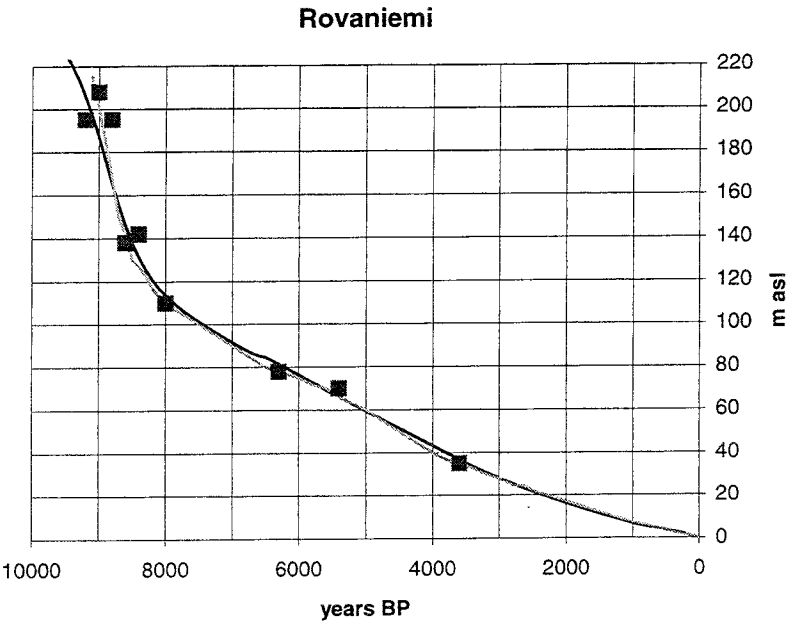

Figure 4-53. *Site 50. Shore level displacement at Rovaniemi according to Saarnisto (1981).*

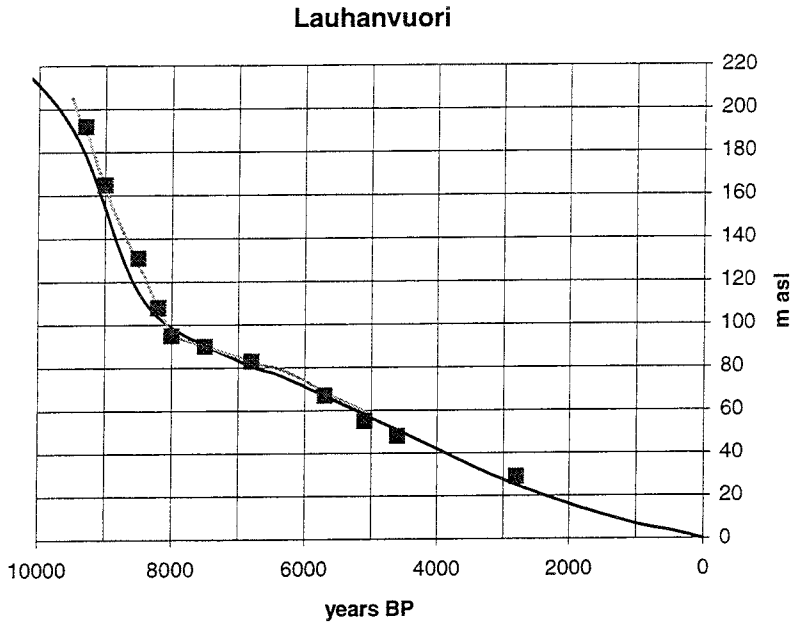

***Figure 4-54**. Site 51. Shore level displacement at Lauhanvuori according to Salomaa (1982) complemented with data from Salomaa & Matiskainen (1983).*

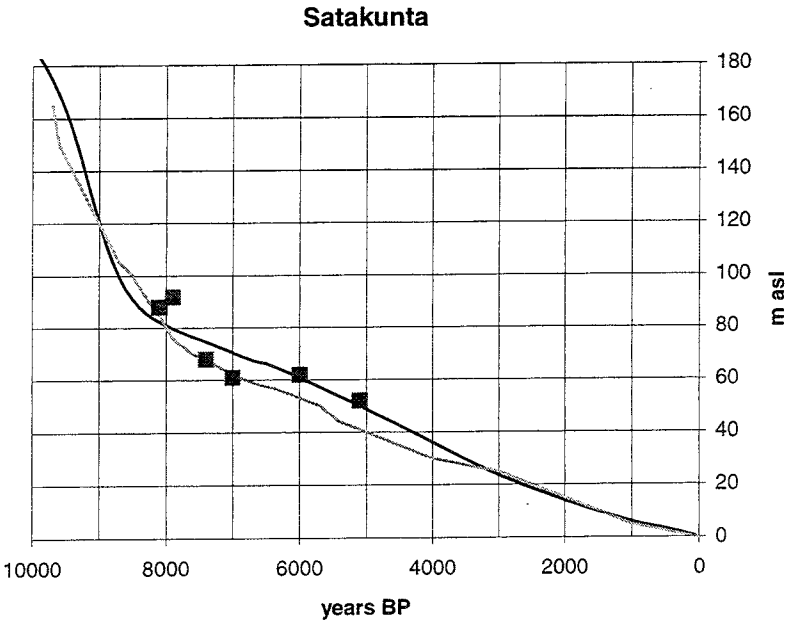

***Figure 4-55**. Site 52. Shore level displacement at Satakunta according to Eronen (1983).*

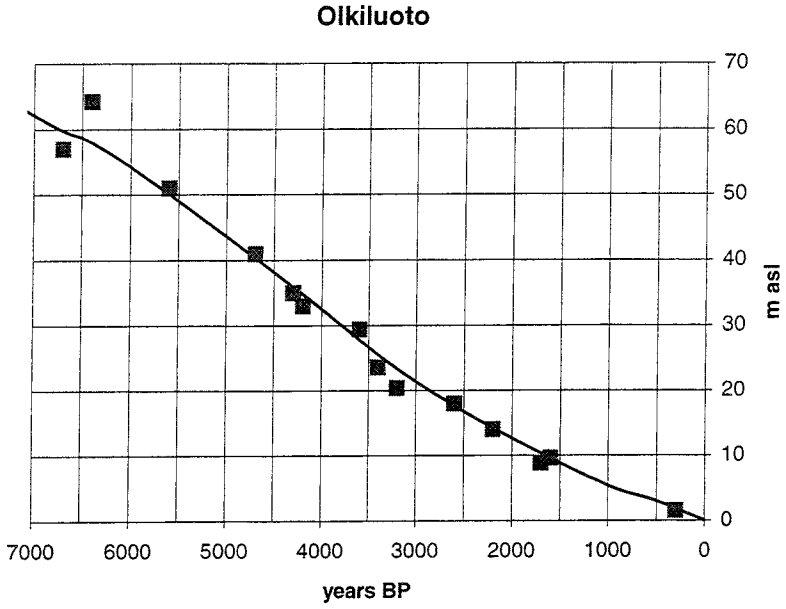

Figure 4-56. *Site 53. Shore level displacement at the Olkiluoto- Pyhäjärvi area according to Eronen et al. (1995).*

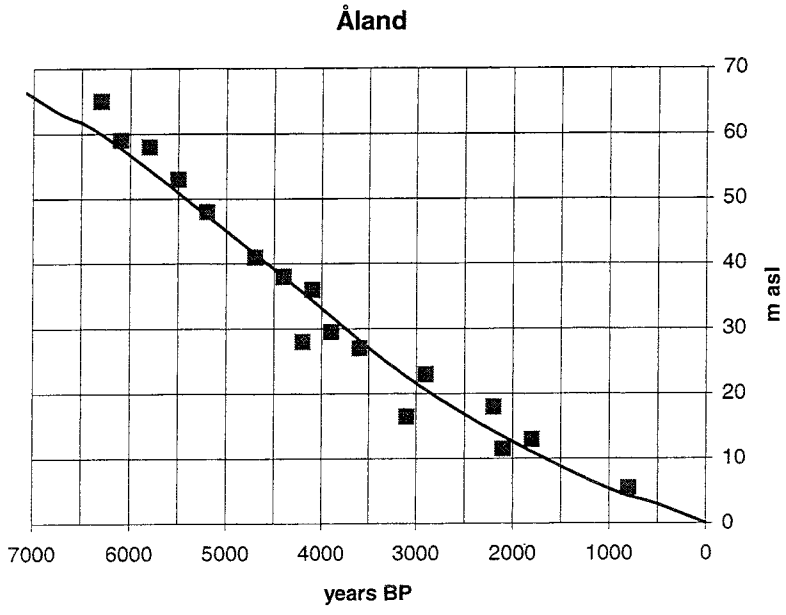

Figure 4-57. *Site 54. Shore level data from Åland according to Glückert (1978).*

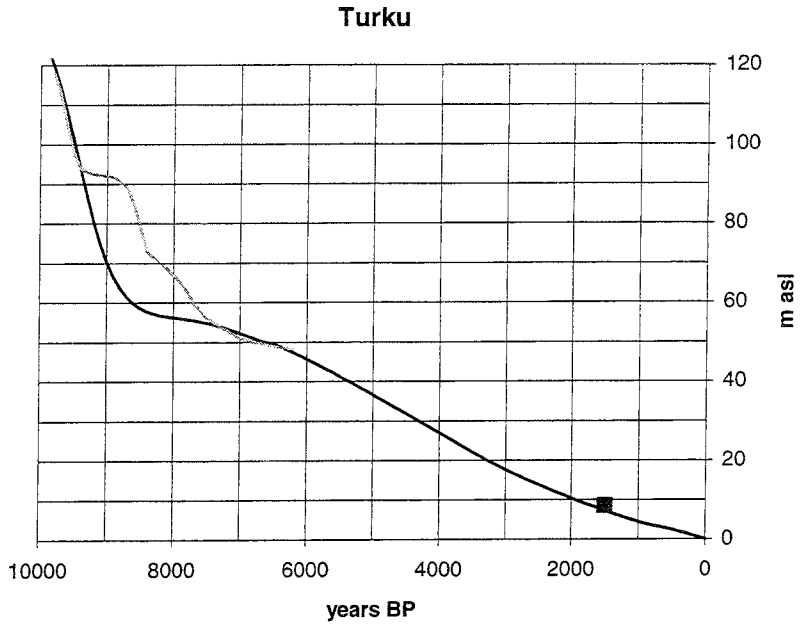

Figure 4-58. *Site 55. Shore level displacement at Turku according to Glückert (1976) supplemented by a date from Salonen et al.(1984). The shore level curve comprises mainly the Ancylus transgression.*

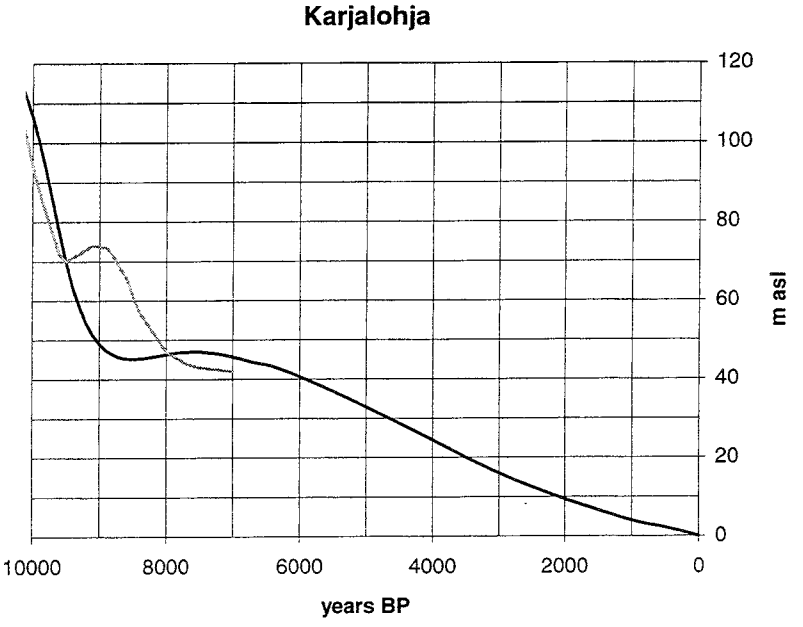

Figure 4-59. *Site 56. Shore level displacement at Karjalohja according to Glückert & Ristaniemi (1982). The shore level curve comprises mainly the Ancylus transgression.*

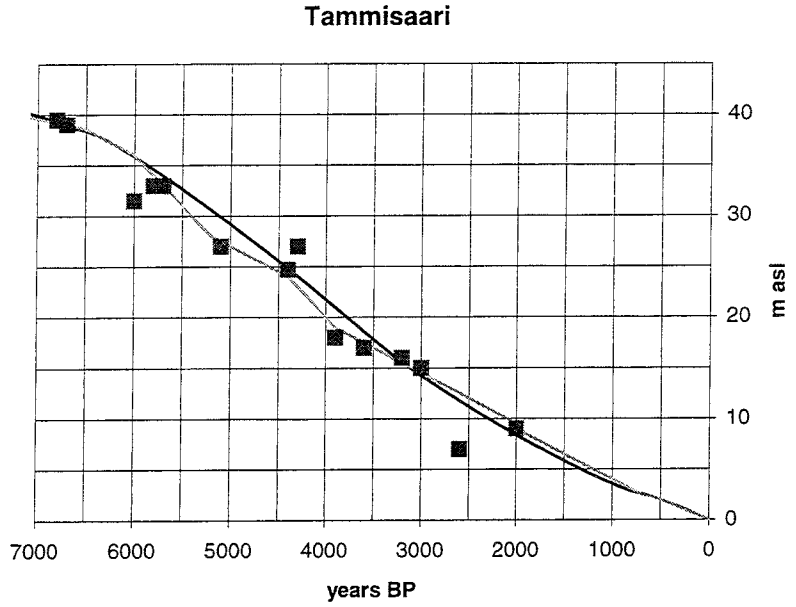

Figure 4-60. *Site 57. Shore level displacement at the Tammisaari-Perniö area according to Eronen et al. (1995).*

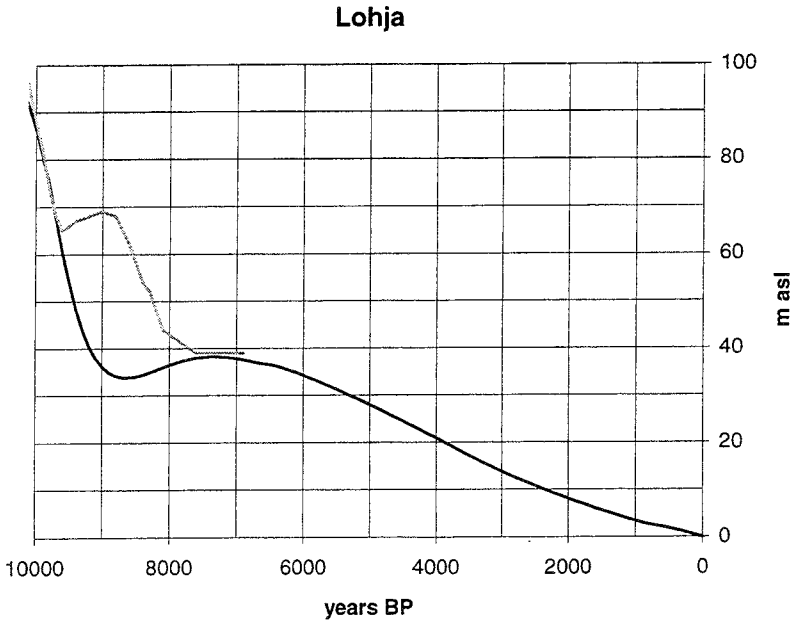

Figure 4-61. *Site 58. Shore level displacement at Lohja according to Glückert & Ristaniemi (1982). The shore level curve comprises mainly the Ancylus transgression.*

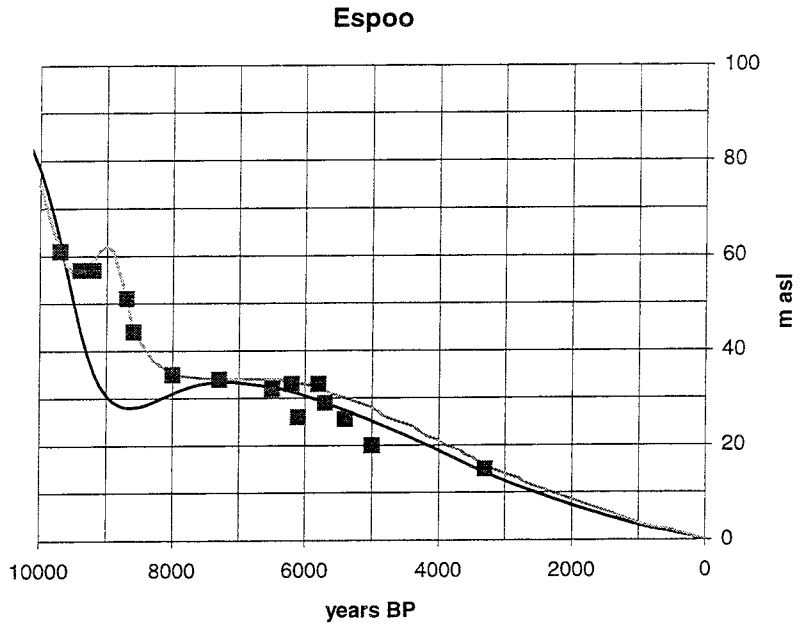

Figure 4-62. *Site 59. Shore level displacement at Espoo according to Hyvärinen (1980, 1984), Glückert & Ristaniemi (1982) and Eronen & Haila (1982).*

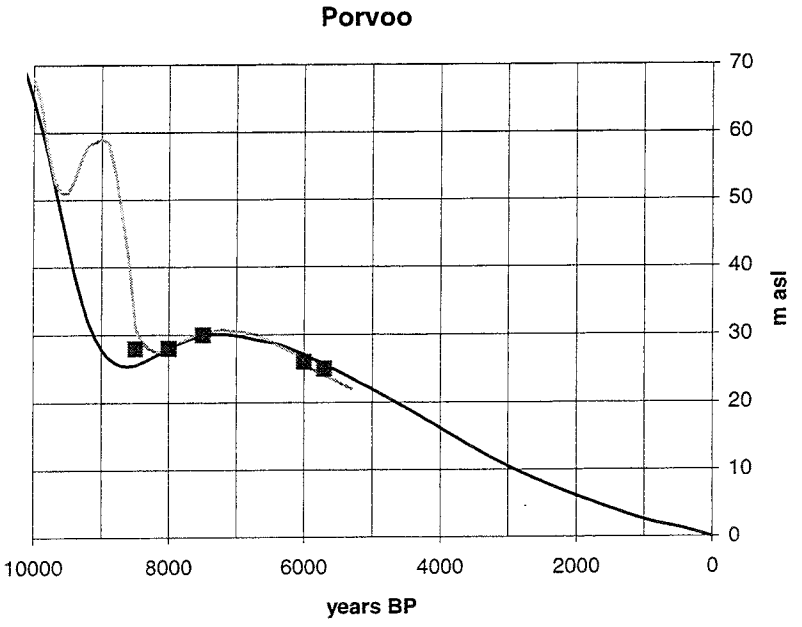

Figure 4-63. *Site 60. Shore level displacement at Porvoo according to Eronen (1983). The shore level curve comprises mainly the Ancylus transgression.*

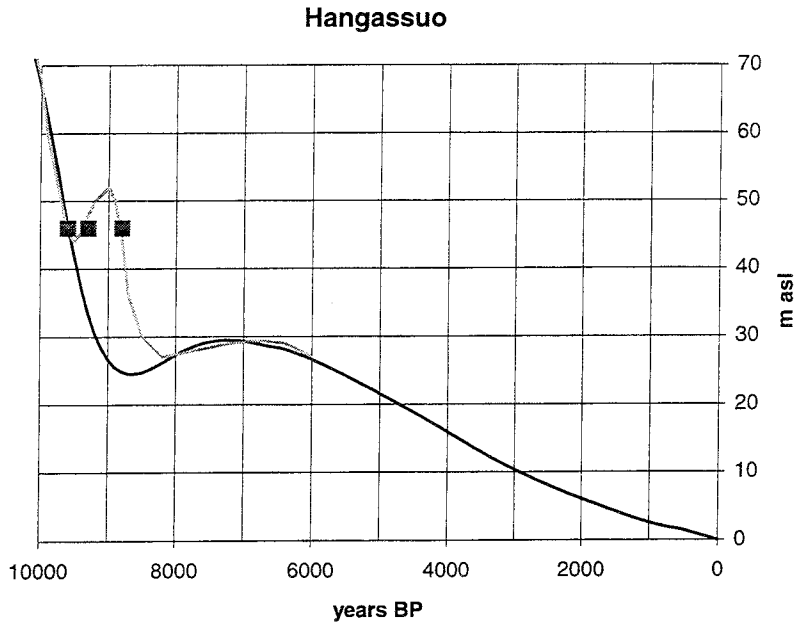

Figure 4-64. Site 61. Shore level displacement at Hangassuo according to Eronen (1976). The shore level curve comprises mainly the Ancylus transgression.

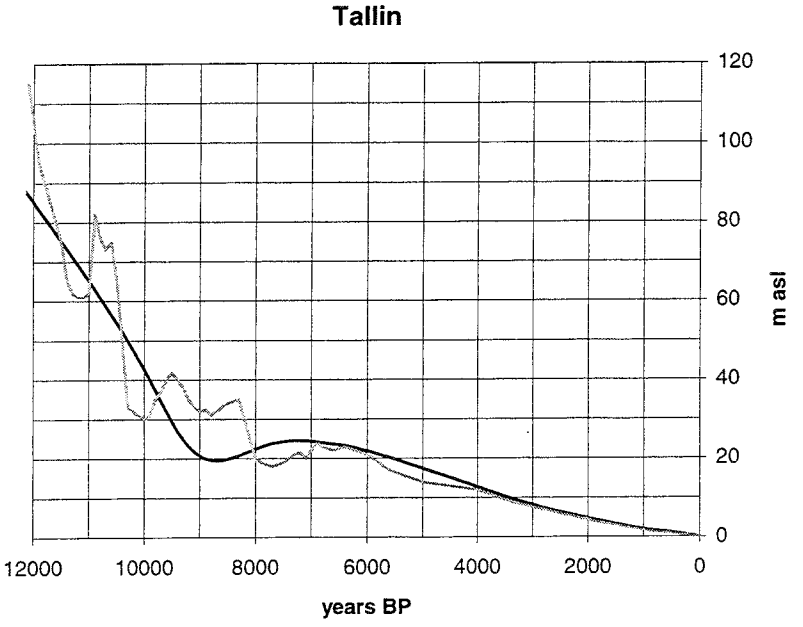

Figure 4-65. Site 62. Shore level displacement at Tallin according to Kessel & Raukas (1979).

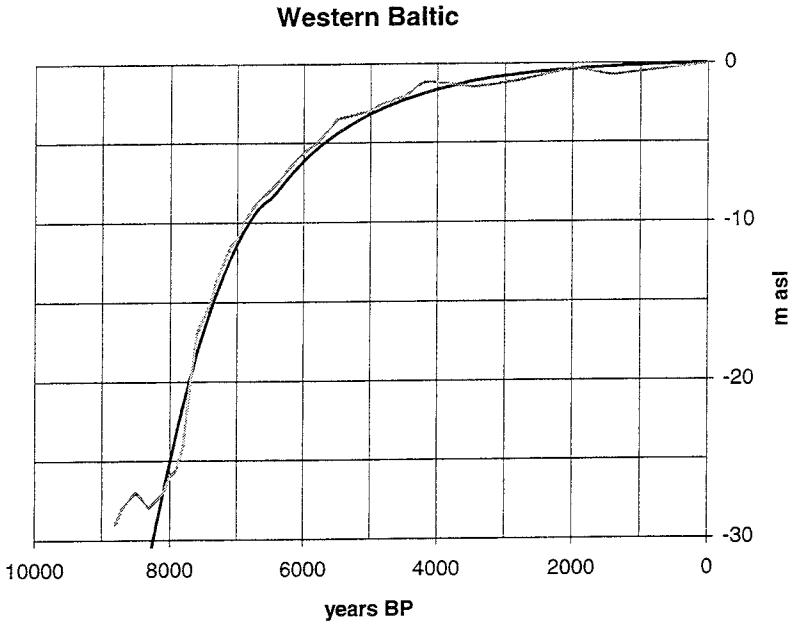

***Figure 4-66**. Site 63. Shore level displacement in the western part of the Baltic in the Bay of Kiel according to Winn et al. (1986) and Klug (1980).*

5 ANALYSIS

5.1 GENERAL

The uplift parameters, used for calculating the theoretical shore level curves, are shown in Table 5-1. The values of A_1, B_1 and A_3 are also presented in maps showing the estimated isolines, Figures 5-1 to 5-3. These maps can be used for determining the specific parameters necessary for calculating the shore level displacement at any optional site.

The uplift parameters are discussed in a regional concept in this chapter. The calculated values of the present uplift and the values of the apparent uplift received from precision levellings and tide gauge measurements are used for calculating the present annual eustatic rise.

5.2 THE SLOW UPLIFT

The parameters used for calculating the slow uplift are designated A_1, B_1 and T_1. The time for the maximal uplift rate (T_1) is estimated to 12 500 calendar years *i.e.* 11 300 years BP. As this is a constant value T_1 is not shown in Table 5-1. T_1 is isochronous in the whole area affected by the Scandinavian ice. That means that the slow uplift occurred as a sympathetic movement. It also implies that a great part of the uplift, especially in the last deglaciated areas, occurred before the sites finally became free of ice.

The values of A_1, half of the total uplift of the slow uplift, are shown in Figure 5-1. This isoline map is based only on the information received from the 63 shore level curves. The configuration of the two highest isolines (400 and 450 m) are just drawn as symmetrical extrapolations as no information exists for this central part.

An isoline map of the values of B_1 is shown in Figure 5-2. The accuracy in the estimations of the declining factor B_1 differs as detailed estimations of B_1 can only be derived from shore level curves comprising information from long time periods. The calculations of the values of B_1 started unprejudiced. However, when a trend in the pattern was discernible some specific values of B_1 were chosen for the final calculations. These values most probably represent mean values valid for the specific region. Figure 5-2 shows that there is a regional gradual trend in B_1, where the south-western part of Fennoscandia has low values and the north-eastern part has high values. High values of B_1 produce flat uplift curves, while low values give steeper curves where most of the recovery occurred close to T_1. The remaining uplift is thus bigger in areas with high values of B_1, which also means that the present rise still is relatively fast in these areas.

Table 5-1. The uplift parameters, used for calculating the theoretical shore level curves. T_1 is 12 500 calendar years BP. This value is not shown in the table as this is a constant value. The values of T_2 and T_3 are given in calendar years BP.

Site	A_1	B_1	A_2	T_2	B_2	A_3	T_3	B_3
1 Varanger	130	6500				30	10200	800
2 Andöja	95	3800	20	12000	-1200	20	10400	600
3 Tromsö	124	3800	28	11800	-600	34	10900	800
4 Lofoten	85	3800				32	10900	1200
5 Näröy	260	3800	30	11800	-300	30	10000	300
6 Verdalsöra	290	4800				50	10400	300
7 Frosta	280	4800				40	10400	300
8 Bjugn	220	3800	28	12400	-500	28	10400	300
9 Hitra	190	3800	34	12200	-800	28	10600	250
10 Fröja	165	3800	28	12000	-1000	18	10200	300
11 Leinöy	100	3800	16	12200	-700	16	10500	600
12 Fonnes	110	3800	35	12400	-800	35	10500	900
13 Sotra	120	3800	40	12400	-800	34	10600	650
14 Bömlo	112	3800	32	12400	-800	32	10800	900
15 Yrkje	115	3800	34	12200	-700	34	10200	400
16 Jären	95	3800	43	12400	-1000	38	10600	800
17 Kragerö	225	3300				45	10600	500
18 Porsgrunn	245	3300				50	10500	500
19 Vestfold	245	3300				55	10600	800
20 Oslo	380	3300				55	10400	200
21 Östfold	330	3300				45	10600	300
22 Ski	360	3300				40	10600	500
23 Vendsyssel	113	3500						
24 Vedbäck	107	2500						
25 Söborg SÖ	98	2500						
26 St Bält	62	2500						
27 Kroppefjäll	270	3800	18	11600	-250	22	11000	200
28 Hunneberg	238	3800	15	12400	-300	17	11200	200
29 Central Bohuslän	235	3800	4	12000	-100	15	11000	200
30 Ljungskile	220	3800	4	11600	-100	6	11000	150
31 Risveden	205	3800	15	12600	-300	15	11100	150
32 Göteborg	170	3800	4	12000	-200	6	10900	150
33 Sandsjöbacka	159	3800	4	12000	-200	6	10900	150
34 Fjärås	153	3800						
35 Varberg	137	3800						
36 Falkenberg	124	3800						
37 Halmstad	118	3300						
38 Bjäre Peninsula	103	3300						
39 Barsebäck	95	2500						
40 Blekinge	127	2500						
41 Oskarshamn	176	3300						
42 Gotland	170	3300						
43 Rejmyra	245	4800				40	10500	400
44 Stockholm area	235	6500				55	10400	700
45 Eskilstuna	245	6500				70	10400	600
46 Gästrikland	300	8000				90	10500	800
47 Hälsingland	340	8000				115	10300	900
48 Ångermanland	345	8000				130	9400	1000
49 S. Västerbotten	360	8000				125	9400	1000
50 Rovaniemi	325	8000				90	9800	600

Site	A_1	B_1	A_2	T_2	B_2	A_3	T_3	B_3
51 Lauhanwuori	310	9500				80	9900	600
52 Satakunta	270	9500				80	10100	600
53 Olkiluoto	245	9500						
54 Åland	260	8000						
55 Turku	215	8000				60	10400	600
56 Karjalohka	200	8000				55	10700	500
57 Tammisaari	180	8000				55	10600	500
58 Lohja	175	8000				50	10700	500
59 Espo	160	8000				47	10600	500
60 Porvoo	150	6500				40	10600	600
61 Hangassuo	147	6500				45	10700	500
62 Tallin	145	4800				25	10600	800
63 W Baltic	37	2500						

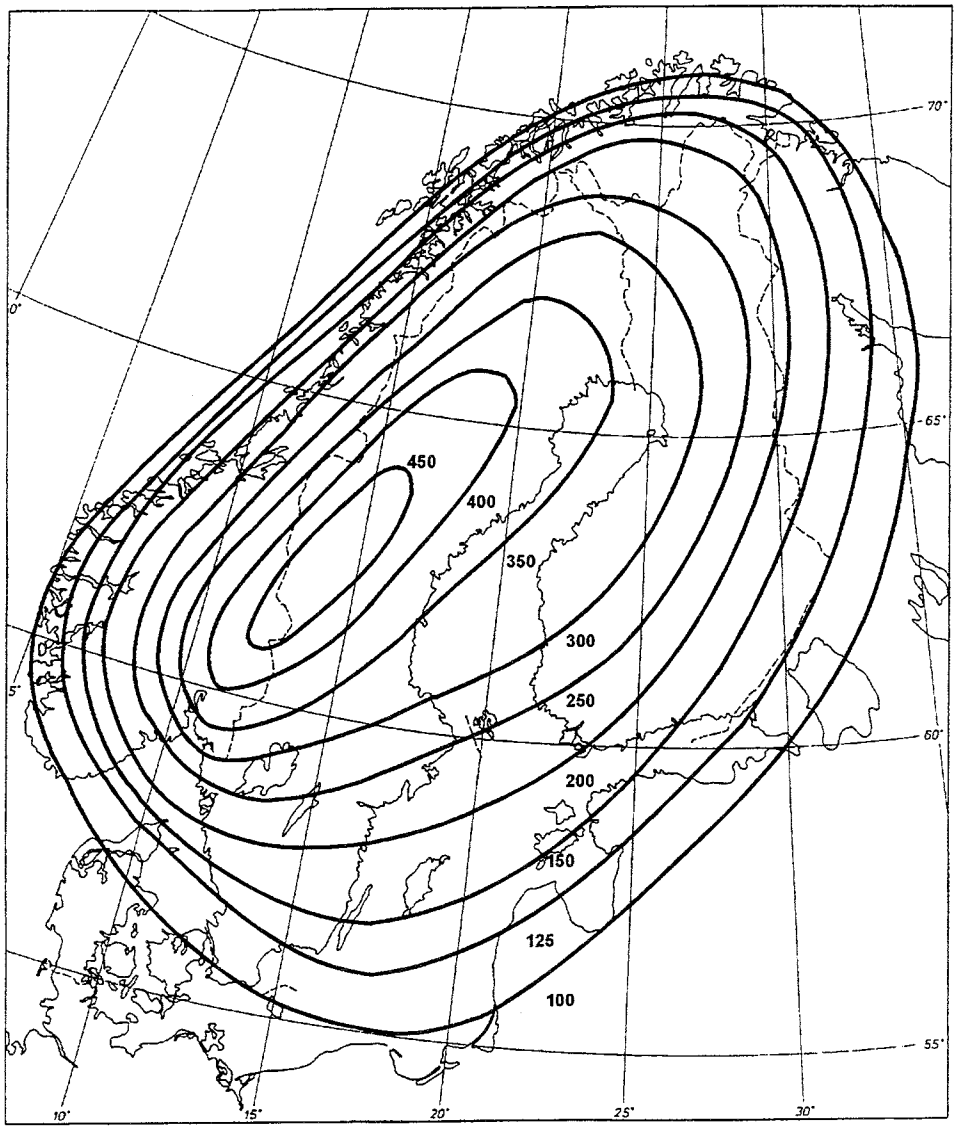

Figure 5-1. *The values of A_1 (m), i.e. half of the total uplift for the slow uplift mechanism.*

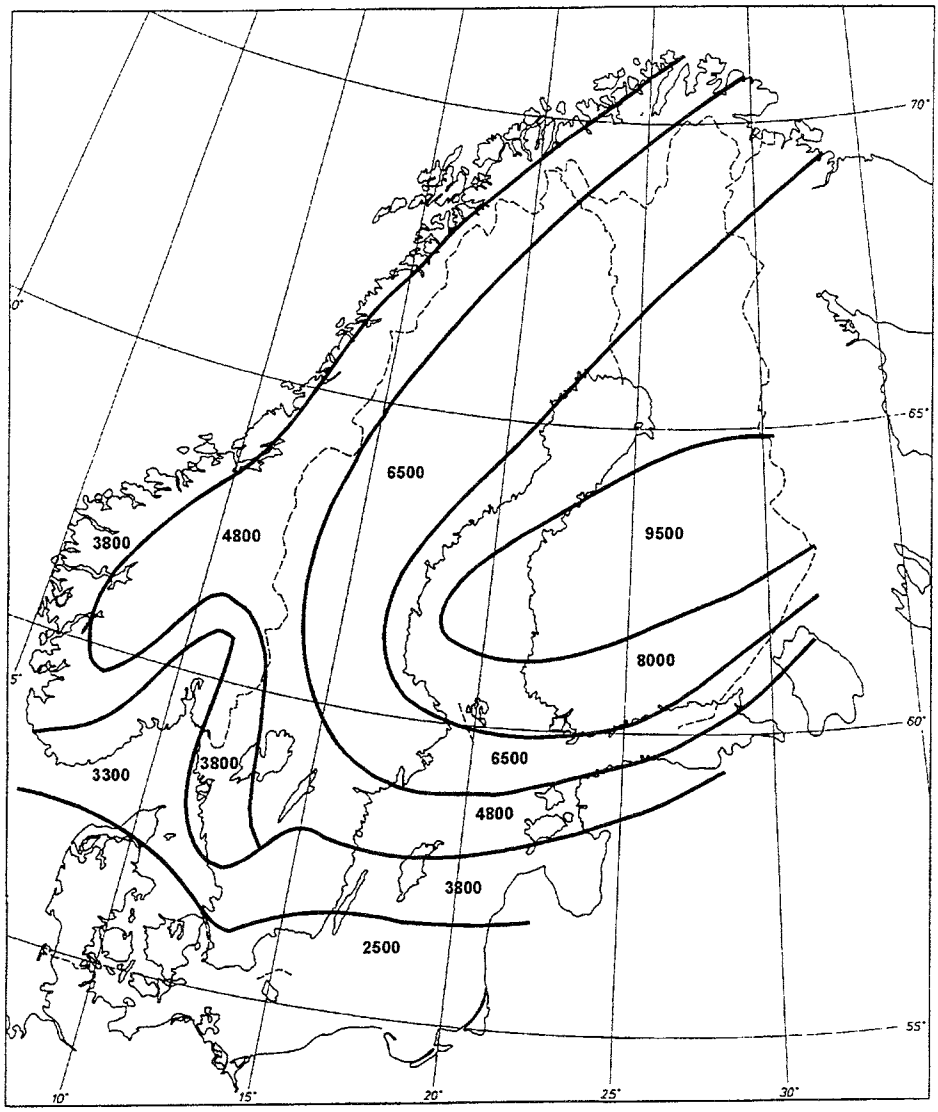

Figure 5-2. *The values of B_1, i.e. the declining factor for the slow uplift.*

5.3 THE FAST SUBSIDENCE

Several shore level curves from the Norwegian west coast show a Late Weichselian transgression. Sites which record this transgression are situated outside the Younger Dryas ice marginal zone. The transgression is named the Younger Dryas Transgression and proposed a result of glacio-isostatic subsidence by Anundsen (1985).

The fast subsidence can be deduced from shore level curves not only from the Norwegian west coast but also from the northern part of the Swedish west coast. The values of the parameters of the fast subsidence are reported in Table 5-1. Sites situated close to the Younger Dryas ice marginal zone are

affected in a higher degree than sites further from the ice margin. The values of A_2 are therefore higher for the sites close to the ice margin. At the south-western part of Norway A_2 is estimated to c. 40 m while A_2 at Sandsjöbacka (site 33) is estimated to 4 m. Sandsjöbacka is situated c.100 km outside the Younger Dryas ice margin.

According to Table 5-1 T_2 is estimated to 12 000 $\pm$ 400 cal years BP (10 850 $\pm$ 400 years BP). It cannot be concluded whether this confidence interval, according to the calculations, is due to uncertainties in the original shore level data or whether differences in T_2 actually exist. In spite of this uncertainty, it can be concluded that the growth of ice, giving rise to the Younger Dryas advance, started as early as the beginning of Alleröd (or possibly even earlier).

5.4 THE FAST UPLIFT

The fast uplift is deduced from all shore level curves from the central parts of Fennoscandia, while sites in southern Sweden and Denmark are not visibly affected by the fast uplift. The parameters of the fast uplift are reported in Table 5-1 and in Figure 5-3.

There is a methodical problem involved in the calculations of A_3, B_3 and T_3 as the functions of the fast uplift and the fast subsidence concur. It is therefore necessary to have information of both the fast subsidence and the fast uplift to obtain regionally comparable values of the uplift parameters. Shore level curves, from areas deglaciated after 10 000 y BP, have no information concerning the fast subsidence. During the modelling, with these curves, the values of T_3 could be changed backwards with the same conformity of the curves when the values of A_3 and B_3 contemporary were increased. Consequently there were infinite solutions at those sites. However, most of these solutions could be disregarded as they give unlikely values. The T_3 values falling closely after the deglaciation are regarded as the most likely values and the associated parameters are presented in Table 5-1. The estimated values for A_3 and B_3 are adequate for calculating theoretical shore level curves but should be regarded as approximate values if used for interpretations concerning the total amount of the glacio-isostatic uplift. This disadvantage can hopefully be improved in the future by proceeding modelling, as the framework is now established.

The values of T_3, Table 5-1, show regional differences. At the northern part of the Swedish west coast T_3 is approximately 11 000 $\pm$ 100 cal years BP (10 000 $\pm$ 100 years BP). In Norway and in central Fennoscandia most values of T_3, with some few exceptions, fall c. 10 500 $\pm$ 100 cal years BP (9 500 $\pm$ 100 years BP). At 5 sites in the northern parts of Sweden and Finland T_3 is between 10 100 and 9 400 cal years BP (9 100 - 8 500 years BP). The regional differences in T_3 indicate that this parameter is related to the time of the local deglaciation.

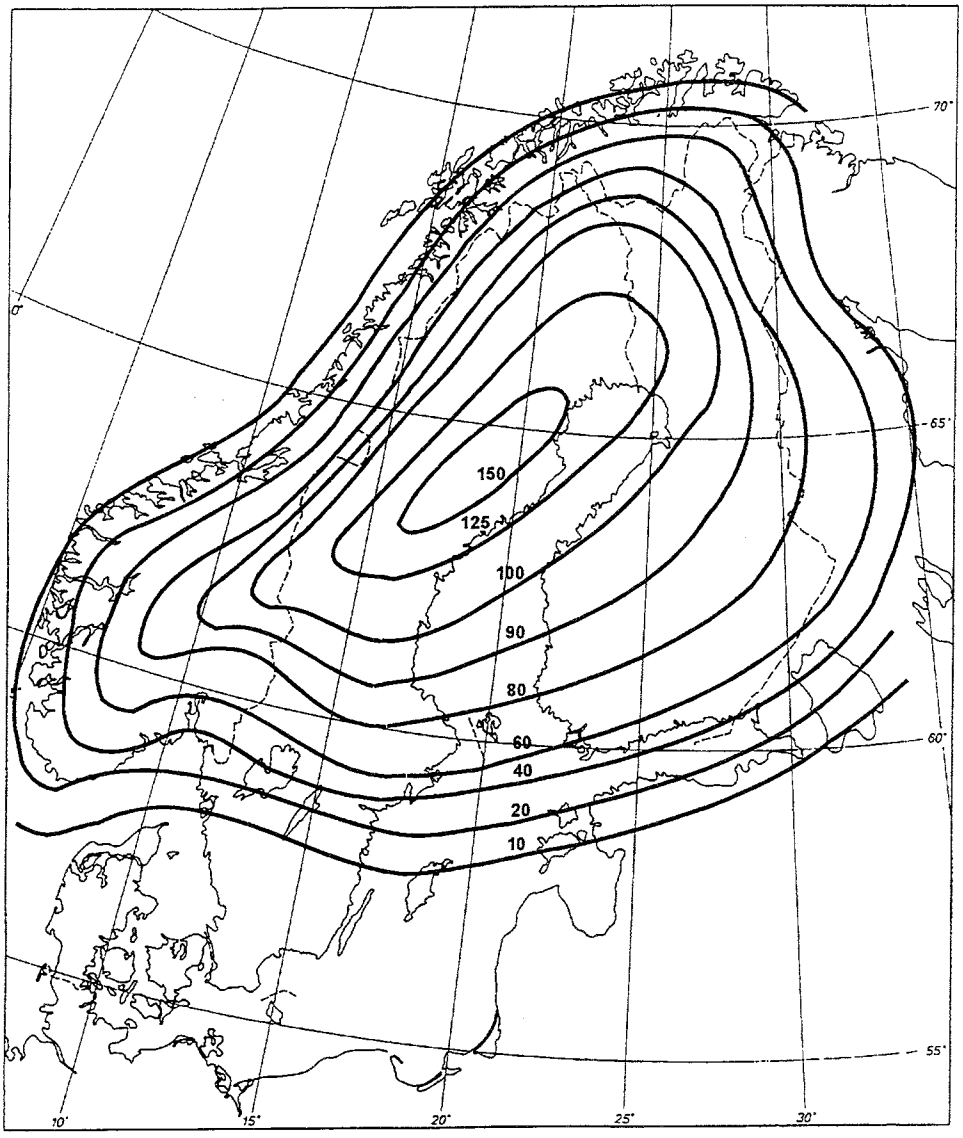

Figure 5-3. *The values of A_3 (m), i.e. half of the total uplift for the fast uplift mechanism.*

5.5 MECHANISMS OF THE GLACIO-ISOSTATIC UPLIFT

The mechanisms of the glacio-isostatic uplift are generally discussed based on geophysical assumptions regarding rheological conditions. In this paper the mechanisms of the glacio-isostatic uplift are discussed based on shore level and lake tilting data.

The applied calculations indicate that there are two mechanisms involved in the glacio-isostatic uplift, one slow and the other fast. The main uplift, still in progress, acts slowly. The results from lake-tilting investigations (Påsse 1996) show that the slow uplift is in progress with a declining course in the southern parts of Sweden. The shore level modelling shows that the slow

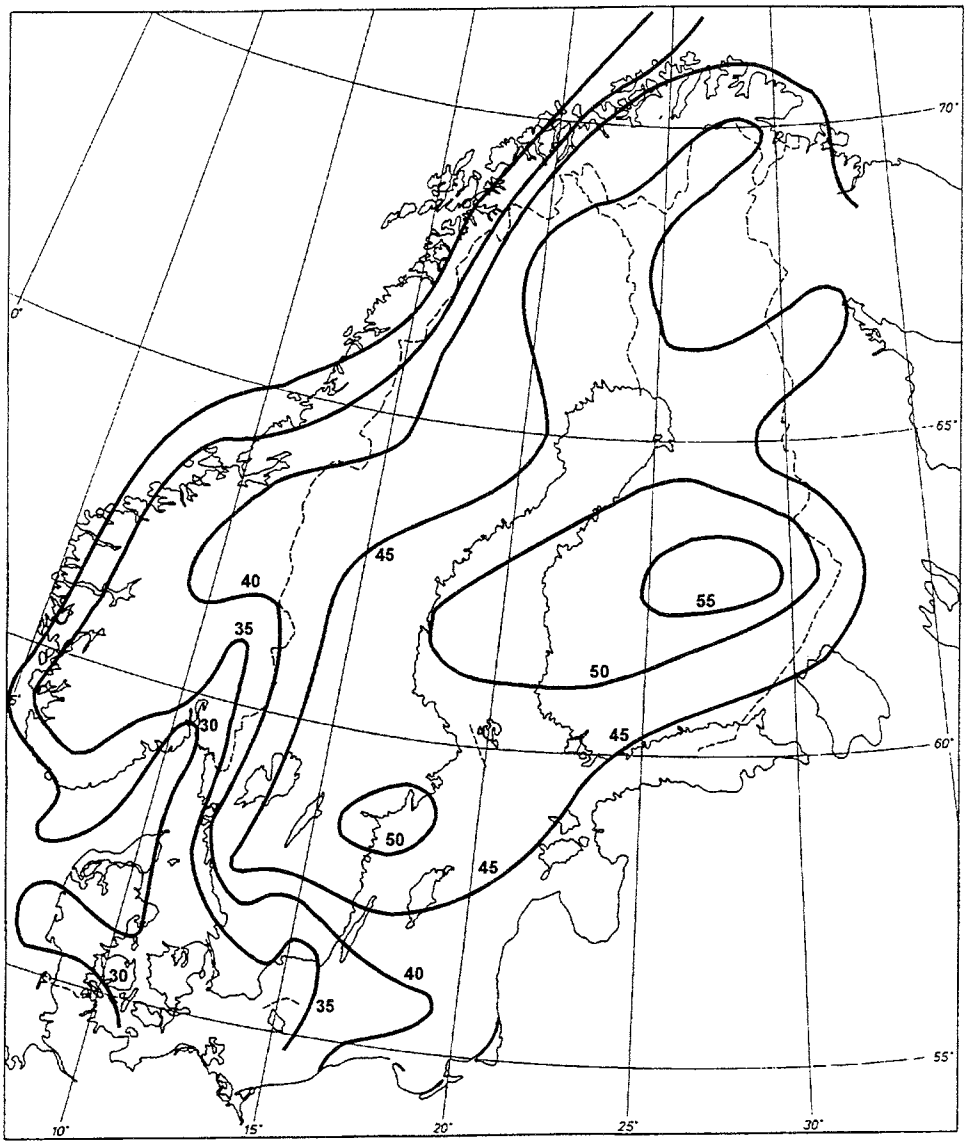

Figure 5-4. *The depth to Moho in km from seismic profiles. The map is redrawn from Kinck et al. (1993).*

uplift is in progress in the whole area earlier covered by the Scandinavian ice. The peripheral areas, which today seem to submerge, are thus still affected by a slow uplift. The reason for the submergence is an ongoing eustatic rise.

The course of the slow uplift is determined by two variables, the size of the uplift (A_1) and a declining factor (B_1). The configuration of the isolines of the present apparent uplift, Figure 2-1 and 2-2, shows a maximum in the Skellefteå area. This maximum is conventionally used for estimating the "centre of the glacio-isostatic uplift" or "the ice divide of the latest glaciation". This interpretation is based on the assumption of a constant declining factor. However, one of the main conclusions, presented in this

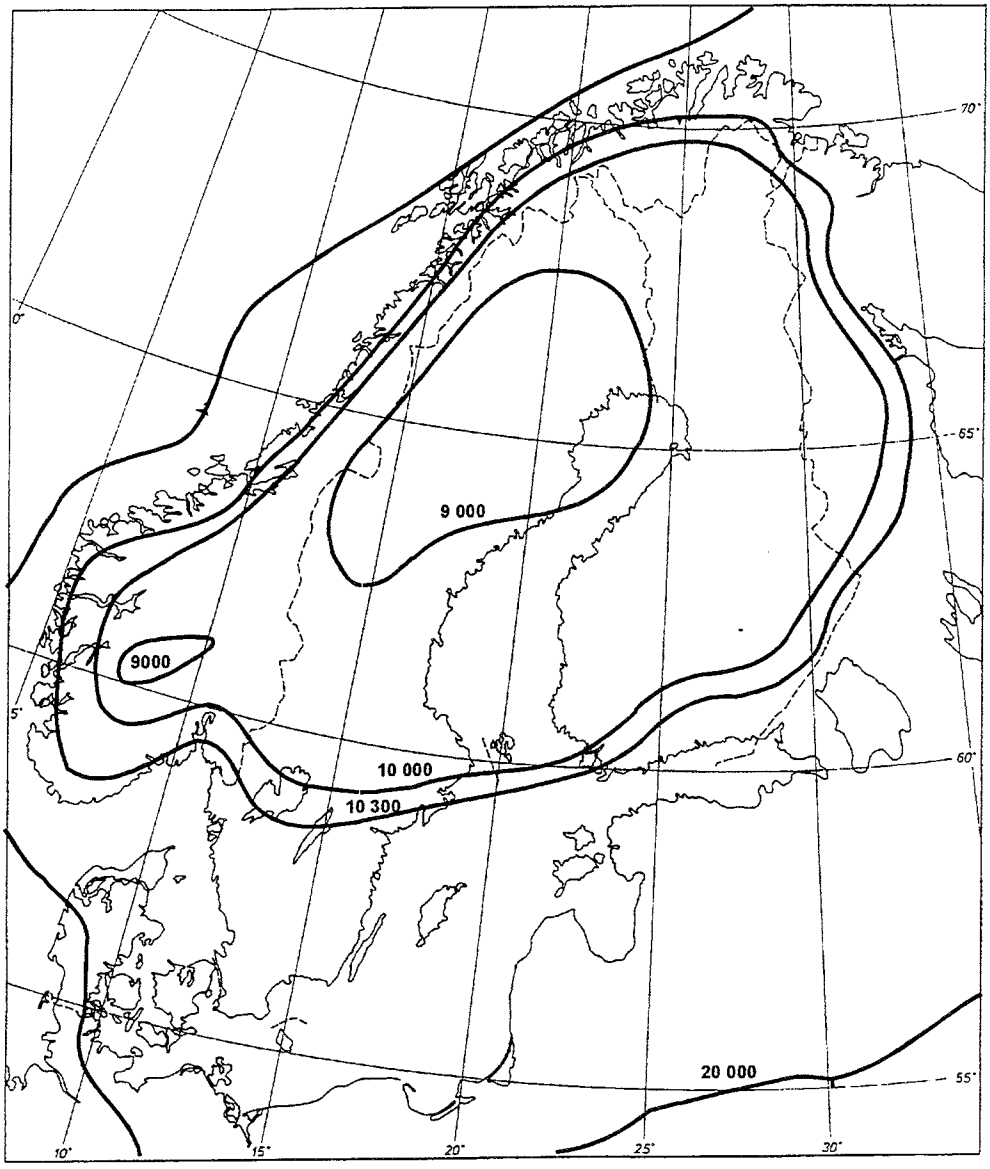

Figure 5-5. *Positions of the ice marginal during different stages (in years BP) of the latest deglaciation. The fast uplift mechanism has been detected from shore level curves from the area which was covered by ice during the Younger Dryas (10 300 y BP), but also from a peripheral zone outside the Younger Dryas ice marginal.*

paper, is that there are regional differences in the rate of the declining. Figure 5-1 infers that "the centre of the glacio-isostatic uplift" and therfore also "the ice divide of the last glaciation" was situated in central Sweden, in the county of Jämtland.

Kinck *et al.* (1993) have presented a map of the Moho depths from seismic profiles, Figure 5-4. Resemblances exist between this map and the map showing the variations in the values of the declining factor B_1, Figure 5-2. This congruence is interpreted as a relationship between the crustal

thickness and the declining factor. In areas with great crustal thickness the glacio-isostatic uplift is slower than in areas with thinner crust.

The fast mechanism gave rise to a crustal subsidence during the Younger Dryas restored by a fast uplift during Preboreal time. The subsidence is apparent in shore level curves in a peripheral zone outside the Younger Dryas ice margin. The fast uplift is apparent in shore level curves from areas in central Fennoscandia which were deglaciated rapidly during Preboreal time but also within the peripheral zone outside the Younger Dryas ice margin.

The course of the fast subsidence and the fast uplift is in response to the deglaciation pattern. The deglaciation of the peripheral parts of the Scandinavian ice, from the maximal Weichselian extension to the Younger Dryas terminal zone, lasted c. 10 000 years, Figure 5-5. The deglaciation from the Younger Dryas terminal zone to the area in northern Sweden where the glaciation terminated lasted c. 1000 year. The fast uplift mechanism is visible in shore level curves from sites situated in the area affected by this rapid deglaciation.

The fast mechanism can be assumed to have been active also during the deglaciation of the peripheral zone. However, due to the slow rate of deglaciation in this zone the result of this mechanism was "hidden" under the vanishing ice. A comparison between the map showing the isolines of A_3, Figure 5-3, and the deglaciation map, Figure 5-5, show similar configurations. These similarities further confirm the dependence of the fast mechanism to the pattern of the deglaciation. The fast subsidence was obviously caused by a renewed downloading of the crust during the glacial advance which culminated during the Younger Dryas. The shore level curves show that the growth of the ice thickness, at least in the marginal parts of the ice, already started at the beginning of Alleröd or possibly somewhat earlier. This means that the cause of the Younger Dryas readvance should not only be explained by the well-known climatic deterioration during the Younger Dryas. A "glacial-tilting", caused by the slow uplift mechanism which had its maximum during the actual time, may have triggered a marginal thickening of the ice.

The model has given information concerning the crustal movements outside the ice margin. The fast subsidence and the fast uplift are visible in shore level curves from sites c. 100 km outside the ice margin. The fast mechanism thus created a sympathetic crustal movement more than 100 km outside the ice margin.

The values of A_3 in the areas outside and inside the Younger Dryas ice margin are not exactly comparable (Chapter 5.4). However, this condition does not considerably influence the **configuration** of the isolines in Figure 5-3. This figure shows a maximum of the fast uplift west of the Skellefteå area in the county of Västerbotten. A comparison between Figures 5-1 and 5-3 show that the maxima of A_1 respectively A_3 are situated at different places. This condition supports the assumption of different causes of the slow and the fast mechanisms. The two mechanisms gave rise to tilting in

somewhat different directions in the south eastern part of Norway and in western central Sweden in the counties of Värmland, Dalarna and Härjedalen.

The existence of the two uplift mechanisms implies that there are two physical processes involved in the glacio-isostatic rebound. Ekman & Mäkinen (1996) have proved by repeated high-precision relative gravity measurements that a viscous inflow of mantle is a necessary part of the ongoing uplift process. The present uplift is due to the slow mechanism. This means that this mechanism can be linked to viscous flow and that the fast mechanism needs another explanation. This explanation may be compression followed by decompression.

5.6 THE PRESENT UPLIFT AND EUSTATIC RISE

The present absolute uplift (v_o mm/y) has been calculated using formula 3-7 by taking t = 1 year. The values obtained at each site are reported in Table 5-2.

The apparent postglacial uplift in Fennoscandia has recently been estimated in two different ways by Ekman (1996). He presents his results in two maps which are shown in Figures 2-1 and 2-2. The map shown in Figure 2-1 is deduced from precision levellings, tide gauge measurements and some results from lake-level stations. The values achieved from this map are designated $v_{p.l.}$ mm/y. The map shown in Figure 2-2 is deduced solely from data from sea level stations and the values achieved from this map are designated $v_{s.l.s.}$ mm/y. The values of the present apparent uplift estimated by these two methods, at the sites used in this investigation, are reported in Table 5-2.

The values calculated by formula 3-7 are different to the values of the present apparent uplift received from precision levellings and tide gauge measurements as the latter are influenced by the eustatic rise. The present annual eustatic rise is estimated by calculating the differences between v_o - $v_{s.l.s.}$ and v_o- $v_{p.l.}$ receptively. These values are reported in Table 5-2 and in Figures 5-6.

Table 5-2. The present absolute and relative uplift and the present eustatic rise. The absolute uplift (v_o mm/y) is calculated by formula 3-7. The values of the relative uplift from sea level records ($v_{s.l.s.}$ mm/y) and precision levellings ($v_{p.l.}$ mm/y) are taken from Ekman (1996) The two last columns in the table show the present eustatic rise calculated from the differences between the calculated absolute values and the relative values taken from Ekman (1996).

Nr	Site	v_o	$v_{s.l.s.}$	$v_{p.l.}$	$v_o - v_{s.l.s.}$	$v_o - v_{p.l.}$
1	Varanger	2,86		1,3		1,56
2	Andöja	1,24		0,1		1,14
3	Tromsö	1,83		0,6		1,23
4	Lofoten	1,41		0,6		0,81
5	Näröy	3,7		2,4		1,3
6	Verdalsöra	5,03		4		1,03
7	Frosta	4,84		3,8		1,04
8	Bjugn	3,11	2,1	1,9	1,01	1,21
9	Hitra	2,62	1,6	1,5	1,02	1,12
10	Fröja	2,25	1,3	1,2	0,95	1,05
11	Leinöy	1,42	0,4	0,2	1,02	1,22
12	Fonnes	1,62	0,2	-0,1	1,42	1,72
13	Sotra	1,69	0,2	-0,1	1,49	1,79
14	Bömlo	1,65	0,3	0	1,35	1,65
15	Yrkje	1,61	0,2	0	1,41	1,61
16	Jären	1,34	0,05	-0,2	1,29	1,54
17	Kragerö	2,96	1,4	1,3	1,56	1,66
18	Porsgrunn	3,22	1,7	1,6	1,52	1,62
19	Vestfold	3,33	2,3	2,7	1,03	0,63
20	Oslo	4,84	3,8	4,1	1,04	0,74
21	Östfold	4,22	3,1	3,2	1,12	1,02
22	Ski	4,64	3,6	3,6	1,04	1,04
23	Jylland	1,49	0,25	0,3	1,24	1,19
24	Vedbäck	1,05	-0,2	-0,25	1,25	1,3
25	Söborg SÖ	0,96	-0,25	-0,25	1,21	1,21
26	St Bält	0,61	-0,6	-0,6	1,21	1,21
27	Kroppefjäll	3,83	2,4	2,7	1,43	1,13
28	Hunneberg	3,37	2,1	2,3	1,27	1,07
29	Central Bohuslän	3,27	2	2	1,27	1,27
30	Ljungskile	3,12	1,8	2	1,32	1,12
31	Risveden	2,9	1,7	1,6	1,2	1,3
32	Göteborg	2,41	1,2	1,2	1,21	1,21
33	Sandsjöbacka	2,25	1	1	1,25	1,25
34	Fjärås	2,17	0,95	0,95	1,22	1,22
35	Varberg	1,94	0,77	0,7	1,17	1,24
36	Falkenberg	1,76	0,7	0,6	1,06	1,16
37	Halmstad	1,48	0,3	0,3	1,18	1,18
38	Bjäre Peninsula	1,29	0,3	0,2	0,99	1,09
39	Barsebäck	0,93	-0,2	-0,25	1,13	1,18
40	Blekinge	1,24	0,3	0,3	0,94	0,94
41	Oskarshamn	2,21	1,2	1,15	1,01	1,06
42	Gotland	2,14	1,4	1,3	0,74	0,84
43	Rejmyra	4,26	3,1	3,4	1,16	0,86
44	Stockholm area	5,12	3,75	3,95	1,37	1,17
45	Eskilstuna	5,35	3,95	4,2	1,4	1,15

Nr	Site	v_o	$v_{s.l.s.}$	$v_{p.l.}$	$v_o - v_{s.l.s.}$	$v_o - v_{p.l.}$
46	Gästrikland	7,35	6,1	6,2	1,25	1,15
47	Hälsingland	8,48	7,25	7,25	1,23	1,23
48	Ångermanland	8,9	7,6	7,7	1,3	1,2
49	S. Västerbotten	9,22	8,2	8,2	1,02	1,02
50	Rovaniemi	7,87	6,6	6,75	1,27	1,12
51	Lauhanwuori	7,92	6,8	6,8	1,12	1,12
52	Satakunta	6,92	5,8	5,8	1,12	1,12
53	Olkiluoto	6,3	5,1	5,1	1,2	1,2
54	Åland	6,22	5	5	1,22	1,22
55	Turku	5,18	4,05	4,05	1,13	1,13
56	Karjalohka	4,78	3,6	3,6	1,18	1,18
57	Tammisaari	4,32	3,1	3,1	1,22	1,22
58	Lohja	4,19	2,9	3	1,29	1,19
59	Espo	3,83	2,75	2,8	1,08	1,03
60	Porvoo	3,26	2,1	2,3	1,16	0,96
61	Hangassuo	3,21	1,8	2,35	1,41	0,86
62	Tallin	2,58	1,9	2	0,68	0,58
63	W Baltic	0,36	-1,1	-1,1	1,46	1,46

The mean values of the calculations v_o - $v_{s.l.s.}$ and v_o- $v_{p.l.}$ mm/y receptively both give 1.2 mm/y (1.19 receptively 1.18 mm/y). The annual present eustatic rise can thus be estimated to 1.2 mm/y. This value is in accordance to the estimations compiled by e.g. Emery&Aubrey (1991), Nakiboglu& Lambeck (1991) and Ekman (1996).

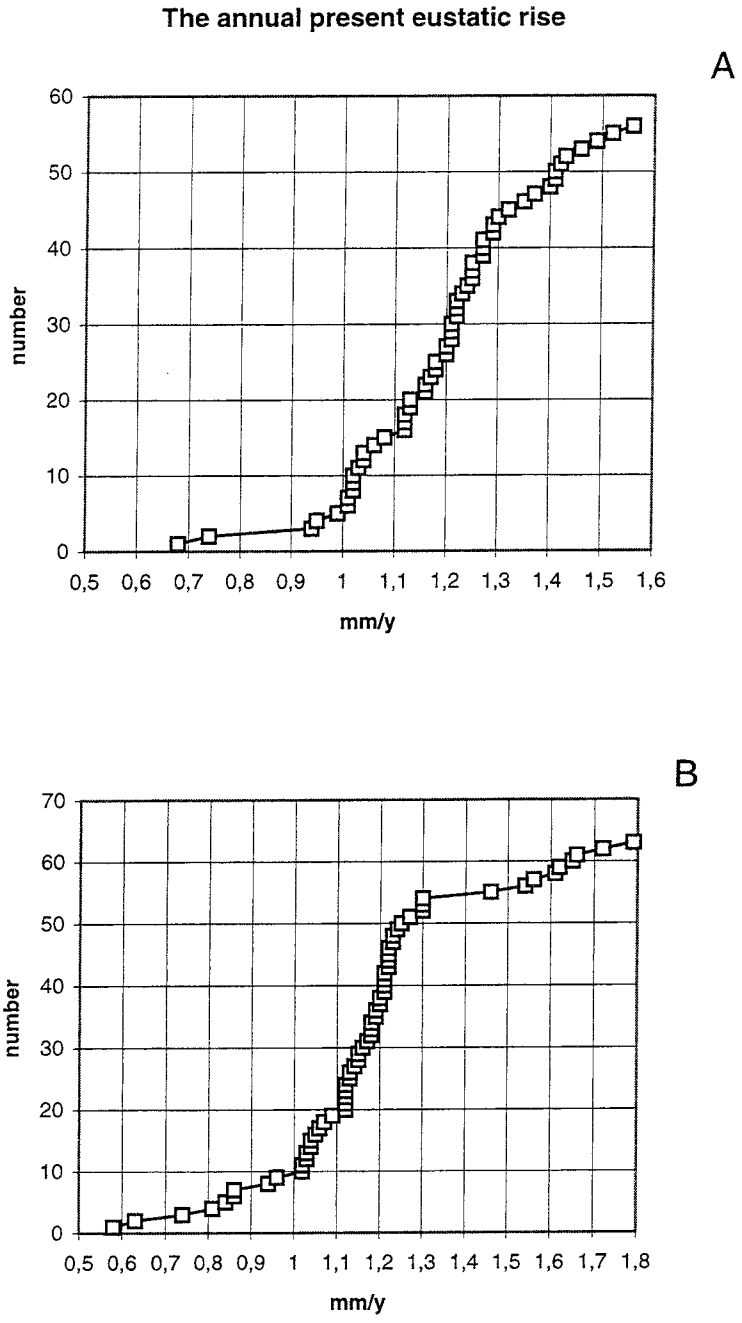

Figure 5-6. A. *The annual present eustatic rise calculated as the difference between the absolute present uplift (v_o mm/y) and the present apparent postglacial uplift deduced from sea level stations ($v_{s.l.s.}$ mm/y) according to Ekman (1996). The y-axis shows the number of calculations and the x-axis shows the difference $v_o - v_{s.l.s.}$ mm/y.*

B. *The present eustatic rise calculated as the difference between the absolute present uplift (v_o mm/y) and the present apparent postglacial uplift deduced from precision levellings, tide gauge measurements and some results from lake-level stations ($v_{p.l.}$ mm/y) according to Ekman (1996). The present annual eustatic rise is estimated at 1.2 mm/y.*

5.7 LAKE-TILTING INFORMATION

Lake shorelines are tilted in the same manner as marine shorelines by crustal movements but are not affected by eustasy. Lake shorelines are related to one fixed level, *i.e.* to the level of the outlet. For this reason they are very useful for empirical estimations of crustal changes.

The depth of the water in a lake is unaffected by glacio-isostatic uplift in the outlet area. However, in other parts of the lake, where the crustal uplift is faster or slower in reference to the rate at the outlet area, the water level changes in reference to the crust. This mechanism creates a tilting of the lake, in the same way as tipping a vessel. If the outlet is situated in a part of the lake that has the fastest rate of uplift, the rest of the lake will be continuously transgressed.

In lakes which have been transgressed, terrestrial and littoral peat today exist at fairly great depths and are in many places covered by gyttja. By dating littoral peat at different depths a record of the ancient levels of the lake surface can be estimated. Graphically the results can be plotted as time-depth curves. These curves show the differences between the amount of the glacio-isostatic uplift at the outlet and at the sampling site. Unfortunately, the lake-tilting information gives no absolute values of the uplift, but by exaggerating the time-depth-function an important tool is achieved for modelling.

The results of an investigation using the lake-tilting method has recently been presented by Påsse (1996). Four lakes in southern Sweden have been investigated, Figure 5-7. An example of the graphs received in the lake-tilting investigations is shown in Figure 1-1.

The lake-tilting investigations show that the difference in uplift between the outlet and the sampling site could be expressed as

$$\Delta U = 0.6366 \times \Delta A \, (arctan \, (T / B) - arctan \, ((T - t) / B)) \qquad 5\text{-}1$$

where ΔU is the difference in uplift between the outlet and the sampling site (in m), ΔA is half of the difference of the total uplift between the outlet and the sampling site (in m), T is the time for the maximal uplift rate (in calendar years), t is the variable time (in calendar years) and B is a declining factor (in calendar years). The sizes of ΔU and ΔA are not only dependent on the course of the glacio-isostatic uplift but also dependent on the distance between the outlet and the sampling site

Formula 5-1 has the same form as the general uplift formula 3-5. The uplift parameters T and B, estimated by the shore level modelling, should thus be equal to the results primarily received by the lake-tilting investigations. The values of ΔA, T and B estimated from the investigations of the four lakes are reported in Table 5-3.

Table 5-3. The most likely values of ΔA, T and B according to the statistical analyses at four lakes in the lake-tilting investigation presented by Påsse (1996).

	ΔA m	T cal. y BP	B year
Lake Fegen	11,2-12	13000-13500	3700-3875
Lake Vanderydsvattnet	7,1-8,7	12300-13500	4105-4325
Lake Säven	6,25-8	11500-12600	4300-4350
Lake Sommen	12-17	10700-12900	5900-6000

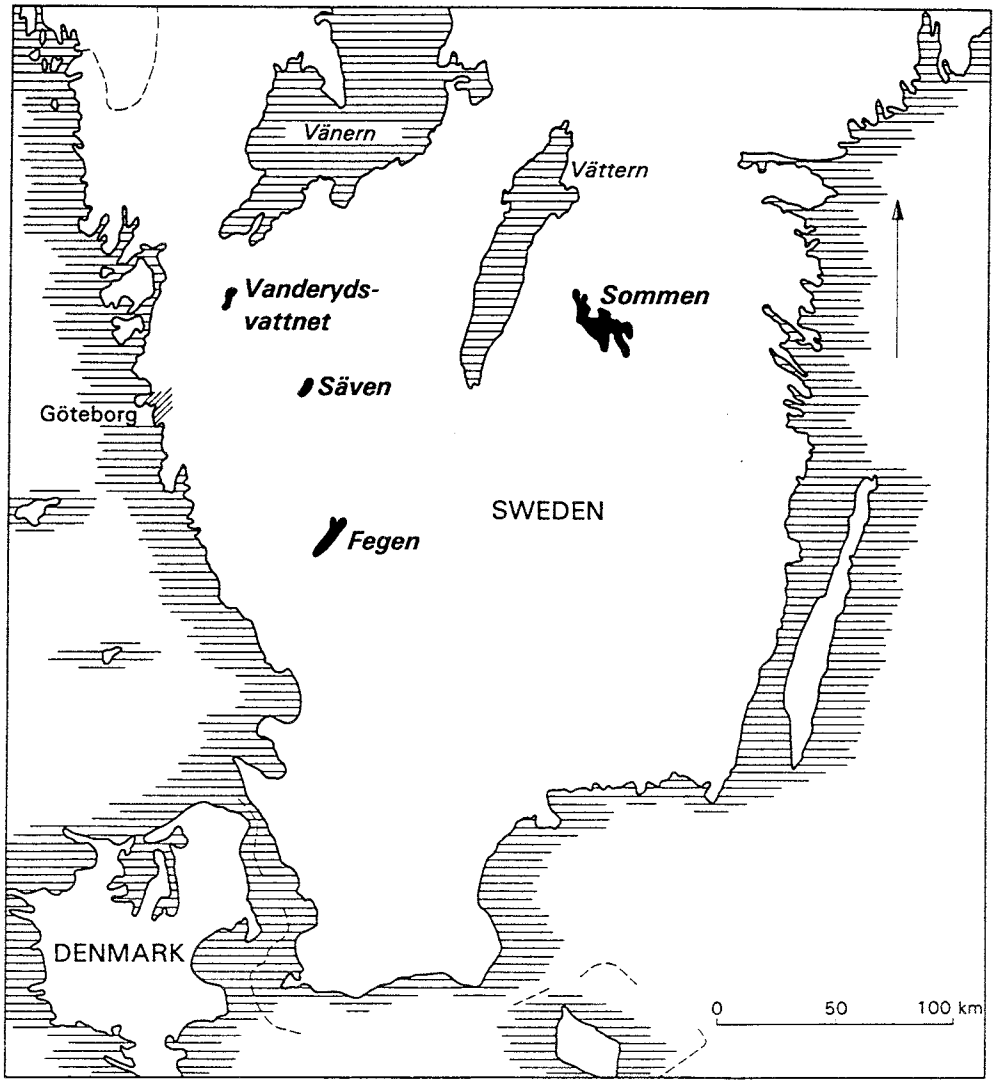

Figure 5-7. Location of the lakes investigated with the lake-tilting method (Påsse 1996).

According to Table 5-3 T is limited to an interval between 10 700 - 13 500 cal years BP. Whether the maximal uplift occurred as a synchronous event or not could not be concluded by the lake-tilting data. However, the shore level modelling indicates a constant value of 12 500 cal years BP for T (T_1), which persists in the interval estimated within the lake-tilting analysis.

The iterations in the shore level modelling always started with the shore level curve from Sandsjöbacka (site 33) as this site is situated at the same isobase as Lake Fegen. B (B_1) was estimated to 3700-3875 in the lake-tilting study and 3800 in the shore-level modelling. Table 5-3 shows that there is a significant difference between the value of B_1 at Lake Sommen compared to the other sites. According to Figure 5-2, B_1 is estimated to 4 800 within the shore level modelling, while B is estimated to 5 900 - 6 000 in the lake-tilting investigation. In chapter 5.5 a relationship is discussed between the crustal thickness and the declining factor B_1. This relationship is a result of the modelling and has therfore not been applied in the calculations (Chapter 8). The crustal thickness at Lake Sommen, Figure 5-4, indicates that B_1 should most probably have a value close to 6 000, which originally was estimated according to the lake-tilting data.

6 THE FUTURE SHORE LEVEL DISPLACEMENT

The future development regarding the glacio-isostatic uplift, the eustasy and the shore level displacement can be predicted in Fennoscandia using the results from the modelling. In this chapter some sites in Sweden are shown as examples of these predictions, 6-1 to 6-6. The predictions are based on the assumption that the crustal and eustatic developments follow the trend that exist today. Regarding the glacio-isostatic uplift this assumption can most probably be applied as long as no new glaciation starts. Regarding the eustatic development it is possible that climatic alterations may change the present eustatic trend. The future glacio-isostatic uplift is thus somewhat easier to predict then the eustatic movement and the connected shore-level displacement. The predictions are presented in two ways, as curves showing only the crustal uplift and as shore-level displacement curves, which include the eustatic trend according to formula 3-8. The predictions extend 10 000 years. Future time is designated as negative time.

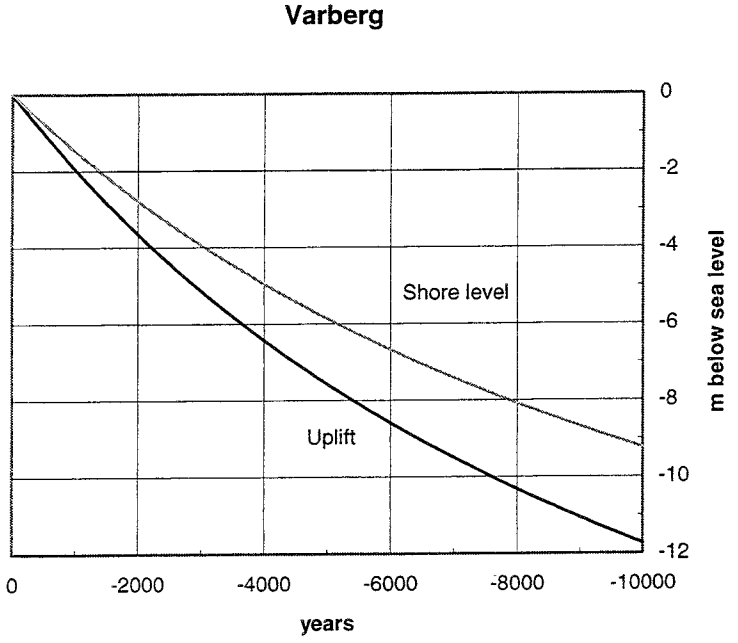

Figure 6-1. *Predicted shore level displacement, grey curve, and the glacio-isostatic rise, black curve, at Varberg, site 35. The uplift parameters used are in accordance with Table 5-1.*

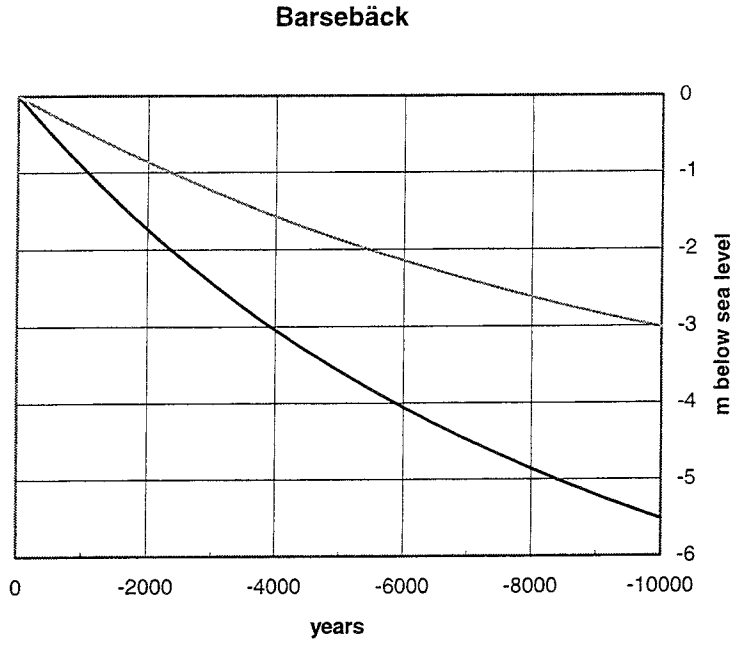

Figure 6-2. Predicted shore level displacement, grey curve, and the glacio-isostatic rise, black curve, at Barsebäck, site 39. The uplift parameters used are in accordance with Table 5-1.

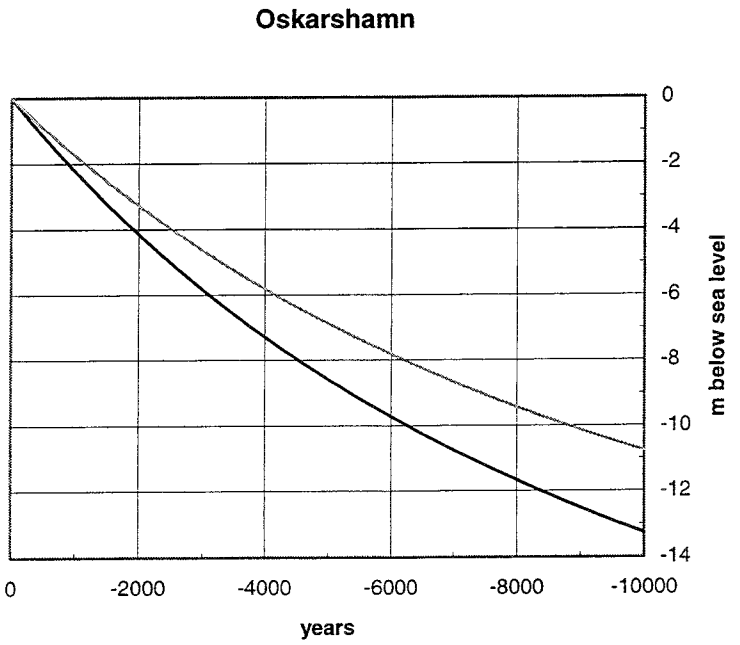

Figure 6-3. Predicted shore level displacement, grey curve, and the glacio-isostatic rise, black curve, at Oskarshamn, site 41. The uplift parameters used are in accordance with Table 5-1.

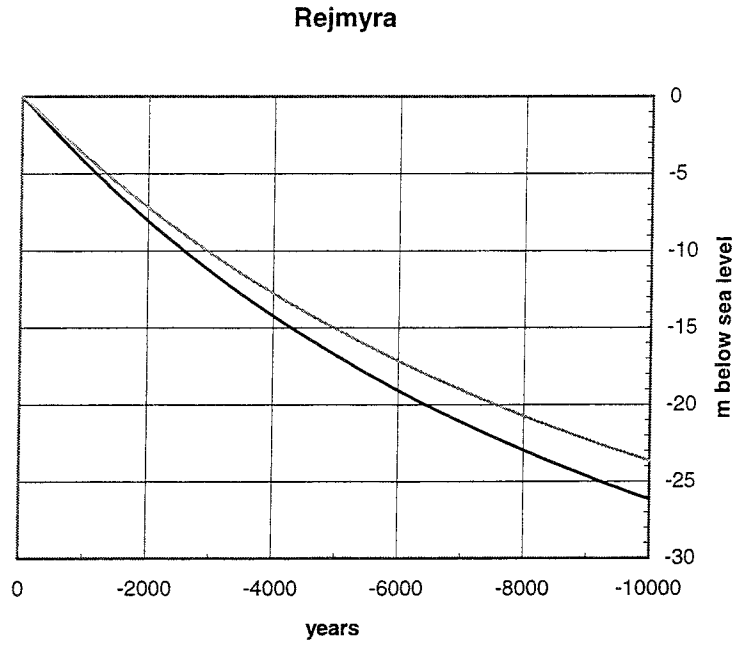

***Figure 6-4**. Predicted shore level displacement, grey curve, and the glacio-isostatic rise, black curve, at Rejmyra, site 43, W of Nyköping. The uplift parameters used are in accordance with Table 5-1.*

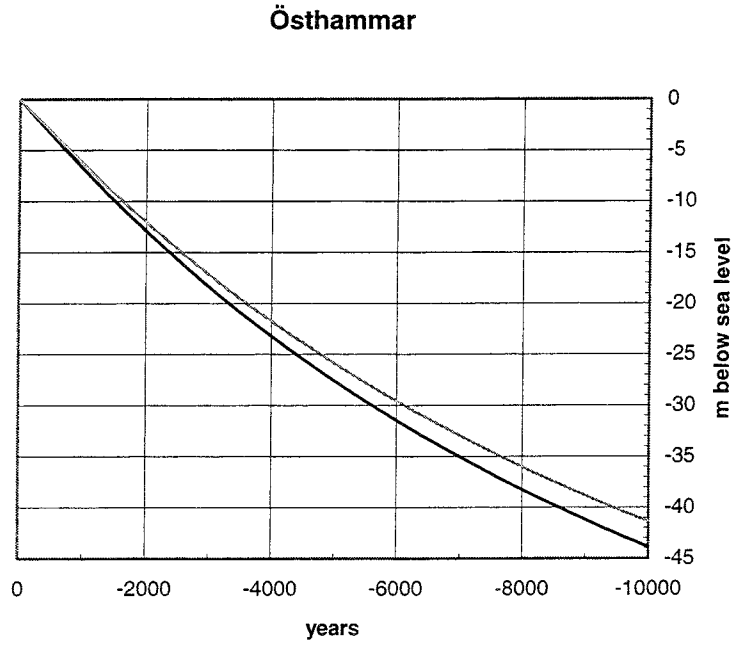

***Figure 6-5**. Predicted shore level displacement, grey curve, and the glacio-isostatic rise, black curve, at Östhammar in the county of Uppland. The uplift parameters used in the calculation are A_1= 275, B_1= 8000 A_3= 80, B_3= 700 and T_3= 10 400.*

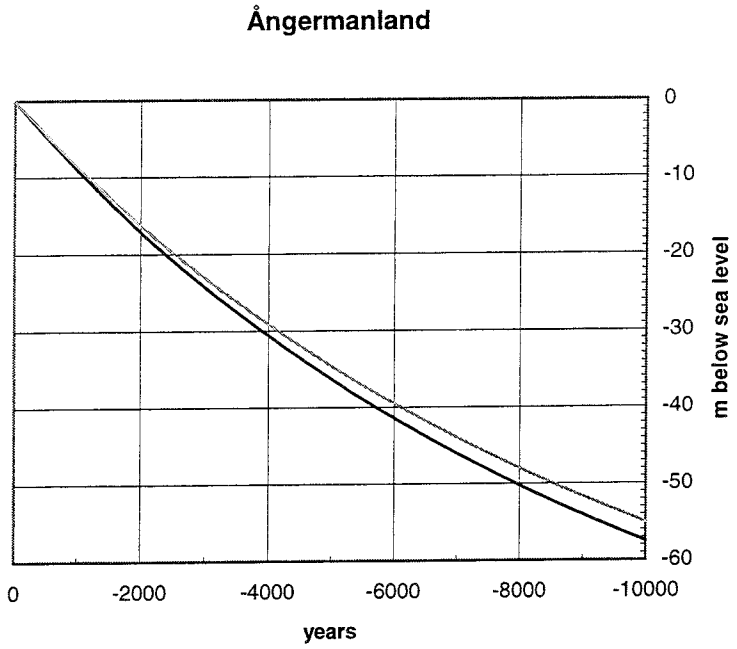

Figure 6-6. *Predicted shore level displacement, grey curve, and the glacio-isostatic rise, black curve, at Ångermanland, site 48. The uplift parameters used are in accordance with Table 5-1.*

7 THE BALTIC

7.1 GENERAL

Shore level curves from the coasts around the Baltic Sea are affected by raised water levels during the two lake stages, the Baltic Ice Lake and the Ancylus Lake. This means that parts of the Baltic shore level curves are not congruous to the marine shore level curves. The differences between the curves can be used for calculating the water level changes and also to deduce the actual thresholds during the different stages of the Baltic, Figure 7-1. The research concerning the development of the Baltic Sea since the last deglaciation has resulted in an immense number of publications. A review of this topic has recently been presented by Björck (1995), which contains most of the relevant references regarding the development of the Baltic Sea.

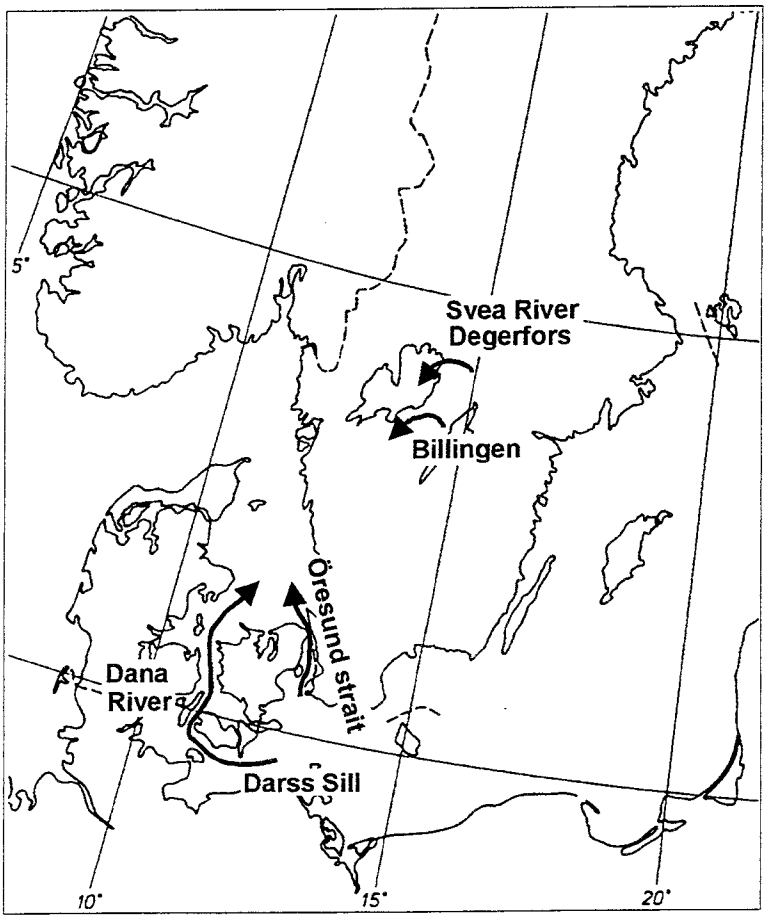

Figure 7-1. *The position of the four different outlets that have determined the water level during the different stages of the Baltic basin since the last deglaciation.*

7.2 THE BALTIC ICE SEA

The shore level curves from Blekinge (site 40) and Oskarshamn (site 41), Figures 4-43 and 4-44, are the only two curves that comprise the first stage of the Baltic. Comparisons between these curves and calculated curves of the corresponding marine shore level displacement, show that the water level within the Baltic basin, until 12 000 ± 100 BP, was in level with the sea. The shore level displacement in the southern part of the Öresund Strait, where a threshold exists at c. -7 m, is shown in Figure 7-2. The shore level curve indicates that this threshold was isolated c. 12 000 BP. A calculated shore level curve for the Darss Sill (c. -20 m) shows that this connection, between the Baltic and the sea, was closed *c.* 13 500 BP, Figure 7-3. The narrow strait at Öresund was thus the only connection to the sea during this stage and explains the "lacustrine" conditions in the Baltic during this phase. A sea facies at the beginning of the development of the Baltic has been proposed by Nilsson (1968) who names this stage the Baltic Ice Sea.

7.3 THE BALTIC ICE LAKE

After the isolation 12 000 ± 100 BP the water level in the Baltic increased due to the uplift (the shore level displacement) of the threshold. The difference between the water level of the Baltic and the sea can be calculated by using the shore level curve from Oskarshamn, Figure 4-44. These values are plotted in Figure 7-4 and compared to the calculated rate of the shore level displacement at the threshold at Öresund. This figure proves that the water level rise at Oskarshamn is related to the raised threshold at Öresund. The increase of the water level in the Baltic Ice Lake continued until approximately 10 400 ± 100 BP, when the opening of a threshold in the Billingen area caused a catastrophic drainage. Before that the water level in the Baltic had reached c. 26 m above sea level according to Figure 7 -4.

7.4 THE YOLDIA SEA

After the drainage of the Baltic Ice Lake the shore level in the Baltic followed the marine water level *c.* 800 - 1000 years. Due to the crustal uplift there was a fast gradual lowering of the connection between the Baltic and the sea. The Yoldia Sea thus became an inland sea during the latter part of this stage. This stage ended when the threshold at Degerfors was emerged *c.* 9 500 ± 100 y BP.

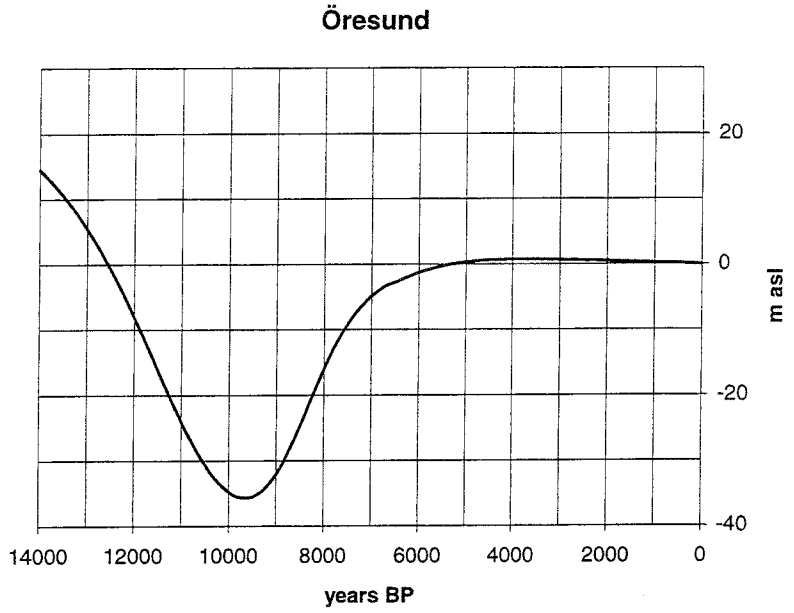

Figure 7-2. *Shore level displacement at the Öresund Strait calculated with A_1 = 72 and B_1 = 2 500. The threshold at c. -7 was isolated c. 12 000 BP.*

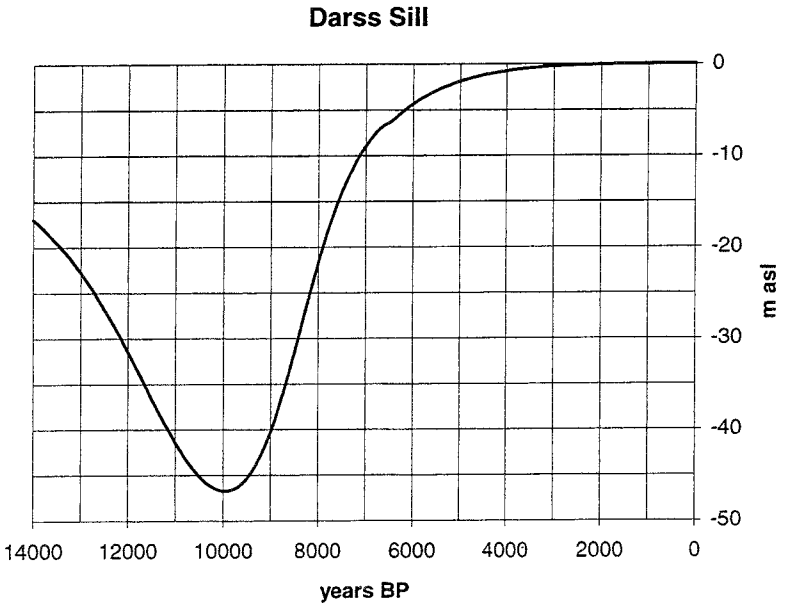

Figure 7-3. *Shore level displacement at the Darss Sill calculated with A_1 = 50 and B_1 = 2 500. The threshold at c. -20 was isolated c. 13 500 BP.*

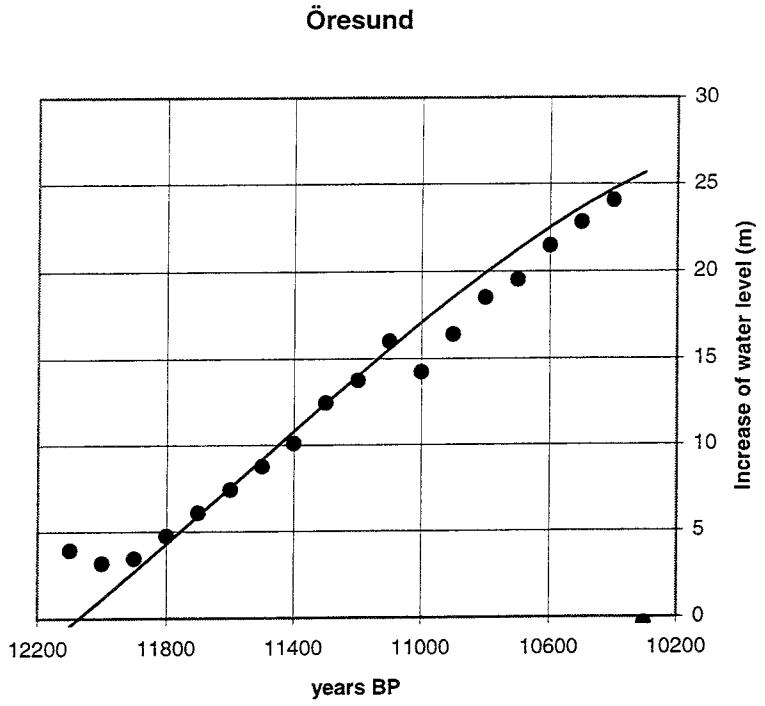

Figure 7-4. *The water level rise in the Baltic Ice Lake. The water level rise recorded at Oskarshamn (site 41) is shown with dots. This rise is related to the calculated rate of shore level displacement at the threshold at Öresund, black line. The transgression in the Baltic Ice Lake continued to c. 10 400 ± 100 BP and reached a level of c. 26 m before the drainage.*

7.5 THE ANCYLUS LAKE

A very fast transgression, the Ancylus transgression, started in the Baltic when the threshold at Degerfors was isolated and the Baltic was drained by the Svea River. The rise of the water level within the Baltic followed the rise of the threshold at Degerfors, which was very fast during this period. The rise of the threshold at Degerfors is calculated with $A_1 = 270$, $B_1 = 4800$, $A_3 = 40$, $B_3 = 400$ and $T_3 = 10\ 500$. This rise is shown in Figure 7-5. The exact time of the isolation at Degerfors is unknown. In Figure 7-5 the transgression is assumed to have started 9 500 BP. However, whether the transgression started 100 years before or after this date is of minor importance for the calculation. When the water level, after a transgressive phase of *c.* 250 - 300 years, had reached a level of *c.* 22 - 23 m a new outlet, the Dana River, was opened in the southern part of the Baltic. This alteration of the outlet occurred *c.* 9 300 - 9 250 BP, a date which also represents the maximum of the Ancylus transgression. After this maximum the water level of the Baltic decreased in phase with the shore level displacement at the Darss Sill, Figure 7-5. This stage may be named the Ancylus regression. The threshold at Dana River was reached by the marine transgression at *c.* 8 000 BP, Figure 7-3. This date defines the end of the Ancylus Lake.

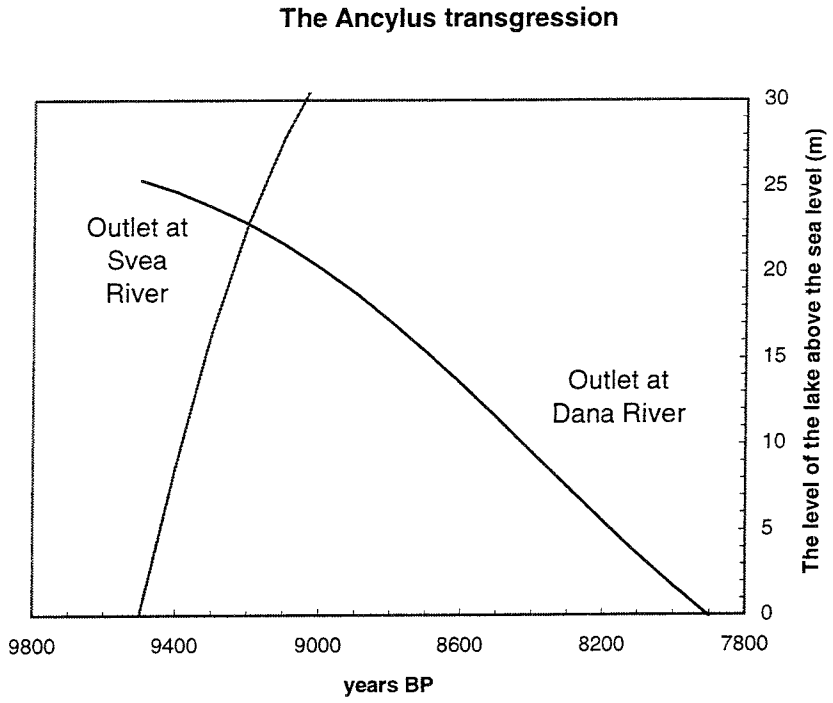

Figure 7-5. *The water level changes during the Ancylus Lake are estimated by combining the results of the calculated shore level displacements at the outlets at Svea River and Dana River.*

7.6 THE LITORINA SEA

The sea intruded the Baltic through the Storebält (the Great Belt) *c.* 8 000 BP. About 500 - 600 years later a connection to the sea also was opened through the Öresund strait. The Baltic was once again on a level with the sea. This stage of the Baltic is named the Litorina Sea. The initial phase of the Litorina Sea is commonly considered to be a separate stage, the Mastogloia Sea. This sub-stage is defined by brackish conditions, caused by the shallow connections between the sea and the Baltic during this time. The changes of the water level of the Baltic since the last deglaciation are summarised in Figure 7-6.

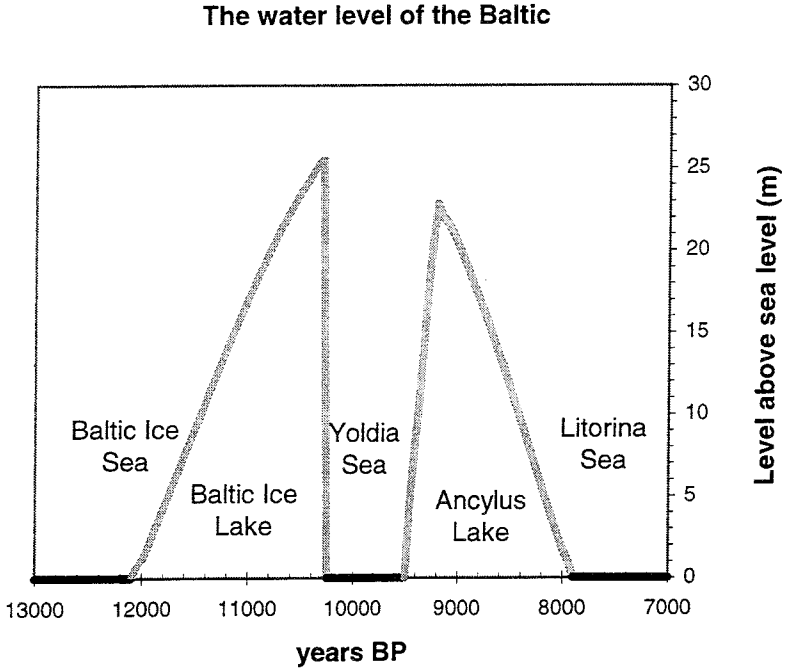

Figure 7-6 *Calculated changes of the water level of the Baltic.*

8 DISCUSSION

Creating a mathematical model for the shore level displacement means that the results are unknown in advance. This implies that one must start the modelling by making assumptions concerning which types of functions to apply. It is not until the results are available that these assumptions can be evaluated. Drawbacks, controversial interpretations but also advantages of the presented model are discussed in this chapter.

Arctan-functions were chosen for the calculations of the glacio-isostatic uplift in this model. The *arctan*-function is a symmetrical function where the initial inclining phase of the glacio-isostatic uplift is mirrored in the declining phase. This symmetry has most probably given a too simplified picture of the course of the uplift during the initial phase when most of the area was still glaciated. A more likely result would probably be obtained for the initial phase if the uplift was restrained in some way during this "loaded" phase. However, the *arctan*-function seems to fit the empirical information for the declining "unloaded" phase.

There is only one shore level curve available that includes the initial phase of the uplift. This curve is from Andöya, site 2, from the northernmost part of Norway (Vorren *et al.* 1988). The theoretical shore level curve for this site differs c. 10 m from the empirical curve for dates older then 16 000 BP (Figure 4-3). This deviation is probably due to an overstatement caused by the use of the symmetrical *arctan*-formulas. However, it cannot be excluded that this deviation is due to a deficiency in the eustatic function as the eustatic function used in this paper is only derived from data ranging back to 14 000 BP.

Late Weichselian shore level information from the Swedish west coast indicated, in an early phase of the modelling, that the glacio-isostatic uplift was not increased exponentially going backwards in time. This observation initiated the use of *arctan*-functions. The use of these functions involve a point at which the glacio-isostatic uplift has its fastest rate. This point (T_1) is estimated to have a constant value of 12 500 cal y BP (11 300 y BP). However, it cannot be excluded that this date may be after (!).

A constant value of T_1 can be physically explained. The slow uplift is caused by viscous inflow of mantle material towards the centre of the depressed dome. During the initial part of the crustal recovery the rate of this inflow was low even in areas which were already deglaciated. At the point when the inflow to the centre had reached a maximum that implied a maximal flow of the mantle material at every spot in the depressed dome.

As the symmetry of the *arctan*-function may probably have given a too simplified picture of the uplift for the initial phase, the question arises how much the values of A_1 have been affected by this shortcoming. A_1 is half of the total uplift (m). If this figure is doubled this would mean the total uplift, but also a doubling of an eventual error. The values of the total uplift should thus be used with caution.

Mörner (1980a) has presented a map, which has become the conventional picture of the total Fennoscandian uplift. This map is made by assuming the glacio-isostatic uplift to start 12 900 BP. The total uplift is then estimated by simply extrapolating the 13 000 year shore lines (!) to an assumed centre of uplift.

A regional trend of the declining factor (B_1) was established during the modelling, where the south-western parts of Fennoscandia showed low values while the north-eastern part showed high values. During the final calculations the estimations of B_1 became somewhat affected by the knowledge of this trend. A relationship between the crustal thickness and the declining factor was later detected during the analysis. This new information can be used for improving the model as irregularities in the regional pattern of the crustal thickness can be utilised for more detailed estimations of B_1.

The way of estimating B_1 shows the complexity in the procedure of modelling. New information can be discernible but can not be used before the first link is "proved". New information regarding the Ancylus transgression, has been "discernible" through the modelling. However, this knowledge has not been used in the modelling as it would have meant a revision of several of the Finnish curves. If this revision had been performed at the time of the modelling it probably would have been regarded as arrangements to suit.

One of the main results in the presentation is that the glacio-isostatic uplift is composed of two mechanisms. Mörner (1977, 1980a) has previously concluded a double nature of the Fennoscandian uplift. However, the mechanisms concluded by Mörner (1977, 1980a) are essentially different from the mechanisms presented by the present author. Mörner (1977, 1980a) suggests that the uplift since 8 000 BP is predominated by a linear "tectonic" mechanism, while the glacio-isostatic mechanism has been low since 8 000 BP and died out 2 000 - 3 000 years ago.

Several uncertainties within the model are illuminated in this chapter. Most of these uncertainties concern the initial part of the glacio-isostatic uplift. The reliability regarding the latest development is assumed to be satisfactory. This means that most of the discussed uncertainties do not affect the predictions made in this paper.

The presented model is a framework for improving future calculations. Adding more empirical information, by using short shore level curves, single dates of shore lines, the Ancylus transgression limit etc., would improve results. Revision in several shore level curves regarding the time of

the Ancylus transgression would change the uplift parameters somewhat in the Baltic area. Using the new information regarding the relationship between the crustal thickness and the declining factor B_1 would not only improve the model but also add new information for rheological calculations.

REFERENCES

Andersen O. B., Kejlsö E. & Remmer O. 1974. Secular movements within Jutland as determined from repeated precise levellings. Geodaet. Inst. Skr. 3. rk. 40. 1 - 70.

Andrews J.T. 1970. A Geomorphological Study of Post-Glacial Uplift, with Particular Reference to Arctic Canada: Institute of British Geographers. Special Publication No. 2., 1-156.

Anundsen K. 1985. Changes in shore-level and ice-front position in Late Weichselian and Holocene, southern Norway. Norsk Geografisk Tidskrift 39, 205 - 225.

Åse L.-E. 1970. Kvartärbiologiska vittnesbörd om strandförskjutningen vid Stockholm under de senaste c. 4000 åren. Geologiska Föreningens i Stockholm Förhandlingar 92, 49 - 78.

Asklund B. 1935. Gästrikländska fornstrandlinjer och nivåförändringsproblemen. Sveriges geologiska undersökning C 391, 1 - 119.

Bakkelid S. 1979. Et forelöpig totalbilde av landhevningen i Norge. Norges Geografiske Oppmålning, 1- 22.

Bard E., Hamelin B., Fairbanks R. G. & Zindler A. 1990. Calibration of the ^{14}C timescale over the past 30,000 years using mass spectrometric U - Th ages from Barbados corals. Nature 345, 405 - 409.

Becker B., Kromer B. & Trimborn, P. 1991. A stable- isotop tree-ring timescale of the Late Glacial/Holocene boundary. Nature 353, 647 - 649.

Bennike O. & Jensen J. B. 1995. Near-shore Baltic Ice Lake deposits in Fakse Bugt, southeast Denmark. Boreas 24, 185-195.

Berglund M. 1995. The Late Weichselian deglaciation, vegetational development and shore displacement in Halland, southwestern Sweden. University of Lund, Department of Quaternary Geology, Thesis 35, 1 - 113.

Bergqvist E. 1977. Postglacial Land Uplift in Northern Sweden: Some Remarks on Its Relation to the Present Rate of Uplift and the Uncompensated epression: Geologiska Föreningens i Stockholm Förhandlingar 99, 347-357.

Bergsten F. 1954. The Land Uplift in Sweden from the Evidence of the Old Water Marks: Geografiska annaler, 36, p. 81 - 111.

Bird E. C. F. & Klemsdal T. 1986. Shore displacement and the origin of the lagoon at Brusand, southwestern Norway. Norsk Geografisk Tidskrift 40, 27 - 35.

Björck S. 1979. Late Weichselian stratigraphy of Blekinge, SE Sweden, and water level changes in the Baltic Ice Lake. University of Lund, Department of Quaternary Geology, Thesis 7, 1 - 248.

Björck S. 1995. A reviw of the history of the Baltic Sea, 13.0-8.0 ka BP. Quaternary International 27, 19 - 40.

Björck S. & Digerfeld G. 1982. Late Weichselian shore displacement at Hunneberg, southern Sweden, indicating complex uplift. Geologiska Föreningens i Stockholm Förhandlingar 104, 132 - 155.

Björck S. & Digerfeld G. 1991. Alleröd- Younger Ryas sea level changes in southwestern Sweden and their relation to the Baltic Ice Lake development. Boreas 20, 115 - 133.

Bloom A.L. 1967. Pleistocene shorelines: a new test of isostasy. Geol. Soc. Am. Bull. 78, 1477-1494.

Brunnberg L., Miller U. & Risberg J. 1985. Project Eastern Svealand: Development of the Holocene landscape. ISKOS 5, 85 - 91.

Cato I. 1992. Shore displacement data based on lake isolations confirm the postglacial part of the Swedish Geochronological Time Scale. Sveriges geologiska undersökning Ca 81, 75 - 80.

Cathles L. M. 1975. The viscosity of the earth's mantle. Princeton University Press, Princeton, New Jersey,1-386.

Celsius A. 1743. Anmärkning om vatnets förminskande så i Östersiön som Vesterhafvet. Kongl. Swenska Wetenskaps Academiens Handlingar 4, 33-50.

Clark R. D., Farrell W. E. & Peltier W. R. 1978. Global changes in postglacial sea level: a numerical calculation. Quaternary Research 9: 265 - 278.

Corner G. D. 1980. Preboreal deglaciation chronology and marine limits of the Lyngen - Storfjord area, Troms, North Norway. Boreas 9, 239 - 249.

Christensen C. 1993. Land and sea. In: Hvass & Stovgaard (eds). Digging into the past - 25 years of Archaeology in Denmark. Aarhus Universitetsforlag, 20-23.

Daly R. A. 1934. The Changing World of the Ice Age. Hafner, New York, 1 - 271.

Damon P. E., Long A. & Grey D. C. 1966. Fluctuation of atmospheric ^{14}C during the last six millennia. Journal of Geophysical Reasearch 71, 1055 - 1063.

Damon P. E., Lerman J. C. & Long A. 1978. Temporal fluctuations of atmospheric ^{14}C: causal factors and implications. Annual Review of Earth Planet Sciences 6, 457 - 494.

Danielsen A. 1970. Pollen-analytical Late-Quaternary studies in the Ra district of Östfold, southeast Norway. Årsbog for universitetet i Bergen, mat.-naturv. serie 1969:14, 1-143.

Digerfeldt G. 1975. A standard profile for Littorina transgression in western Skåne, South Sweden. Boreas 4, 125 - 142.

Donner J. 1980. The detemination and dating of synchronous Late Quaternary shorelines in Fennoscandia. In: N.A. Mörner (Ed.), Earth Rheology, Isostasy and Eustasy. Wiley, New York; N.Y, 285 - 293.

Ekman M. 1986. A reinvestigation of the world's second longest eries of sea level observations: Stockholm 1774 - 1984. National Land Survey of Sweden, Professional Papers 1986:4.

Ekman M. 1996. A Consistent Map of the Postglacial Uplift of Fennoscandia. Terra Nova 8, 158 - 165.

Ekman M. & Mäkinen J. 1996. Recent postglacial rebound, gravity change and mantle flow in Fennoscandia. Geophysical Journal International 126, 229-234.

Emery K. O. & Aubrey D. G. 1991. Sea levels, land levels, and tide gauges. Springer-Verlag, 1-237.

Eronen M. 1976. A radiocarbon-dated Ancylus transgression site in south-eastern Finland. Boreas 5, 65 - 76.

Eronen M. 1983. Late Weichselian and Holocene shore displacement in Finland. In D.E. Smith & G. Dawson (eds.): Shorelines and Isostasy. Institute of British Geographers, Special Publication 16, Academic Press, 1983, 183-207.

Eronen M. & Haila H. 1982. Shorelines displacement near Helsinki, southern Finland, during the Ancylus Lake stage. Annales Academiae Scientiarum Fennicae AIII 134, 111 - 129.

Eronen M., Glückert G., van de Plassche O., van der Plicht J. & Rantala P. 1995. Land uplift in the Olkiluoto-Pyhäjärvi area, southwestern Finland, during the last 8 000 years. Nuclear Waste Commission of Finnish Power Companies, Report YJT-95-17, 1- 26.

Fairbanks R.G. 1989. A 17, 000- years glacio-eustatic sea lrvel record: influence of glacial melting rates on the Younger Dryas event and deep- ocean circulation. Nature 342, 637 - 642.

Fairbridge R.W. 1961. Eustatic changes in sea level. Physics and Chemistry of the Earth 4, 99-185.

Fjeldskaar W. & Cathles L. 1991. Rheology of mantle and lithosphere inferred from post-glacial uplift in Fennoscandia. In: Sabdini *et al.* (eds): Glacial isostasy, sea-level and mantle rheology, Kluwer Academic Publishers, 1 - 19.

Glückert G. 1976. Post-glacial shore-level displacement of the Baltic in SW Finland. Annales Academiae Scientiarum Fennicae AIII 134, 1 - 92.

Glückert G. 1978. Östersjöns postglaciala strandförskjutning och skogens historia på Åland. Publication Department of Quaternary Geology, University of Turku, 1 - 106.

Glückert G. & Ristaniemi O. 1982. The Ancylus transgression west of Helsinki, South Finland - A preliminary report. Annales Academiae Scientiarum Fennicae AIII 134, 99 - 134.

Godwin H., Suggate R. P. & Willis E. H. 1958. Radiocarbon dating of the eustatic rise in ocean-level. Nature 181, 1518 - 1519.

Hafsten U. 1983. Shore-level changes in South Norway during the last 13,000 years, traced by biostratigraphical methods and radiometric datings. Norsk Geografisk Tidskrift 37, 63 - 79.

Hald M. & Vorren T. O. 1983. A shore displacement curve from the Tromsö district, North Norway. Norsk Geologisk Tidskrift 63, 103 - 110.

Henningsmoen K. E. 1979. En karbon-datert strandforskyvningskurve fra söndre Vestfold. 239 - 247. In. Nydal, R., Westin, S., Hafsten, U. & Gulliksen, S.: Fortiden i sökelyset. Trondheim. (Univ. forl.)

Hyvärinen H. 1980. Relative sea-level changes near Helsinki, southern Finland during early Litorina times. Bullentin of the Geological Society of Finland 52, 207 - 219.

Hyvärinen H. 1984. The Mastogloia stage in the Baltic Sea history: Diatom evidence from southern Finland. Bullentin of the Geological Society of Finland 56. 1-2, 99 - 115.

Jelgersma S. 1961. Holocene sea level changes in the Netherlands. Meded. Geol. Sticht., C, VI, 7. 1-100.

Kääriäinen E. 1963. Land uplift in Finland computed by aid of precise levellings. Fennia 89, 15 - 19.

Kääriäinen E. 1966. The second levelling of Finland in 1935 - 1955. Veröff. Finn. Geodät. Inst. 61, Helsinki, 1 - 331.

Kaland P. E. 1984. Holocene shore displacement and shorelines in Hordaland, western Norway. Boreas 13, 203 - 242.

Kaland P. E., Krzywinski, K. & Stabell B. 1984. Radiocarbondating of the transitions between marine and lacustrine sediments and their relation to the development of lakes. Boreas 13, 243 - 258.

Kessel H. & Raukas A. 1979. The Quaternary History of the Baltic, Estonia. In: V. Gudelis & L.-K. Königsson (eds), The Quaternary History of the Baltic, 127 - 146. Acta Universitatis Upsaliensis Symposia Universitatis Upsaliensis Annum Quingentesimum Celebrantes 1. Uppsala

Kinck J. J., Husebye E. S. & Larsson F. R. 1993. The Moho depth distribution in Fennoscandia and the regional tectonic evolution from Archean to Permian times. Precambrian Research, 64, 23 - 51.

Kjemperud A. 1986. Late Weichselian and Holocene shore displacement in the Trondheimsfjord area, central Norway. Bores 15, 61 - 82.

Klein J., Lerman J. C., Damon P. E. & Ralph E. K. 1982. Calibration of radiocarbon dates. Radiocarbon 24, 103 - 150.

Klug H. 1980. Der Anstieg des Ostseespiegels im deutchen Küstenraum set dem Mittelatlantikum. Eiszeitalter und Gegenwart 30, 237 - 252.

Krzywinski K. & Stabell B. 1984. Late Weichselian sea level changes at Sotra, Hordaland, western Norway. Boreas 13, 159 - 202.

Lambeck K. 1991. A model for Devensian and Flandrian glacial rebound and sea-level change in Scotland. In*:* Sabdini *et al.* (eds): Glacial isostasy, sea-level and mantle rheology, Kluwer Academic Publishers, 33-61.

Libby W. F. 1955. Radiocarbon dating. Chicago: University of Chicago Press.

Liljegren R. 1982. Paleoekologi och strandförskjutning i en Littorinavik vid Spjälkö i mellersta Blekinge. University of Lund, Department of Quaternary Geology, Thesis 11, 1 - 95.

Lisitzin E. 1974. Sea-level changes. Elsevier Scientific Publishing Co. 1974.

Lotter A. 1991. Absolute dating of the Late-Glacial period in Switzerland using annually laminated sediments. Quaternary Research 35, 321 - 330.

Lundqvist G. 1962. Geological radiocarbon datings from the Stockholm station. Sveriges geologiska undersökning C 589, 1 - 23.

Madsen V., Nordmann V., Andersen J., Boggild O. B., Callisen K., Jessen A., Jessen K., Mertz E. L., Milthers V., Ravn J. P. J. & Ödum H. 1928. Summary of the geology of Denmark. Danmarks Geologiska Undersökning.V. 4.

McConnell R. K. 1968. Viscosity of the Mantle from Relaxation Time Spectra of Isostatic Adjustment: J. Geophys. Res.73, 7089-7105.

Miller U. & Robertsson A. -M. 1982. The Helgeandsholmen excavation: An outline of biostratigraphical studies to document shore displacement and vegetational changes. PACT 7, 311 - 327.

Miller U. & Robertsson A. -M. 1988. Late Weichselian and Holocene environmental changes in Bohuslän, Southwestern Sweden. Geographia Polonica 55, 103 - 111.

Möller J. J. 1984. Holocene shore displacement at Nappstraumen, Lofoten, North Norway. Norsk Geologisk Tidskrift 64, 1 - 5.

Mörner N. A. 1976. Eustatic changes during the last 8,000 years in view of radiocarbon calibration and new information from the Kattegatt region and other northwestern European coastal areas. Palaeogeography, Palaeoclimatology, Palaeoecology, 19, 63 - 85.

Mörner N. A. 1977. Past and present uplift in Sweden glacial isostasy, tectonism and bedrock influence. Geologiska Föreningens i Stockholm Förhandlingar 99, 48 - 54.

Mörner N. A. 1980a. The Fennoscandian Uplift: Geological Data and their Geodynamical Implication. In: Earth Rheology, Isostasy, and Eustasy. Ed. N.-A. Mörner. Avon, 251 - 283.

Mörner N. A. 1980b. The Northwest European " sea -level laboratory" and regional Holocene eustasy. Palaeogeography, Palaeoclimatology, Palaeoecology, 29, 281 - 300.

Nakada M. & Lambeck K. 1987. Glacial rebound and relative sea-level variations: a new appraisal. Geophysical Journal Royal Astronomical Society 90, 171 - 224.

Nakada M. & Lambeck K. 1989. Late Pleistocene and Holocene sea-level change in the Austrailian region and mantle rheology. *Geophysical Journal 96.* 497 - 517.

Nakiboglu S. M. & Lambeck K. 1991. Secular sea-level change. *In:* Sabdini *et al.* (eds): Glacial isostasy, sea-level and mantle rheology, Kluwer Academic Publishers, 237-258.

Nilsson E. 1968. Södra Sveriges senkvartära historia. Geokronologi, issjöar och landhöjning. Kungliga Svenska Vetenskapsakademiens Handlingar. Fjärde serien. Band 12. Nr 1, 1 - 117.

Norrman J. O. 1964. Vätterbäckenets senkvartära strandlinjer: En studie över relationen strandlinjegradient-ålder:Geologiska Föreningens i Stockholm Förhandlingar 85, 391-413.

Olsson I. U. 1968. Modern aspects of radiocarbon dating. Earth Science Review 4, 203 - 218.

Påsse T. 1983. Havsstrandens nivåförändringar i norra Halland under Holocen tid. Göteborgs universitet. Geologiska institutionen A 45,1 - 174.

Påsse T. 1986. Beskrivning till jordartskartan Kungsbacka SO. Sveriges geologiska undersökning Ae 56, 1 - 106.

Påsse T. 1987. Shore displacement during the Late Weichselian and Holocene in the Sandsjöbacka area, SW Sweden. Geologiska Föreningens i Stockholm Förhandlingar 109, 197 - 210.

Påsse T. 1988. Beskrivning till jordartskartan Varberg SO/ Ullared SV. Sveriges geologiska undersökning Ae 86, 1 - 98.

Påsse T. 1990a. Emperical estimation of isostatic uplift using the lake-tilting method at Lake Fegen and at Lake Säven, southwestern Sweden. Mathematical Geology 22, No. 7, 803 - 824.

Påsse T. 1990b. Beskrivning till jordartskartan Varberg NO. Sveriges geologiska undersökning Ae 102, 1 - 117.

Påsse T. 1996. Lake-tilting investigations in southern Sweden. SKB Technical Report 96-10, 1-34.

Peltier W. R., 1976. Glacial isostatic adjustments - II: The inverse problem. Geophysical Journal Royal Astronomical Society 46, 605 -646.

Peltier W. R. 1988. Lithospheric thickness, Antarctic deglaciation history, and ocean basin discretization effect in a global model of postglacial sea level changes: a summary of some sources of nonuniqueness. Quaternart Reaserch 29. 93 - 112.

Peltier W. R. 1991. The ICE-3G model of late Pleistocene deglaciation: construction, verification, and applications. In: R. Sabadini et al. (Editors), Glacial,Isostasy, Sea-level and Mantle Rheology. Kluwer, Dordrecht, 95 - 119.

Persson C. 1979. Shore displacement during Ancylus time in the Rejmyra area, south central Sweden. Sveriges geologiska undersökning C 755, 1 - 23.

Persson G. 1962. En transgressionslagerföljd från Limhamn. Geologiska Föreningens i Stockholm Förhandlingar 84, 47 - 55.

Persson G. 1973. Postglacial transgressions in Bohuslän, Southwestern Sweden. Sveriges geologiska undersökning C 684, 1 - 47.

RAK (Rikets allmänna kartverk) 1971. Geodetic activities in Sweden 1967-1970. Geographical Survey Office of Sweden A 38, 1 - 19.

RAK (Rikets allmänna kartverk) 1974. Sveriges andra precisionsavvägning 1951-1967. Geographical Survey Office of Sweden A 40, 1-91.

Ramfjord H. 1982. On the Late Weichselian and Flandrian shoreline displacement in Naeröy, Nord-Tröndelag, Norway. Norsk Geologisk Tidskrift 62, 191 - 205.

Renberg I. & Segerström U. 1981. The initial points on a shoreline displacement curve for southern Västerbotten, dated by varve-counts of lake sediments. Striae 14, 174 - 176.

Richardt N. 1996. Sedimentological examination of the Late Weichselian sea-level history following deglaciation of northern Denmark. Geological Society Special Publication 111, 261 - 273.

Ringberg B. 1989. Upper Late Weichselian lithostratigraphy in western Skåne, southernmost Sweden. Geologiska Föreningens i Stockholm Förhandlingar 111, 319 -337.

Risberg J. 1991. Palaeoenvironment and sea level changes during the early Holocene on the Södertörn penisula, Södermanland, eastern Sweden. Stockholm University, Department of Quaternary Research. Report 20, 1 - 27.

Robertsson A. -M. 1991. Strandförskjutningen i Eskiltunatrakten för ca 9 000 till 4 000 år sedan. Sveriges geologiska undersökning, Rapporter och meddelanden 67, 1 - 27.

Saarnisto M. 1981. Holocene emergence history and stratigraphy in the area north of the Gulf of Bothnia. Annales Academiae Scientiarum Fennicae AIII 130, 1 - 42.

Salomaa R. 1982. Post-glacial shoreline displacement in the Lauhanvuori area, western Finland. Annales Academiae Scientiarum Fennicae AIII 134, 81 - 97.

Salomaa R. & Matiskainen H. 1983. Rannan siirtyminen ja arkeologinen kronologia Etelä-Pohjanmaalla. Arkeologian päivät 7 -8.4. 1983 Lammin Biolog. tutkimusasemalla. Karhunhammas 7, 21 - 36.

Salonen V. - P., Räsenen M. & Terho A. 1984. Palaeolimnology of ancient Lake Mätäjärvi. Third Nordic Conference on the application of scientific methods in archaelogy. Mariehamn, Åland, Finland, 8-11. October 1984. Iskos 5, 233 - 288.

Sandegren R. & Johansson H. E. 1931. Beskrivning till kartbladet Göteborg. Sveriges geologiska undersökning Aa 173, 1 - 141.

Shepard F. P. 1963. Submarine Geology. Harper and Row, New York, N.Y. 2nd ed., 1-557.

Simonsen O. 1969. Some remarks in May 1968 on the secular movements within Denmark. In. J. A. Mescherikov, Problems of recent crustal movements of the Earth, USSR Acad. Sci., Moscow.

Stabell B. 1980. Holocene shorelevel displacement in Telemark, southern Norway. Norsk Geoglogisk Tidskrift 60, 71 - 81.

Stuiver M. & Reimer P. J. 1993. Extended ^{14}C data base and revised CALIB 3.0 age calibration program.Radiocarbon 35, 215-230.

Suess H. E. 1970. Bristlecone pine calibration of the radiocarbon time-scale 5200 BC to the present. In: Radiocarbon variation and absolute chronology, I. U. Olsson (ed.), 595 - 605. New York: Wiley.

Suutarinen O. 1983. Recomputation of land uplift values in Finland. Reports of the Finnish Geodetic Institute 83:1, 1-16.

Svedhage K. 1985. Shore displacement during Late Weichselian and Early Holocene in the Risveden area, SW Sweden. Göteborgs universitet. Geologiska institutionen A 51, 1 - 111.

Sveian H. & Olsen L. 1984. En strandforsyvningskurve fra Verdalsöra, Nord-Tröndelag.Norsk Geologisk Tidskrift 64, 27 - 38.

Svendsen J. I. & Mangerud J. 1990. Sea-level changes and pollen stratigraphy on the outer coast of Sunnmöre, western Norway. Norsk Geologisk Tidskrift 70, 111 - 134.

Svensson N. -O. 1989. Late Weichselian and Early Holocene shore displacement in the Central Baltic, based on stratigraphical and morphological records from Eastern Småland and Gotland, Sweden. Lund University, Department of Quaternary Geology 25, 1 - 195.

Sörensen R. 1979. Late Weichselian deglaciation in the Oslofjord area, south Norway. Boreas 8, 241 - 246.

Thomsen H. 1982. Late Weichselian shore-level displacement on Nord-Jären, south-west Norway. Geologiska Föreningens i Stockholm Förhandlingar 103, 447 - 468.

Winn K., Averdieck F. R., Erlenkeusser H. & Werner F. 1986. Holocene sea level rise in western Baltic and the question of isostatic subsidence. Meyniana 38, 61-80

Vorren K. -D. & Moe D. 1986. The early Holocene climate and sea-level changes in Lofoten and Vesterålen, North Norway. Norsk Geologisk Tidskrift 66,135 - 143.

Vorren T., Vorren K. -D., Alm T., Gulliksen S., and Lövlie R. 1988. The last deglaciation (20,000 to 11,000 B.P.) on Andöya, northern Norway. Boreas 17, 41-77.

List of SKB reports

Annual Reports

1977-78
TR 121
KBS Technical Reports 1 – 120
Summaries
Stockholm, May 1979

1979
TR 79-28
The KBS Annual Report 1979
KBS Technical Reports 79-01 – 79-27
Summaries
Stockholm, March 1980

1980
TR 80-26
The KBS Annual Report 1980
KBS Technical Reports 80-01 – 80-25
Summaries
Stockholm, March 1981

1981
TR 81-17
The KBS Annual Report 1981
KBS Technical Reports 81-01 – 81-16
Summaries
Stockholm, April 1982

1982
TR 82-28
The KBS Annual Report 1982
KBS Technical Reports 82-01 – 82-27
Summaries
Stockholm, July 1983

1983
TR 83-77
The KBS Annual Report 1983
KBS Technical Reports 83-01 – 83-76
Summaries
Stockholm, June 1984

1984
TR 85-01
Annual Research and Development Report 1984
Including Summaries of Technical Reports Issued during 1984. (Technical Reports 84-01 – 84-19)
Stockholm, June 1985

1985
TR 85-20
Annual Research and Development Report 1985
Including Summaries of Technical Reports Issued during 1985. (Technical Reports 85-01 – 85-19)
Stockholm, May 1986

1986
TR 86-31
SKB Annual Report 1986
Including Summaries of Technical Reports Issued during 1986
Stockholm, May 1987

1987
TR 87-33
SKB Annual Report 1987
Including Summaries of Technical Reports Issued during 1987
Stockholm, May 1988

1988
TR 88-32
SKB Annual Report 1988
Including Summaries of Technical Reports Issued during 1988
Stockholm, May 1989

1989
TR 89-40
SKB Annual Report 1989
Including Summaries of Technical Reports Issued during 1989
Stockholm, May 1990

1990
TR 90-46
SKB Annual Report 1990
Including Summaries of Technical Reports Issued during 1990
Stockholm, May 1991

1991
TR 91-64
SKB Annual Report 1991
Including Summaries of Technical Reports Issued during 1991
Stockholm, April 1992

1992
TR 92-46
SKB Annual Report 1992
Including Summaries of Technical Reports Issued during 1992
Stockholm, May 1993

1993
TR 93-34
SKB Annual Report 1993
Including Summaries of Technical Reports Issued during 1993
Stockholm, May 1994

1994

TR 94-33

SKB Annual Report 1994

Including Summaries of Technical Reports Issued during 1994.
Stockholm, May 1995

1995

TR 95-37

SKB Annual Report 1995

Including Summaries of Technical Reports Issued during 1995.
Stockholm, May 1996

List of SKB Technical Reports 1996

TR 96-01

Bacteria, colloids and organic carbon in groundwater at the Bangombé site in the Oklo area

Karsten Pedersen (editor)
Department of General and Marine Microbiology,
The Lundberg Institute, Göteborg University,
Göteborg, Sweden
February 1996

TR 96-02

Microbial analysis of the buffer/container experiment at AECL´s Underground Research Laboratory

S Stroes-Gascoyne[1], K Pedersen[2], S Daumas[3],
C J Hamon[1], S A Haveman[1], T L Delaney[1],
S Ekendahl[2], N Jahromi[2], J Arlinger[2], L Hallbeck[2],
K Dekeyser[3]
[1] AECL, Whiteshell Laboratories, Pinawa, Manitoba, Canada
[2] University of Göteborg, Department of General and Marine Microbiology, Göteborg, Sweden
[3] Guigues Recherche Appliquée en Microbiologie (GRAM), Aix-en-Provence, France
1996

TR 96-03

Reduction of Tc (VII) and Np (V) in solution by ferrous iron. A laboratory study of homogeneous and heterogeneous redox processes

Daqing Cui, Trygve E Eriksen
Department of Chemistry, Nuclear Chemistry,
Royal Institute of Technology, Stockholm, Sweden
March 1996

TR 96-04

Revisiting Poços de Caldas. Application of the co-precipitation approach to establish realistic solubility limits for performance assessment

Jordi Bruno, Lara Duro, Salvador Jordana,
Esther Cera
QuantiSci, Barcelona, Spain
February 1996

TR 96-05

SR 95

Template for safety reports with descriptive example
SKB
December 1995

TR 96-06

Äspö Hard Rock Laboratory Annual Report 1995

SKB
April 1996

TR 96-07

Criticality in a high level waste repository. A review of some important factors and an assessment of the lessons that can be learned from the Oklo reactors

Virginia M Oversby
VMO Konsult
June 1996

TR 96-08

A reappraisal of some Cigar Lake issues of importance to performance assessment

John Smellie[1], Fred Karlsson[2]
[1] Conterra AB
[2] SKB
July 1996

TR 96-09

The long-term stability of cement. Leaching tests

Ingemar Engkvist, Yngve Albinsson,
Wanda Johansson Engkvist
Chalmers University of Technology,
Göteborg, Sweden
June 1996

TR 96-10

Lake-tilting investigations in southern Sweden

Tore Påsse
Sveriges geologiska undersökning,
Göteborg, Sweden
April 1996

TR 96-11
Thermoelastic stress due to an instantaneous finite line heat source in an infinite medium
Johan Claesson, Göran Hellström
Depts. of Building Physics and Mathematical Physics, Lund University, Lund, Sweden
September 1995

TR 96-12
Temperature field due to time-dependent heat sources in a large rectangular grid
– Derivation of analytical solution
Johan Claesson, Thomas Probert
Depts. of Building Physics and Mathematical Physics, Lund University, Lund, Sweden
January 1996

TR 96-13
Thermoelastic stress due to a rectangular heat source in a semi-infinite medium
– Derivation of an analytical solution
Johan Claesson, Thomas Probert
Depts. of Building Physics and Mathematical Physics, Lund University, Lund, Sweden
May 1996

TR 96-14
Oklo: Des reacteurs nucleaires fossiles (Oklo: The fossil nuclear reactors). Physics study (R Naudet, CEA)
– Translation of chapters 6, 13, and conclusions
V O Oversby
VMO Konsult
September 1996

TR 96-15
PLAN 96
Costs for management of the radioactive waste from nuclear power production
Swedish Nuclear Fuel and Waste Management Co
June 1996

TR 96-16
Diffusion of I^-, Cs^+ and Sr^{2+} in compacted bentonite
– Anion exclusion and surface diffusion
Trygve E Eriksen, Mats Jansson
Royal Institute of Technology, Department of Chemistry, Nuclear Chemistry, Stockholm
November 1996

TR 96-17
Hydrophilic actinide complexation studied by solvent extraction radiotracer technique
Jan Rydberg
Department of Nuclear Chemistry, Chalmers University of Technology, Gothenburg, Sweden and Radiochemistry Consultant Group AB, V. Frölunda, Sweden
October 1996

TR 96-18
Information, conservation and retrieval
Torsten Eng[1], Erik Norberg[2], Jarl Torbacke[3], Mikael Jensen[4]
[1] Swedish Nuclear Fuel and Waste Management Co (SKB)
[2] National Swedish Archives
[3] Department of History, Stockholm University
[4] Swedish Radiation Protection Institute (SSI)
December 1996

TR 96-19
Application of space geodetic techniques for the determination of intraplate deformations and movements in relation with the postglacial rebound of Fennoscandia
Hans-Georg Scherneck, Jan M Johansson, Gunnar Elgered
Chalmers University of Technology, Onsala Space Observatory, Onsala, Sweden
April 1996

TR 96-20
On the characterization of retention mechanisms in rock fractures
Jan-Olof Selroos, Vladimir Cvetkovic
Div. of Water Resources Engineering, Dep. of Civil and Environmental Engineering, Royal Institute of Technology, Stockholm, Sweden
December 1996

TR 96-21
Boring of full scale deposition holes using a novel dry blind boring method
Jorma Autio, Timo Kirkkomäki
Saanio & Riekkola Oy, Helsinki, Finland
October 1996

TR 96-22
Feasibility study for siting of a deep repository within the Malå municipality
Swedish Nuclear Fuel and Waste Management Co., Stockholm
March 1996

TR 96-23

Analysis of the Äspö LPT2 pumping test via simulation and inverse modelling with HYDRASTAR

Douglas Walker (ed.)[1], Lars Eriksson[2],
Lars Lovius[2]
[1] INTERA KB
[2] Starprog AB

December 1996